TÉCNICO LISBOA

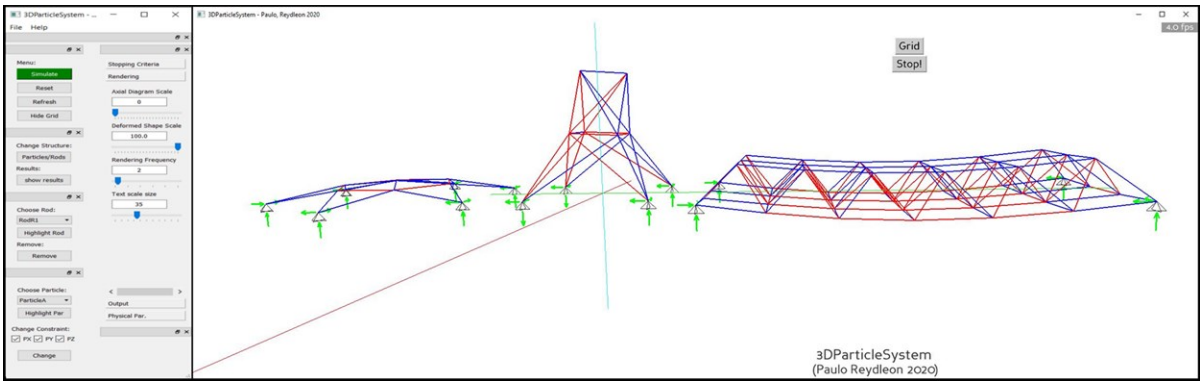

An interactive real-time physics software for structural analysis of space trusses

Reydleon Paiva de Paulo

Thesis to obtain the Master of Science Degree in

Civil Engineering

Supervisors:

Prof. Dr. Vítor Manuel Azevedo Leitão

Prof. Dr. Francisco Afonso Severino Regateiro

Examination Committee

Chairperson: Prof. Dr. António Manuel Figueiredo Pinto da Costa

Supervisor: Prof. Dr. Vítor Manuel Azevedo Leitão

Member of the Committee: Prof. Dr. José Paulo Moitinho de Almeida

Sept 2020

Declaration

I declare that this document is an original work of my own authorship and that it fulfills all the requirements of the Code of Conduct and Good Practices of the Universidade de Lisboa.

“FAOT – Facilitar, Alterar, Otimizar e Transformar”
Reydleon Paulo 2014

Agradecimentos

Aos meus orientadores, Professor Vítor Leitão e Professor Francisco Regateiro, pela ajuda na resolução de problemas ao longo das várias etapas deste trabalho, pelas suas correções e sugestões.

Agradeço a atenção que tiveram comigo durante este ano em que tive o privilégio de receber uma bolsa de estudos "Eng. Augusto Ramalho-Rosa". A importância de uma bolsa de estudos na vida de um estudante como eu é inexplicável e imensurável. Hoje e ao longo da minha vida sempre serei um bolseiro agradecido à Dra. Berta Marinho, Dra. Rita Schreck e ao Eng. Augusto Ramalho-Rosa. Agradeço também a atenção que me foi dada por todos os profissionais dos SAS Ulisboa e do NDA, em particular ao Dr. José Barbosa e à Dra. Rita Wahl.

Agradeço a todos os meus amigos, em particular, ao Eng. Eduardo Lopes, à Sofia Alves, ao Eng. Andrei Vodã e ao Eng. Bruno Alexandre Morais Ribeiro. Um especial agradecimento à Engenheira Ana Beatriz Rodrigues e à sua família: José Ambrósio, José Miguel e Graciete Novais.

Agradeço à minha mãe, Derli, e aos meus irmãos Gabryel e Simão Paulo pelo apoio e por estarem sempre do meu lado. Dedico esta dissertação à minha mãe por me encorajar e que, em fases decisivas da minha vida, me tem apoiado e esclarecido como nenhuma outra pessoa.

Abstract

Space truss is an important theme while learning the first concepts of statics. On the other hand, it has real engineering applications. An example of the application of this technique is the Double Layer Grid (DLG), which is generally the adopted solution in the roofing of factories and airport terminal halls, as it can overcome large spans.

This work presents an interactive software entirely written in Python that aims to help students to understand the behavior of space truss systems. The software allows the user to design structures, analyze them, and then export the results. The CAD software was successfully created from scratch and can perform nonlinear analysis.

The 3DParticleSystem software numerical method is based on the concept of physics engine. Physics engines are widely used as middleware in game engines. In commercial software for structural analysis, this approach is rarely used despite exhibiting some quite convenient features: it allows for new types of analysis (namely, nonlinear and incremental analysis); also allowing to represent the time evolution of a structure once calculations are made in real-time, responding to user input. Such features can be important while learning structural engineering concepts.

The work carried out here further improves the application of physics engines in the field of structural analysis: it first summarizes the implementation of the physically-based modeling/particle system dynamics; it then gives an overview of the PyQt and the Panda3D game engine, tools that were used to create an advanced GUI (Graphical User Interface) to render space trusses.

Keywords: Interactive Structural Analysis, Python 3D physics engine, Panda3D, Nonlinear Analysis, Newton's Second Law, Particle System Dynamics.

Resumo

A treliça espacial é um tema importante ao aprender os primeiros conceitos de estática. Por outro lado, esta tem aplicações reais em engenharia. Um exemplo da utilização desta técnica é o Double Layer Grid (DLG). Esta técnica é geralmente adotada em coberturas de fábricas e terminais de aeroporto, pois pode superar vãos grandes.

Este documento apresenta um software interativo inteiramente escrito em Python que visa ajudar os alunos a compreender o comportamento de treliças espaciais. O software permite criar estruturas, analisá-las, em seguida, exportar os resultados. Este CAD foi criado de raiz e é capaz de realizar análises não-lineares.

O método numérico do 3DParticleSystem software é baseado no conceito de physics engine. Physics engine é uma abordagem normalmente utilizada em game engines. Porém, não tanto na área de engenharia de estruturas. Sendo assim, não é a abordagem mais comum em software comerciais para a análise de estruturas. A grande vantagem desta abordagem é que permite complexos tipos de análises, tais como, análises não-lineares e incrementais. Além disso, permite representar a evolução temporal de uma estrutura uma vez que os cálculos são feitos em tempo real. Tais vantagens podem ser cruciais na aprendizagem de conceitos de engenharia de estruturas.

Este documento contribui numericamente na aplicação de physics engines na análise de estruturas. Primeiramente, apresenta a implementação da metodologia physically based modeling/particle system dynamics. Além disso, dá uma visão global do PyQt e do Panda3D, ferramentas utilizadas para desenvolver a GUI (Graphical User Interface) capaz de representar treliças espaciais.

Palavras-chave: Análise estrutural interativa, Python 3D physics engine, Panda3D, Análise não linear, Segunda Lei de Newton, Particle System Dynamics.

Notation

a	Acceleration vector	$[\mathrm{ms}^{-2}]$
A	Cross-sectional area	$[\mathrm{m}^2]$
c	Damping coefficient	$[\mathrm{kNm}^{-1}\mathrm{s}]$
ρ	Density	$[\mathrm{ms}^{-2}]$
$F\ or\ f$	Generic force	$[\mathrm{kN}]$
L	Length	$[\mathrm{m}]$
m	Mass	$[\mathrm{kg}]$
λ	Mass per unit length	$[\mathrm{kgm}^{-1}]$
Δt	time-step	$[\mathrm{s}]$
k	Stiffness	$[\mathrm{kNm}^{-1}]$
ϵ	Strain	$[-]$
σ	Stress	$[\mathrm{MPa}]$
t	time	$[\mathrm{s}]$
v	Velocity vector	$[\mathrm{ms}^{-1}]$
E	Young's modulus	$[\mathrm{GPa}]$

Acronyms

CSV	Comma-separated values
CAD	Computer-aided design
DLG	Double Layer Grid
DXF	Drawing Exchange Format
FEM	Finite Element Method
FPM	Finite Particle Method
GE	Game engine
GRE	Graphics rendering engine
GUI	Graphical user interface
PS	Particle System approach
PE	Physics engine
TXT	Text file
VFIFE	Vector Form Intrinsic Finite Element method

Contents

List of Figures

List of Tables

1 Introduction

1.1 Motivation

As knowledge evolves, there is a natural increase in technical requirements for structural engineering projects. Thus, software knowledge becomes essential when it comes to obtaining the best solution in the shortest possible time. Therefore, this knowledge is fundamental at the professional level and should be presented to the students during the academic period. Thus, several tools have been developed to employ full numerical structural analysis and to handle structural phenomena, for example, commercial programs such as ANSYS Inc. (2011) and SAP2000 (Computers and Structures Inc. 2011). These programs, however, are designed for advanced users and are challenging to learn and use.

The analysis of trusses (structures composed of bars/rods connected at their ends by hinges and subject to loads applied only at the nodes/hinges) is an important theme in learning the first concepts of structural mechanics. The static equilibrium of plane (2D) trusses is generally presented in the first semesters of engineering courses. During this stage, didactic software are usually introduced to support learning the basics of structural engineering. Usually, these codes implement the linear static model and the direct stiffness method [1]. This is suitable for academic purposes, but entails some limitations: if the student attempts to model a structure that is hypostatic or if the configuration of supports in a model does not render it externally isostatic, most of the didactic software will simply produce an error message saying that the structure cannot be analyzed because it is an unstable structure [2]. Moreover, due to its numerical simplifications, they are not suitable for teaching some topics, such as physical nonlinearity and failure mechanisms, as they do not address these matters effectively or at all.

There are some numerical alternatives to the traditional Finite Element Method (FEM) that may be seen to avoid some of the above difficulties. One such alternative resorts to particle-based methods. These methods are widely used in the development of games and animations but also have applications in structural engineering problems where methods have been devised for problems such as structural form-finding problems [3], and others based on the dynamic relaxation method [4]. Unlike the methods based on finite elements, there is no need to construct a global stiffness matrix and solve it [5]. Typically, a particle-based approach is built on sets of particles that carry all the physical properties and conditions; then, equilibrium is verified at each particle in an iterative process. This approach allows different analyses to be carried out by simply enforcing Newton's laws at each particle, making it possible to address kinematically indeterminate structures [1], discontinuities, failure mechanisms [6], and also physically and geometrically nonlinear problems. For a student learning the basics of structural engineering, the answer to some previous topics can be difficult to relate to the real world. Besides, it takes time and experience to understand the behavior of structures. Thus, a software that allows real-time physics interactive analyses can be a useful tool for an engineering student to start learning these relevant engineering topics.

1.2 Physics engine and Game engine

For the development of an interactive real-time physics software for structural analysis, there are several possible approaches. The one favored here is to use concepts commonly used in computer games. This thesis starts by describing two fundamental concepts: the physics engine and the game engine.

1.2.1 Physics engine

Physics engines are often described as game middleware that are integrated into a game engine to handle some specialized aspects in physics simulation, such as collision detection and dynamics simulation [7]. Physics engines are packages that provide specialized mechanical simulation and are responsible for solving Newton's equation of motion. It handles certain physical systems such as rigid body dynamics, soft body dynamics, fluid dynamics and collision detection. Havok [8], PhysX [9], Open Dynamics Engine [10], and Chipmunk [11] are some of the most popular game-oriented physics engines.

Some developer-friendly physics engines can be included in different applications, such as game engines, digital content creation systems, and effects applications. An example of a developer-friendly physics engine is Pymunk [12], which is built on top of the 2D physics library Chipmunk, for the Python programming language [13]. This physics engine can handle rigid bodies, collision shapes, and constraints/joints. In Figure 1.1, the Pymunk library is used to create an animation of randomly falling balls over a rigid body, constrained by a slide and a pin joint. In this case, it is combined with PyGame [14] as a graphics rendering middleware to render the simulation results.

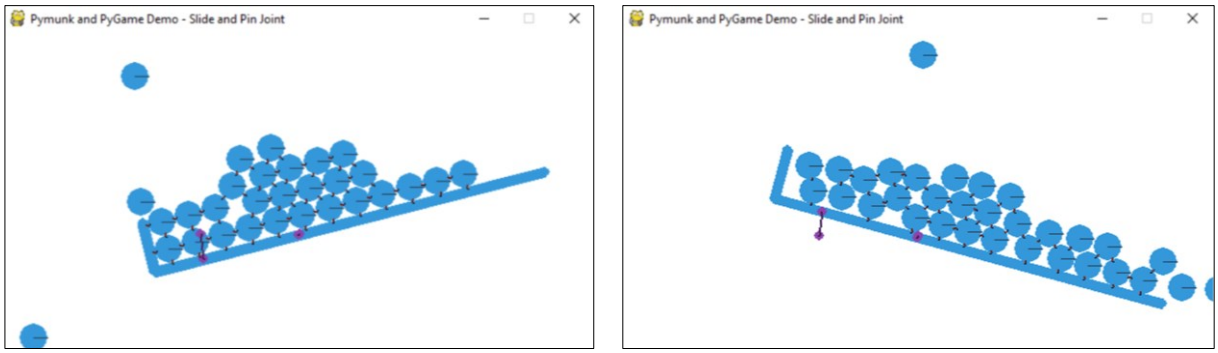

Figure 1.1 – Pymunk and Pygame demonstration. Slide and pin joint [89].

In addition to video game applications, physics engines are widely used in physically-based animations [15]. In the last decade, physics engines are also being used for robotic applications such as Mira – Middleware for Robotic Applications [16] and MuJoCo – A physics engine for model-based control [17].

1.2.2 Game engine

Game engines, all-in-one middleware, normally correspond to a Software Development Kit (SDK), which integrates the functionalities needed to develop a game. These functionalities, also known as middleware, can be graphics/rendering, audio, physics, Artificial Intelligence, multiplayer, synthesis, among others [7]. Some popular commercial game engines with their representative games are Renderware (Grand Theft Auto: San Andreas) [18], Unity (Assassin's Creed: Identity) [19], and Unreal (Borderlands) [20].

1.3 Real-time physics software in structural engineering

Real-time physics simulation has been extensively used in computer games, but its potential has yet to be fully realized in design and education. It is suitable to simulate the behavior of structures under different loading with engineering accuracy and giving real-time feedback [5]. Some didactic programs aim to introduce the first structural engineering concepts and are directly related to the core of this thesis. Of these, two programs stand out, namely, Arcade and PushMePullMe3D.

Arcade [21], created by Kirk Martini (latest release in 2009), is a structural analysis software program for nonlinear dynamic simulation specially tailored for students and classes of architecture and structural engineering courses. It is based on a computation method widely used in computer games to create an interactive real-time linear and nonlinear physical simulation of simple structures.

PushMePullMe3D [22], which is part of the educational project *Expedition Workshed,* is written in Java and is available online. It is based on the idea of using interactive real-time physics, where a co-rotational approach is used to compute the resultant field of displacements in global coordinates, including the effect of large deformations.

Figure 1.2 shows, on the left, the Arcade's GUI, while analyzing an inelastic behavior of a cantilever; on the right, the PushMePullMe3D's GUI is shown while analyzing a space truss.

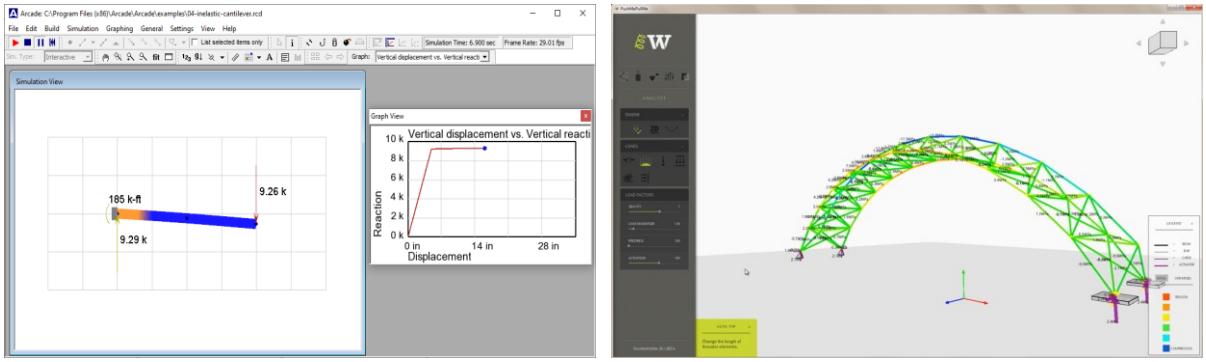

Figure 1.2 – Arcade (left side). PushMePullMe (right side).

1.4 Particle-based methods in structural engineering

Particle-based methods have a real application in advanced civil engineering problems. In recent years, some researchers have put effort into developing particle methods suitable for application to structural analysis. Thus, this chapter provides an overview of two particle-based methods, the Vector Form Intrinsic Finite Element method, VIFIFE, and the Finite Particle Method, FPM.

1.4.1 Vector Form Intrinsic Finite Element method

The Vector Form Intrinsic Finite Element method (VFIFE) is a mathematical calculation method based on vector mechanics for structures with large deformation. The method appears to have been first proposed by Ting, Wang, and Shi in 2002 and is based on an intrinsic modeling approach, an explicit algorithm, and a co-rotational formulation of kinematic, meaning that it is a step-by-step and particle-by--particle cycling iteration computation that follows the motion of the particles.

In a series of three papers, Ting explains the fundamentals of the VFIFE method. In the first paper, the author presents the basics of the method as applied to a plane frame element model [23]. In the second work, the author introduces the formulation for plane solid elements and makes some remarks related to convergence [24]. Finally, the author presents a convected material frame which is used to extend the method for the large deformation and large displacement cases. Some interesting examples are also presented, including the case of bending of a flexible cantilever with contact [25].

The VFIFE is based on some assumptions, which are:

a) the structural system is a finite collection of rigid and/or deformable bodies,
b) the motion of the bodies follows Newton's second law,
c) all the existing bodies must have mass,
d) each body mass is represented by a finite number of particles.

The VFIFE method can be applied to a broad spectrum of problems. For example, it was used to analyze the snap-through of a space truss dome [26] as well as to simulate a 3D frame collapse [27]. With a slightly different implementation, it was used to analyze the nonlinear behavior of steel structures exposed to fire [28]. More recently, it has been used to analyze train and bridge dynamic interaction responses [29].

1.4.2 Finite Particle Method

The Finite Particle Method (FPM) is a numerical analysis method based on VFIFE that focuses more on structural engineering. It was developed in 2008 by Ying Yu and Yao-Hi Luo and presented in two papers [30] and [31] both in Chinese. Then, the principles of FPM are also described in English by Long et al. in [32], which applied the method in the simulation of the collapse of a 3D space structure frame subjected to earthquake excitation. A comparison with FEM results was also included in this last work.

The FPM has already shown its applicability in various types of problems, namely: analyzing kinematically indeterminate bar assemblies [33] and deployable structures [34], making a progressive failure simulation [6] and a collapse analysis of cable nets under dynamic loads [35]. Most recently, it was used to analyze the nonlinear dynamic collapse analysis of semi-rigid steel frames [36]. The following figures present the results of the progressive deformation of the Vogel six-story frame with rigid connections, in Figure 1.3, and with linear semi-rigid connections, in Figure 1.4.

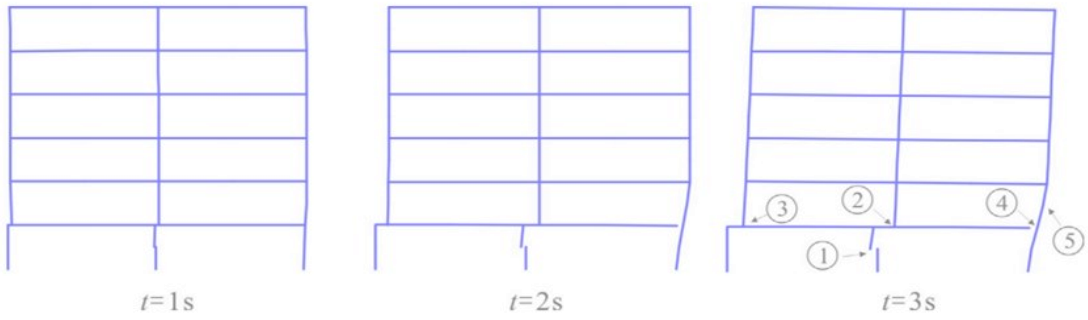

Figure 1.3 – Progressive deformation of a Vogel six-story frame with rigid connections, adapted from [36].

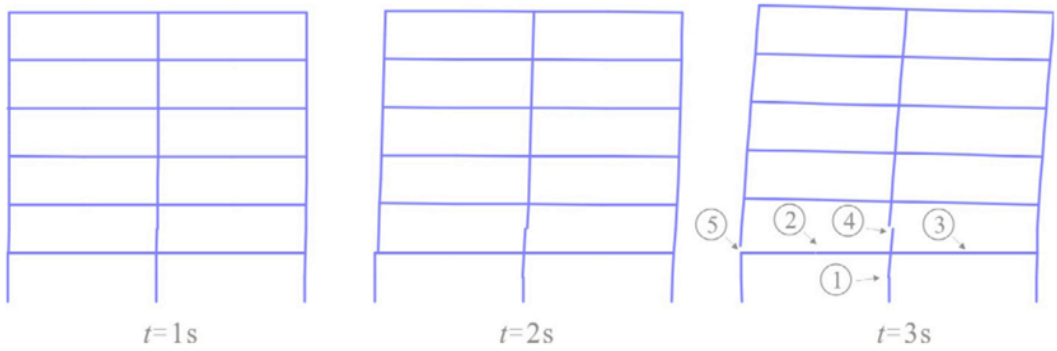

Figure 1.4 – Progressive deformation of a Vogel six-story frame with linear semi-rigid connections. Adapted from [36].

One of the most interesting applications of FPM is the progressive failure simulation of truss structures [6]. In this work, a cantilever-framed structure was analyzed to simulate the roof of an audience stand at Sanmen in China that was destroyed by a typhoon in 2005. Figure 1.5 shows the roof modeled as a cantilever truss structure. Each member of the structure was modeled by a 3D rod element and two particles. The total numbers of particles and rod elements were 416 and 1456, respectively.

A typhoon is one of the most complicated types of dynamic loads. Because the focus of the work was on the failure simulation algorithms, the wind loads were, for simplicity, taken as constant impact loads in the analysis. Moreover, the deformations of the pillars were ignored in the analysis, and so fixed roof supports were considered. The results of this analysis are shown in Figure 1.6.

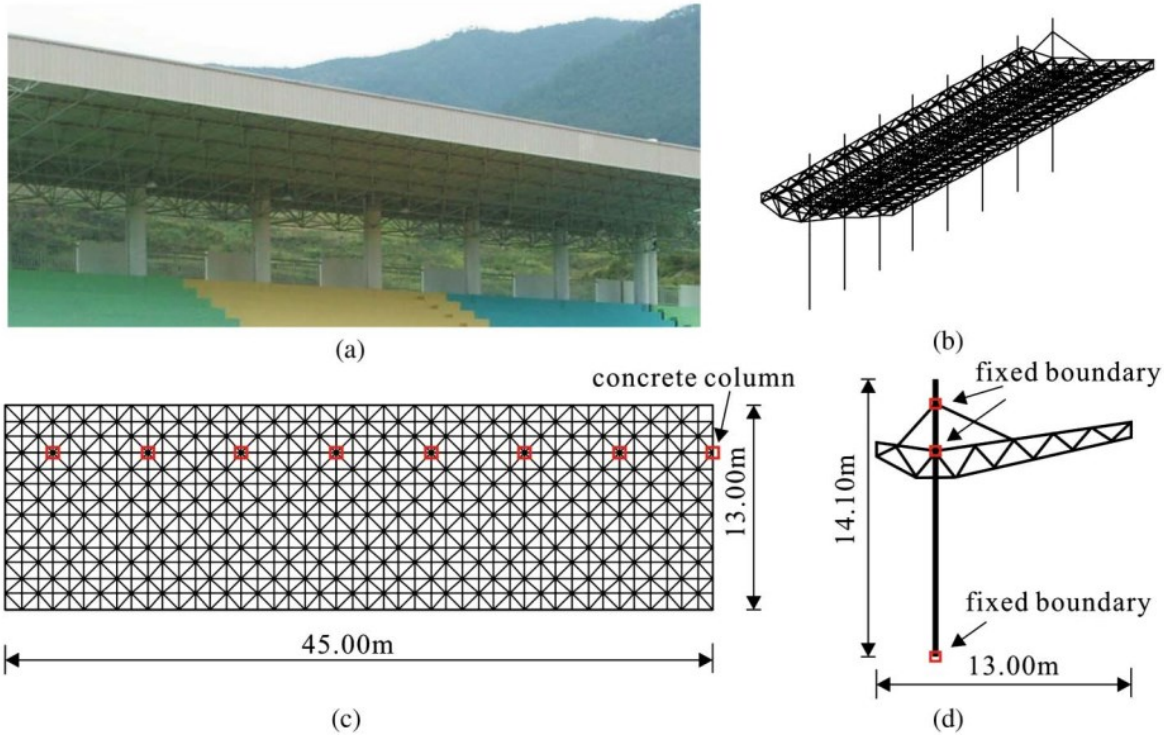

Figure 1.5 – Cantilever-framed structure: (a) structure in use (Image by Y. Yu); (b) axisymmetric view; (c) plane view; (d) vertical view. Adapted from [6]

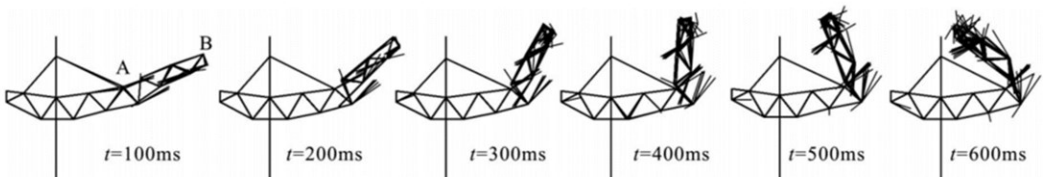

Figure 1.6 – Vertical view of cantilever structure failure process. Adapted from [6].

1.4.2.1 Particle definition

The bodies specified in the VFIFE method correspond in the Finite Particle Method to mass points, the particles. The particles are connected by rods, and the motion of the particles follows Newton's second law. The rod element, which has no mass, connects these particles with point values, and all internal forces and external forces are added to the particles. Equilibrium is instead enforced on each particle, resulting in the internal nodal force and external force being balanced continuously. Figure 1.7 presents the FPM model of a planar frame [36].

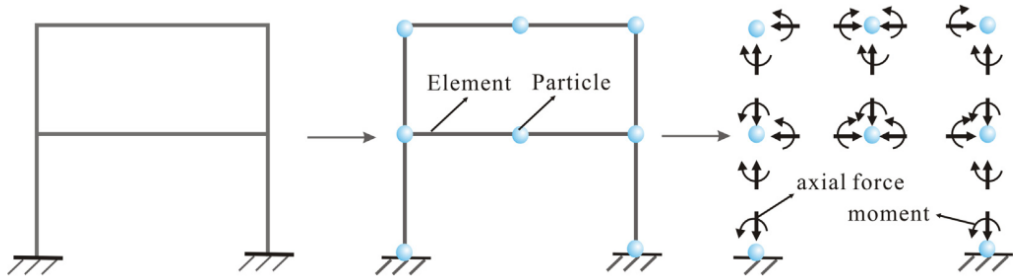

Figure 1.7 – FPM model of a planar frame. Adapted from [36].

1.4.2.2 Modeling material nonlinearity

The particle motion equation is the same for nonlinear materials and linear ones as well. Therefore, the only difference between linear and nonlinear constitutive models in the FPM is how the internal force of each particle is calculated, according to Newton's second law [6][35]. If a nonlinear constitutive model $\sigma = \mathrm{E}(\varepsilon)$ is considered, the only extra task is that of recording the loading-unloading state of the rod element at each time-step.

1.5 Overview and objectives

The objective of this project is to develop an interactive software that supports learning the fundamentals of structural engineering and space trusses. The developed software should have some features commonly found in advanced structural analysis software, but at the same time, be user-friendly and didactic. Thus, one possible approach for the development of this tool is to use the concepts of game engines and physics engines. Moreover, it can provide real-time simulation feedback about structural performance, including internal forces and reactions, to the users [37]. Another advantage of this approach is that it handles kinematically indeterminate structures as well as determinate ones. This feature can be used to instantly see the effect of removing bars and changing nodal constraints during the simulation; allowing even to analyze the instant when the structure becomes a mechanism.

This work is inspired by the work of Martini [38], which was followed by the works of Lopes [39] and Matos [40]. In the project developed by Lopes, a physics engine was written to solve 2D truss problems. Lopes successfully applied the fundamentals of particle system dynamics described by Witkin and Baraff [41][42]. The physics engine was combined with an interactive graphical interface developed in PyGame [14], allowing to explore some of the advantages of the presented approach. In the project

developed by Matos, Lopes' physics engine was extended to 2D frame structure problems. Matos implemented also an adaptation of the Kinetic Damping approach inspired by the approach presented by Michael R. Barnes in [43].

The PSA3D physics engine was written from scratch in Python and was combined with a developed graphics rendering middleware – our graphics rendering engine (GRE), created using the Panda3D game engine [44]. The result of this combination is the game engine named 3DParticleSystem software presented in this work, as summarized in Figure 1.8. The developed software gives the user a unique game-like interaction environment where structural models respond to input in real-time.

The developed Graphical User Interface (GUI) has great importance in the developed work since the real-time visualization, the usability of the software, the rendering quality of the structures and the quality of the results are all very important for understanding the physical phenomena. To this end, the code is optimized to follow Python best practices and advice from Python experts, while respecting the object--oriented programming paradigms. Subsequently, the 3DParticleSystem software results are validated and compared against exact solutions (when available) or results obtained with other programs. The project focuses on two cross-platform frameworks, PyQt [45] and Panda3D [44]. The first is related to the user interface (UI), the second is related to the 3D computer graphics and the canvas.

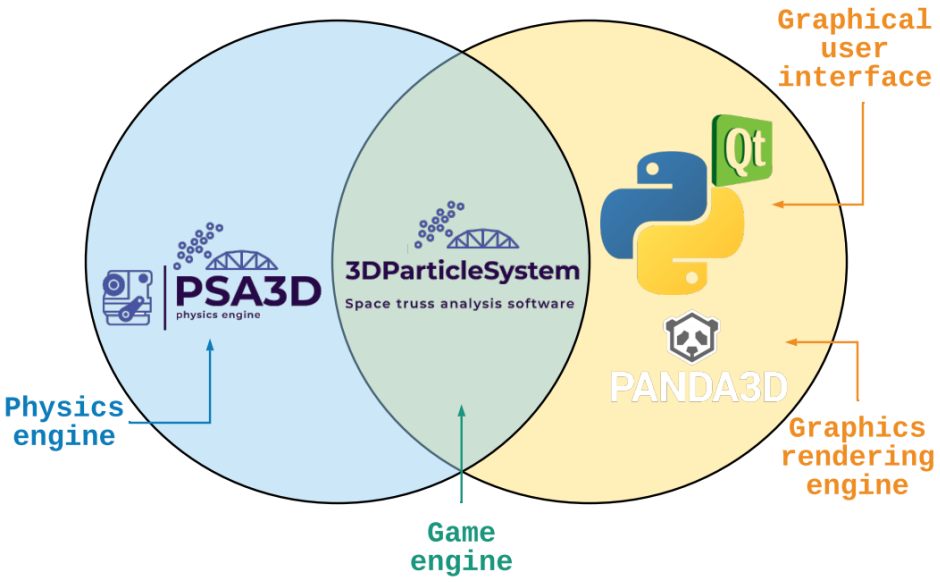

Figure 1.8 – The 3DParticleSystem software Venn diagram.

The developed game engine is applied to express the numerical methods, with emphasis on solving the equations of motion. This approach, as said above, may have some advantages over other numerical methods such as the Finite Element Method (FEM), but it also presents some challenges, such as setting the stopping criterion and the parameters for numerical integration, among others. These will be discussed later

Despite using the game engine concept, the purpose of this work is not to develop a game. Instead, it is intended to benefit from the interaction of games to get all the practical advantages these can give.

There is also an attempt to design a software that resembles others used in civil engineering courses, namely, FTOOL [46], ADINA [47], and SAP2000 [48]. Thus, when using the developed software, the user is getting used to the interface and usability of advanced structural analysis software.

The tasks carried out during this work are summarized in chronological order:

a) Review of particle system dynamics;
b) Development of a physics engine and its validation with 2D truss problems;
c) Development of a Graphical User Interface and a 3D graphical environment;
d) Extension of the numerical approach to 3D problems.

1.6 Document outline

The following list describes the contents to be discussed in each of the chapters of this thesis, from a state-of-the-art literature review to the conclusions drawn from the study. This document is divided into five parts: Introduction, Particle System Approach 3D (The Physics Engine), the 3DParticleSystem Software, Modelling, and Conclusions.

The first part, Introduction, includes the problem statement and critical literature review for the subject under analysis in this thesis.

Chapter 2 – “Particle System Approach 3D (The Physics Engine)” – This chapter contains the description of the developed physics engine. It reviews bar models and fundamental concepts of structural mechanics, including the mechanical behavior of materials. In addition, this chapter contains an overview of the work related to particle system dynamics tools. Then the developed physics engine numerical approach is presented, followed by a review of numerical integration of the equations of motion. Therefore, all steps for the correct implementation of this approach are presented.

Chapter 3 – “The 3DParticleSystem Software” – A computer-aided design software was developed from scratch. Thus, this chapter explains some programming approaches to overcome the technical difficulties faced but without going into much detail on object-oriented programming (OOP) in Python. The fundamental concepts of the implemented procedure are presented on the perspective of a programmer used to the OOP paradigm.

Chapter 4 – “Modeling” – This chapter is about modeling and is divided into two distinct parts. This chapter begins by presenting the numerical results of Approach 1 and 2 of the PSA3D physics engine, which are then compared with ADINA results. Finally, this chapter presents several features of the 3DParticleSystem software, useful in learning fundamental structural engineering concepts.

Chapter 5 – “Conclusions” – This chapter gives an overview of the achievements, along with advantages and disadvantages of the implemented approach. Finally, it discusses some directions for future work.

2 Particle System Approach 3D (The Physics Engine)

This chapter presents the basic theoretical aspects related to the physics engine, together with its implementation and can be summarized in:

- Presentation of the PSA3D physics engine
- Mechanical behavior of materials,
- The fundamentals of particle system dynamics,
- Numerical implementation of Particle System Approach 3D – physics engine,
- The stopping criterion is set.

The PSA3D physics engine, Particle System Approach 3D physics engine (PE), is a 3D physics engine library written from scratch in Python for structural engineering applications. It is based on particle system dynamics, which is a physically-based particle model that follows the laws of classical mechanics. It is designed to solve trusses, from simple 2D trusses to complex 3D truss structures composed by materials with linear and nonlinear behaviors and different stress and strain behaviors: such as elastic and elastic-plastic behaviors. The PSA3D works without having a graphical component, being the results written in the python console.

There are some open source physics engines that implement the particle system dynamics for a similar purpose. Of these, there are two that stand out, ofxMSAPhysics in C ++ [49] and TRAER.PHYSICS 3.0 in Java [50].

2.1 Mechanical behavior of materials

The first step to create the PSA3D physics engine was to implement the mechanical behavior of the materials. As a fundamental engineering theme, solid mechanics is the branch of continuum mechanics that studies the behavior of solid materials when subjected to loads. This topic allows us to describe the behavior of materials as simple laws that can be written as mathematical models, for example, describing the behavior of solid material when subjected to an external load. These laws are commonly known as constitutive laws or equations, and the simplest relationships characterize materials as having elastic, plastic, or elastic-plastic behavior, among others. Compressive and tensile strength tests are generally used to describe the constitutive equations of engineering materials.

2.1.1 Stress and strain

In teaching the fundamental concepts of mechanical behavior of materials in civil engineering, the materials that come to mind are concrete and steel. Concrete resists far better to compressive stresses than to tensile stresses, whereas steel is indifferent to the type of stress it is subjected to. The combination of these two structural materials results in reinforced concrete, which takes advantage of the good behavior of concrete under compression, leaving the task of resisting tensile stresses mainly to the steel. To describe the behavior of these materials, compressive and tensile strength tests are performed.

Taking the simplest case of a thin bar or rod, its normal strain ε can be defined as the elongation per unit length of the bar [51]. Thus, this quantity corresponds to the change in length divided by the original length. It is dimensionless and can be defined as:

$$\varepsilon = \frac{l - l_0}{l_0} = \frac{\delta}{l_0} \tag{1}$$

where ε is the strain at a given point, δ is the elongation or extension of the gauge length, l_0 is the initial length, and l is the length of the rod after load P is applied.

The normal stress is defined as force per unit area and can be described as:

$$\sigma = \frac{P}{A_0} \tag{2}$$

where σ is the stress at a given point, P is the applied force, and A_0 is the original cross-sectional area of the specimen/bar.

Tensile tests are applied to determine the behavior of materials subject to axial tensile load. These tests are performed by fixing the specimen (a bar) on the test apparatus and applying a force to the specimen separating the sleepers from the test machine [52]. By doing this, tensile tests determine how strong a material is and how much it can elongate.

On the other hand, compression tests are applied to determine the behavior of materials subject to axial compressive load. Compression tests are performed by loading the sample between two plates and applying a force to the sample by approaching the crossheads [52].

The relationship between stress and strain can be described as a stress-strain curve. Figure 2.1 shows, on the left, a typical result of a tensile strength test. On the right, it shows a typical stress-strain curve for a compressive strength test.

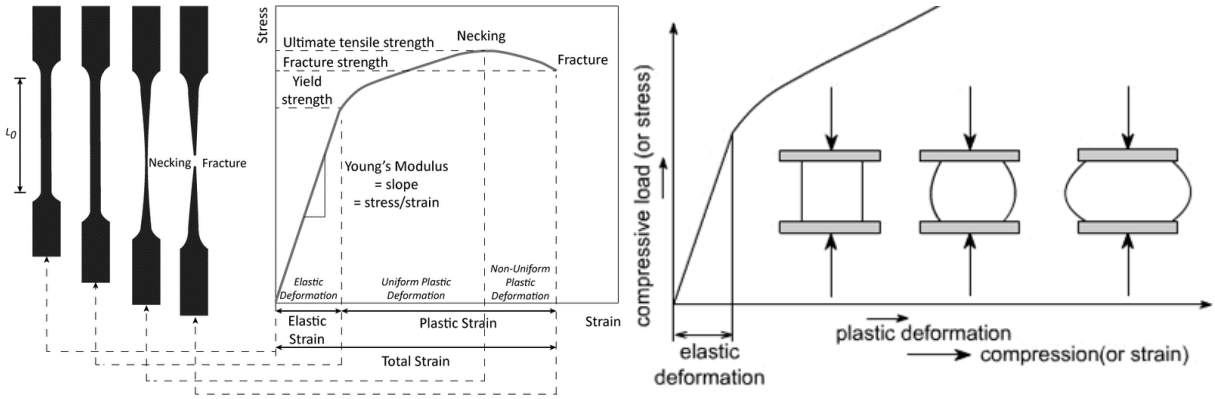

Figure 2.1 – Stress-strain curves. Typical ductile steel tensile test, on the left (adapted from [90]). Compressive strength test, on the right (adapted from [91]).

2.1.2 Elastic behavior

Elastic behavior is a reversible stress/strain behavior, which means that materials undergoing deformation when subjected to loads return to their undeformed shape after the loads are removed, [53]. This reversible behavior may either be linear or nonlinear. The elastic behavior can be either linear elastic or nonlinear elastic.

A rod made of elastic material may be described as an ideally elastic spring and uniaxial Hooke's law states that for small deformations, the relationship between the stress and the strain can be expressed as:

$$\sigma = \mathrm{E} \cdot \varepsilon \tag{3}$$

where σ is the stress (uniaxial force per surface), E is the Young's modulus, also referred to as the modulus of elasticity, and ε is the strain.

Not all materials behave elastically. Therefore, it is necessary to understand the differences between an elastic material, a plastic material, and an elastic-plastic material.

2.1.3 Elastic-plastic behavior

The plasticity of a material can be described as its ability to undergo some permanent deformation without rupture. Generally, plastic behavior is conveniently simplified using idealized models. The most common models are the elastic-perfectly plastic model and the bilinear hardening model [54][55].

The elastic-perfectly plastic model results from the combination in series of elastic and plastic behavior. On the other hand, the bilinear hardening model assumes linear elastic behavior up to the yield limit. Beyond the yield limit, the material exhibits linear plastic deformation. In both cases, the linear strain tensor can be split additively into elastic ε_{e} and plastic ε_{p} parts [56]. Then, the total unit strain can be expressed as:

$$\varepsilon = \varepsilon_p + \varepsilon_e \tag{4}$$

Recovering the result from Equation (3), the elastic strain in a material is linearly proportional to the stress:

$$\sigma = E \cdot \varepsilon_e \rightarrow \varepsilon_e = \frac{\sigma}{E}. \tag{5}$$

Then, the plastic strain can be calculated from the total strain as:

$$\varepsilon_p = \varepsilon - \varepsilon_e = \varepsilon - \frac{\sigma}{E} \tag{6}$$

Figure 2.2 presents the symbolic one-dimensional models for a better understanding of this idealized model. On the left, it presents the elastic-perfectly plastic solid with the yield limit Fy; on the right, the elastic-plastic body with linear strain hardening.

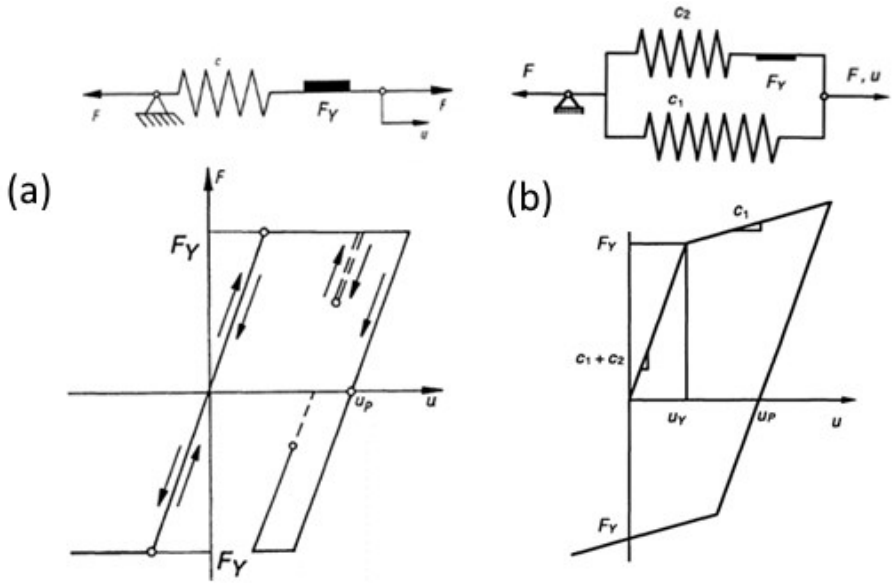

Figure 2.2 – Symbolic one-dimensional models: (a) The elastic-perfectly plastic solid with the yield limit Fy. (b) The elastic-plastic body with linear strain hardening. Adapted from [92].

2.2 Particle System Dynamics

The fundamentals of particle system dynamics (PS) were described by Witkin and Baraff, both from Pixar Animation Studios, in [41][42], and are commonly used in physics-based animation [15]. The PS is a particle-based approach where each particle carries properties such as mass, density, force, and velocity.

Particles may be linked to other particles by means of massless springs (in the case being treated here, mostly elastic truss members) that are in static equilibrium during motion. The forces acting on a particle may be external forces (loads) or internal forces. The internal forces are due to the deformations of members/springs connected to the particle. In this approach, the differential equations of motion of a collection of particles are solved using a time-step simulation.

The main disadvantage of the PS approach is the computational cost as it requires significantly more computational resources than conventional structural analysis [57]. The PS approach for three--dimensional structural models requires an even larger number of iterations. On the other hand, a particle-based method differs from the conventional structural analysis since it does not form a global stiffness matrix [5][57]. Instead, it enforces the equilibrium at each particle, at each step, making the internal nodal force and external force always balanced, enabling new types of analysis such as modeling unstable structures/mechanisms, also being suitable for modeling nonlinearities and discontinuities [6]. A good example of the capabilities of the Particle System approach may be seen in Arcade [21], a two-dimensional implementation developed by Kirk Martini.

In the following example, a complex space truss structure is discretized into simple objects, such as particles and rods. Then, the rods are represented by their equivalent internal forces.

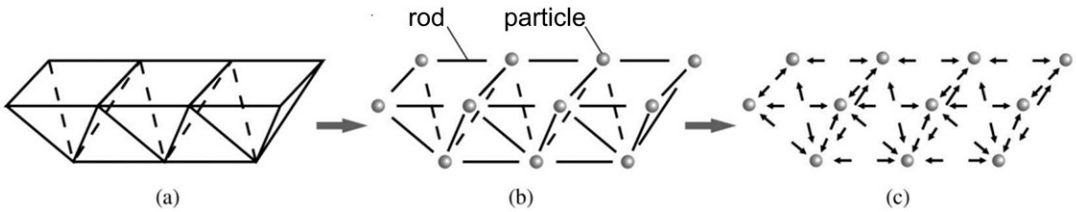

Figure 2.3 – (a) space truss structure; (b) discretization of the structure by particles and elements; (c) particles and forces. Adapted from [6].

2.2.1 Newton's second law

This chapter discusses the forces applied to the particles and how they affect their motion. The basic issue in dynamics problems is solving the fundamental equation of dynamics, also known as Newton's second law. First, to establish a consistent reading with recent literature, the notation used here is that presented in [6] by Ying Yu. Thus, the motion of an arbitrary particle i follows Newton's second law and can be expressed as:

$$m_i \ddot{x}_i = F_i^{ext} + F_i^{int} = F_i^{unb} \tag{7}$$

where $\mathrm{m_i}$ is the mass of particle i; x_i is the displacement vector; $\ddot{x}_i$ is the acceleration vector. $\mathrm{F}_i^{\mathrm{ext}}$, $\mathrm{F}_i^{\mathrm{int}}$, and $\mathrm{F}_i^{\mathrm{unb}}$ are the external force, internal nodal force, and unbalanced force, respectively.

The forces acting on a particle of a space rigid truss is shown in Figure 2.4.

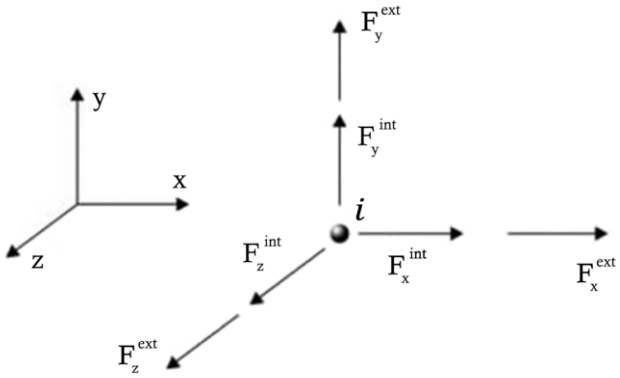

Figure 2.4 – Forces acting on a particle of a rigid space truss. Adapted from [30].

The unbalanced force corresponds to the sum of the applied load with the forces of the rods meeting at particle i, latter decomposed at each direction. After adding the support reaction contribution, the unbalanced force is given by:

$$F_i^{\mathrm{unb}} = \mathrm{F}_i^{\mathrm{ext}} + \mathrm{F}_i^{\mathrm{int}} + \mathrm{F}_i^{\mathrm{reaction}} \tag{8}$$

Equation (7) can also be written as:

$$m_i \begin{bmatrix} \ddot{x}_{i,x} \\ \ddot{x}_{i,y} \\ \ddot{x}_{i,z} \end{bmatrix} = \begin{bmatrix} F_{i,x}^{ext} \\ F_{i,y}^{ext} \\ F_{i,z}^{ext} \end{bmatrix} + \begin{bmatrix} F_{i,x}^{int} \\ F_{i,y}^{int} \\ F_{i,z}^{int} \end{bmatrix} + \begin{bmatrix} F_{i,x}^{reaction} \\ F_{i,y}^{reaction} \\ F_{i,z}^{reaction} \end{bmatrix} = \begin{bmatrix} F_{i,x}^{unb} \\ F_{i,y}^{unb} \\ F_{i,z}^{unb} \end{bmatrix} \tag{9}$$

2.2.2 Particle definition and particle mass

The structure is divided into a set of particles as in Figure 2.3. The mass of the structure, that is the mass of the rods/bars composing the structure, is divided proportionally between the particles, and these can simulate the characteristics of the structure. The particles have mass and are connected by massless rod elements. The mass of each rod element $\mathrm{m_{rod}}$ is equally divided between the particles defines the rod and this contribution is defined as an equivalent mass $\mathrm{m_\alpha}$. Thus, the mass of a given particle i is defined as:

$$\mathrm{m_i} = \sum_{\alpha=1}^{\mathrm{n}} \mathrm{m_\alpha} \tag{10}$$

$$\mathrm{m_\alpha} = 0.5 \cdot \mathrm{m_{rod}} \; ; \; \mathrm{m_{rod}} = \lambda \cdot \mathrm{L} \tag{11}$$

where n is the number of rods connected to the particle i, $\mathrm{m_\alpha}$ is the mass contributed from each rod element and assigned to particle i. Moreover, λ is the mass per unit length of the rod element, and L is the length of the rod element.

2.2.3 Local deformation coordinate system of a space rod element

The positive and the negative convention of the local coordinate system is set according to the space rod unit vector. The figures below show three rods (rod1, rod2 and rod3) connected by three nodes (A, B and C). On the left, it shows the positive sign convention. On the right, it shows the negative sign convention.

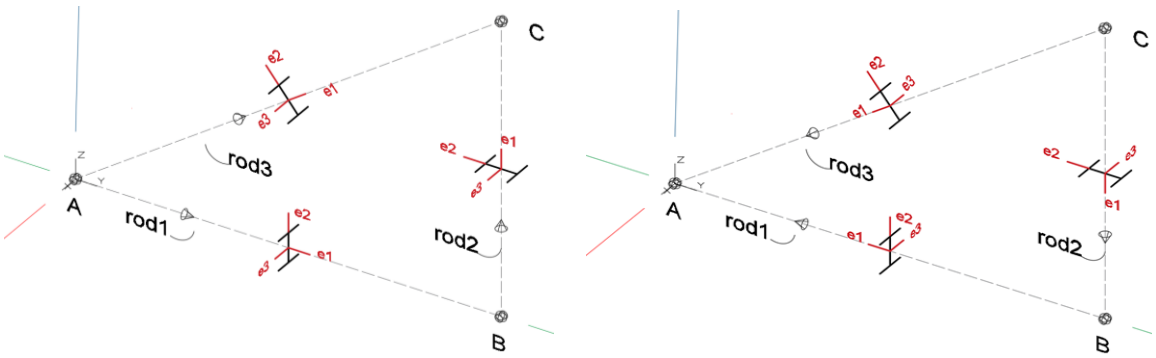

Figure 2.5 – The local coordinate system of space rod – positive sign convention (left) and negative sign convention (right).

For a generic 3D rod, connected by two nodes, M and N, the vector $\mathrm{e_1}$ is the normalized vector that defines the rod and can be calculated with Equation (12). Then, to find the next orthogonal component, an auxiliary vector $\mathrm{e_{1'}}$ should be calculated. Thus, if $\mathrm{e_{1z}} \neq 0$, this vector may be the projection of the vector $\mathrm{e_1}$ in the $\mathrm{X0Y}$ plane ($\mathrm{z} = 0$). Otherwise, it corresponds to $\overrightarrow{\mathrm{e_{1'}}} = [0\,,0\,,1]$. Next, the vector $\mathrm{e_{3'}}$ is given by the normalized cross product between $\mathrm{e_{1'}}$ and $\mathrm{e_1}$, as follows in Equation (15).

$$\overrightarrow{e_1} = \frac{\overrightarrow{MN}}{\left\|\overrightarrow{MN}\right\|} = \left[e_{1x} \;\; e_{1y} \;\; e_{1z}\right] \tag{12}$$

$$\overrightarrow{e_{1'}} = \left[e_{1x} \;\; e_{1y} \;\; 0\right], if \;\; e_{1z} \neq 0 \tag{13}$$

$$\overrightarrow{e_{1'}} = [\,0\;0\;1], if\;\; e_{1z} = 0 \tag{14}$$

$$\overrightarrow{e_{3'}} = \frac{\overrightarrow{e_{1'}} \times \overrightarrow{e_1}}{\|\overrightarrow{e_{1'}} \times \overrightarrow{e_1}\|} \tag{15}$$

Then, another auxiliary vector $\mathrm{e}_{2'}$ is calculated as the cross product between e'_3 and e_1:

$$\overrightarrow{e_{2'}} = (\overrightarrow{e_{3'}} \times \overrightarrow{e_1}) = \left[e_{2'x}\;\; e_{2'y}\;\; e_{2'z}\right]. \tag{16}$$

To calculate vector $\overrightarrow{\mathrm{e}_2}$ there are two cases: the first case is when $\mathrm{e}_{2'_\mathrm{z}}$ is equal to zero, where the positive direction of $\overrightarrow{\mathrm{e}_2}$ corresponds to the unit vector in the negative y-direction ($\overrightarrow{\mathrm{e}_2} = [\,0, -1, 0]$), as shown in Figure 2.5 with rod2. The second case is when $\mathrm{e}_{2'\mathrm{z}}$ is nonzero ($\mathrm{e}_{2'\mathrm{z}} \neq 0$), where the positive direction of $\overrightarrow{\mathrm{e}_2}$ is always the direction of gravity, as shown in Figure 2.5 with rod1 and rod3. Then, to ensure this established convention, e_2 is given by correcting vector $\mathrm{e}_{2'}$ with the following conditions:

$$sgn = -1, if\; e_{2y} < 0, \tag{17}$$

$$sgn = -1, if\; e_{2y} \geq 0, \tag{18}$$

$$\overrightarrow{e_2} = sgn \cdot \overrightarrow{e_{2'}} = \left[e_{2x}\;\; e_{2y}\;\; e_{2z}\right]. \tag{19}$$

Finally, vector e_2 corresponds to the cross product between e_3 and e_1 and can be expressed as

$$\overrightarrow{e_3} = \overrightarrow{e_1} \times \overrightarrow{e_2} = \left[e_{3x}\;\; e_{3y}\;\; e_{3z}\right]. \tag{20}$$

The relationship between the local coordinates and the global coordinates is described as:

$$\widehat{\mathrm{X}} = \mathrm{TX} \tag{21}$$

$$T = \begin{bmatrix} \overrightarrow{e_1} \\ \overrightarrow{e_2} \\ \overrightarrow{e_3} \end{bmatrix} = \begin{bmatrix} e_{1x} & e_{1y} & e_{1z} \\ e_{2x} & e_{2y} & e_{2z} \\ e_{3x} & e_{3y} & e_{3z} \end{bmatrix} \tag{22}$$

where $\widehat{\mathrm{X}}^{\mathrm{T}} = (\mathrm{x}_1, \mathrm{x}_2, \mathrm{x}_3\,)$ corresponds to the local coordinates, $\mathrm{X}^{\mathrm{T}} = (x, \mathrm{y}, \mathrm{z})$ to the global coordinates, and T is the transformation matrix described in Equation (22).

2.2.4 Calculation of the internal nodal forces

In this work, two approaches are presented to calculate internal nodal force: one considering small displacements and another considering large displacements.

2.2.4.1 Small Displacements

Recalling Hooke's law for linear springs, the force is linearly proportional to the amount of elongation/deformation (from the rest length) and acts in the opposite direction to the deformation. Thus, the internal force in a given 3D rod k, connecting particles 1 and 2, can be written as in Equation (23): [6][41].

$$f^{int}_{k,local\;axis} = \varepsilon_{n+1} \cdot EA;\;\; \varepsilon_{n+1} = \frac{L_{n+1} - r}{r} \tag{23}$$

$$L_{n+1} = \|X_{2'} - X_{1'}\|\;;\;\; r = \|X_2 - X_1\| \tag{24}$$

where r is the rest length of rod k. $\mathrm{L_{n+1}}$ and $\varepsilon_{\mathrm{n+1}}$ are the length and strain at the given time, respectively. E is the Young's modulus, and A is the cross-sectional area of rod k.

Figure 2.6 shows the initial configuration and the current configuration used to calculate the deformation.

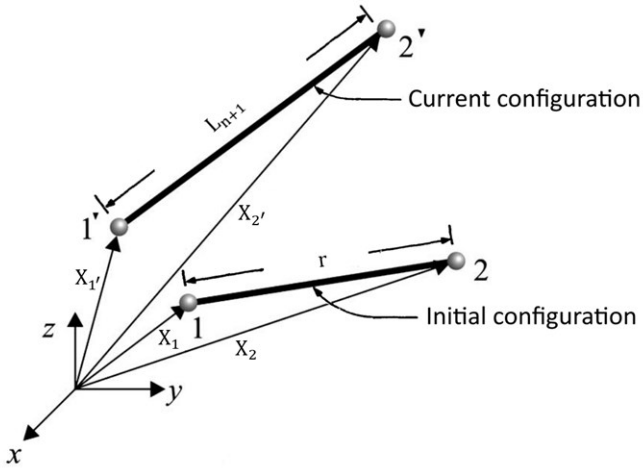

Figure 2.6 – A simple rod element with its initial and current configuration.

2.2.4.2 Large Displacements

Large displacements analysis can be achieved by using the approach described in [6][35][33], in which Yu Yung presents the Finite Particle Method, suitable for modeling geometric nonlinearity behavior.

Figure 2.7 shows the process in which the fictitious motion is illustrated: firstly, it removes the rigid body motion of rod k; then, the axial force of each particle are calculated, taking into account the geometric nonlinearity. This process assumes a reversed motion, from $1'2'$ to 12, and then a forward motion.

The reversed motion starts with a fictitious position at the time $\mathrm{t_b}$ (a). The first step is a fictitious reversed translation $(-\Delta \mathrm{x_1})$ (b); which is followed by a fictitious reversed rotation $(-\Delta\theta)$ (c), and then it calculates the deformed shape in time $\mathrm{t_a}$ (d). The forward motion starts with a known shape at time $\mathrm{t_a}$ and can be summarized as a rotation $(\Delta\theta)$ (e) and a translation $(\Delta \mathrm{x_1})$ (f). In this process, only the direction of the rod axial force is changed.

The axial force in rod k can be written as:

$$f^{\mathrm{int}}_{\mathrm{k,local\ axis}} = f_{\mathrm{n+1}} = f_{\mathrm{n}} + \Delta f_{\mathrm{n}} = \left(\sigma_{\mathrm{n}} \mathrm{A_n} + \frac{\mathrm{E_n A_n}}{\mathrm{L_n}} \Delta \mathrm{L}\right) \mathrm{e}_{1'2'} \tag{25}$$

where f_{n} is the axial force of rod k at time t_{a}; Δf_{n} is the incremental axial force of rod k at time t_b; σ_n is the axial stress at time $\mathrm{t_a}$; $\mathrm{A_n}$ is the cross-sectional area of rod k; E_n is the Young's modulus; $\Delta \mathrm{L}$ is length variations of rod k between time t_a and $\mathrm{t_b}$; L_{n} is the length of rod k at time $\mathrm{t_a}$; $\mathrm{e}_{1'2'}$ is the directional vector of rod k at time t_b.

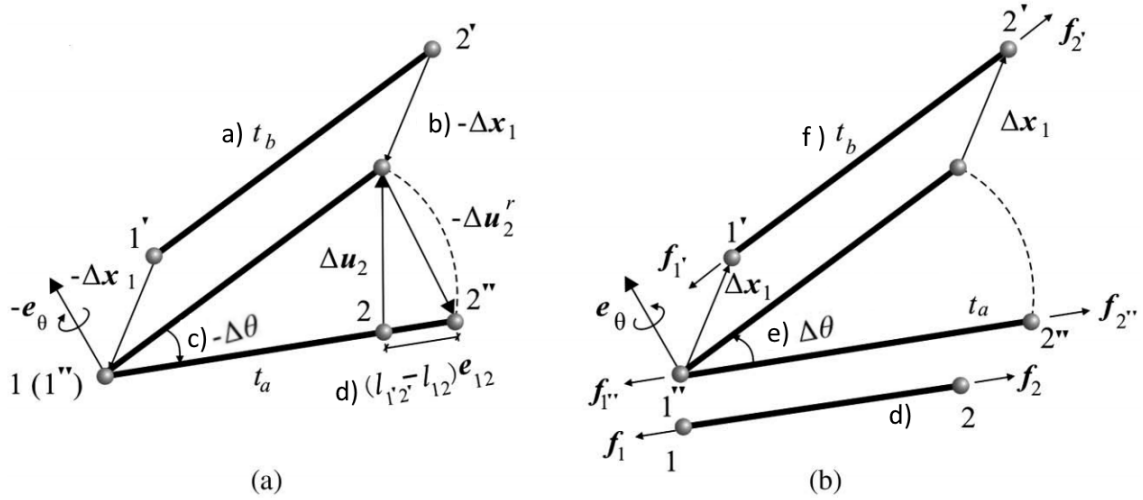

Figure 2.7 – (a) Reversed motion. (b) Forward motion. Adapted from [6].

2.2.4.3 Internal nodal force

The rod's internal forces can be transformed from principal axes to the global axis with the following linear transformation:

$$f_k^{int} = T^T f_{k,local\ axis}^{int} = \left[f_{k,x}^{int}\ f_{k,y}^{int}\ f_{k,z}^{int}\right]^T \tag{26}$$

The relationship between the rod's internal forces and the forces acting on each particle is given by the particle 1 (linked to the beginning of the rod) receiving the force $f_{\mathrm{k}}^{\mathrm{int}}$ and particle 2 (at the end of the rod) receiving the same force in the opposite direction, according to the static equilibrium condition [35]. Then, it can be stored in a 1x6 vector as follows:

$$f_k^{int} = \left[f_{k,1}^{int^T} \quad | \quad f_{k,2}^{int^T}\right] = \left[f_k^{int^T} \quad | \quad -f_k^{int^T}\right] \tag{27}$$

where $f_{\mathrm{k,1}}^{\mathrm{int}^T} = f_{\mathrm{k}}^{\mathrm{int}^{\mathrm{T}}}$ and $f_{\mathrm{k,2}}^{\mathrm{int}^T} = -f_{\mathrm{k}}^{\mathrm{int}^{\mathrm{T}}}$ are the forces at 1 and 2, respectively.

Finally, the internal nodal force of the particle i can be identified by the summation of the internal/axial forces from all rods connected to it and can be given as follows in Equation (28).

$$F_i^{int} = \begin{bmatrix} F_{i,x}^{int} \\ F_{i,y}^{int} \\ F_{i,z}^{int} \end{bmatrix} = \begin{bmatrix} f_{1,x}^{int} \\ f_{1,y}^{int} \\ f_{1,z}^{int} \end{bmatrix} + \cdots + \begin{bmatrix} f_{n,x}^{int} \\ f_{n,y}^{int} \\ f_{n,z}^{int} \end{bmatrix} = \sum_{k=1}^{n} \left(\begin{bmatrix} f_{k,x}^{int} \\ f_{k,y}^{int} \\ f_{k,z}^{int} \end{bmatrix} \right) \tag{28}$$

where $\mathrm{F}_{\mathrm{i}}^{\mathrm{int}}$ is the internal nodal force acting on the particle i, f_k is the equivalent internal forces provided by rod k connected to particle i, and n is the number of rods connected to particle i.

2.2.5 Convergence and stability

The main idea of this approach is to "follow" the particle motion caused by the unbalanced forces. The information regarding the position, velocity, and acceleration of each particle are calculated iteratively [5]. The system converges to an equilibrium position around which it oscillates and eventually stabilizes when the unbalanced forces become very small/zero. Convergence is usually achieved by damping the nodal movements using artificial viscous damping [41] or considering a form of kinetic energy damping [43].

2.2.5.1 Particle System Approach

In the Particle System approach (PS), the axial force in each rod results by adding the rod's damping forces with its internal forces. The rod's damping force, also described as the ideal viscous drag in Witkin's notation [41], can be considered as a way of extracting energy from the system to bring it to rest. The damping coefficient, c, only affects how convergence is achieved. However, it must be chosen to avoid slow convergence due to either over or under damping. The rod's damping force depends on the relative velocities between the particles and can be expressed as:

$$f^{dmp}_{k,local\ axis} = c \cdot \Delta v_{local\ axis} = c \cdot (v_{2,local} - v_{1,local}) \tag{29}$$

where c is the damping coefficient, $v_{\mu,local}$ is the velocity on the local axis of edge μ linking nodes 1 and 2.

Rewriting the equation by using matrix notation, this amount is given by:

$$f^{dmp}_{k,local\ axis} = c \cdot A\,T(v_2 - v_1) \tag{30}$$

$$A = \begin{bmatrix} 1 & 0 & 0 \\ 0 & 0 & 0 \\ 0 & 0 & 0 \end{bmatrix}, T = \begin{bmatrix} \overrightarrow{e_1} \\ \overrightarrow{e_2} \\ \overrightarrow{e_3} \end{bmatrix} = \begin{bmatrix} e_{1x} & e_{1y} & e_{1z} \\ e_{2x} & e_{2y} & e_{2z} \\ e_{3x} & e_{3y} & e_{3z} \end{bmatrix}, v_\mu = \begin{bmatrix} v_{x,\mu} \\ v_{y,\mu} \\ v_{z,\mu} \end{bmatrix} \tag{31}$$

where v_μ is the velocity at end μ on the global axis, given by $v_{\mu,local} = T\,v_\mu$.

In this approach, the axial force of rod k can be written as:

$$f^{axial}_{k,local\ axis} = f^{int}_{k,local\ axis} + f^{dmp}_{k,local\ axis} = EA \cdot \varepsilon + f^{dmp}_{k,local\ axis} \tag{32}$$

where $f^{axial}_{k,local\ axis}$ is the resulting internal force. $f^{int}_{k,local\ axis}$ is the internal force given by Equation (23) and $f^{dmp}_{k,local\ axis}$ is the damping force.

The axial force evaluated in Equation (32) must be calculated on the global axis and stored as presented in equations (27) and (28). This amount will then be transmitted to each particle as internal nodal forces.

2.2.5.2 Kinetic Damping approach

Kinetic Damping approach is usually associated with the Dynamic Relaxation (DR) method. A detailed overview of this approach can be found in “Form Finding and Analysis of Tension Structures by Dynamic Relaxation” by Michael R. Barnes [43]. The DR method has been used in many works, such as, “Fictitious Time Step for the Kinetic Dynamic Relaxation Method” [58]. Kinetic damping involves tracking the kinetic energy of the system and setting the velocities of the particles to zero whenever a maximum is detected (see [43]). Kinetic damping is based on the fact that, for a system made of masses in harmonic motion, maximum kinetic energy corresponds to the minimum potential energy. The iterative application of kinetic damping gradually brings the system to the stable equilibrium configuration [5].

This method can be divided into two stages: the first stage consists of solving the equation of motion. The second stage consists of correcting the positions of all the particles whenever a peak of kinetic energy occurs.

2.2.5.2.1 Stage 1 – Numerical integration

Newton's second law dictates the motion of particle i in direction x at time t:

$$F_i^{unb} = m_i \dot{v}_i^n \tag{33}$$

Considering a small time step, Δt, the acceleration at mid-interval (time t), $\dot{v}_i^n$, can be approximated in centered finite difference form ([43]) as:

$$\dot{v}_i^n = \frac{v_i^{n+\frac{1}{2}} - v_i^{n-\frac{1}{2}}}{\Delta t} \tag{34}$$

The velocity at time $t + \frac{\Delta t}{2}$ can be then calculated from the previous equation as:

$$v_i^{n+\frac{1}{2}} = v_i^{n-\frac{1}{2}} + \Delta t \cdot \dot{v}_i^n \tag{35}$$

Replacing Equation (33) in Equation (35), the velocity at time $t + \frac{\Delta t}{2}$ is given by:

$$v_i^{n+\frac{1}{2}} = v_i^{n-\frac{1}{2}} + \Delta t \cdot \frac{F_i^{unb}}{m_i} \tag{36}$$

The variation of the coordinates is then reconstructed and, by simply adding this difference to the previous position, the new coordinates become:

$$x_i^{n+1} = x_i^n + \Delta t \cdot v_i^{n+\frac{1}{2}} \tag{37}$$

Thus, the first stage is composed of Equation (36) and Equation (37), which allows us to compute the velocities and positions of the particles.

2.2.5.2.2 Stage 2 – Kinetic Damping approach

Generally, the kinetic energy of undamped oscillations of the structure is traced when a peak in the total kinetic energy of the system is detected; consequently, all velocities are set to zero. The kinetic energy of the whole structure is calculated as follows in [58] and can be written as:

$$K^{n+1} = \frac{1}{2}\sum_{i=1}^{q} m_i \left(v_i^{n+\frac{1}{2}}\right)^2 \tag{38}$$

where K^{n+1} is the kinetic energy of the system of particles. m_i is the mass of particle i. $v_i^{n+\frac{1}{2}}$ is the velocity of particle i and q is the number of particles.

In Kinetic Damping approach formulation, a decrease of the kinetic energy indicates that a peak has been passed [43][58]. At this time, the stored coordinates are x_i^{n+1}, as represented in the figure below. For simplification, it is assumed that the kinetic energy attains its peak at $t - \frac{\Delta t}{2}$. All particles coordinates must be then recalculated/restarted at this peak instant.

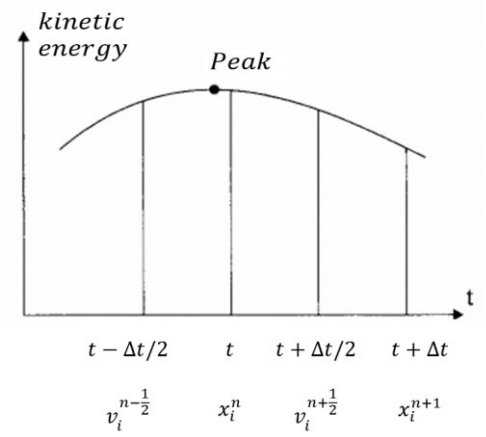

Figure 2.8 – The trace of a typical kinetic energy peak. Adapted from [93].

The coordinate at time $t - \frac{\Delta t}{2}$ can be given by subtracting this difference from the previous position. Thus, the coordinate backward returns to:

$$x_i^{n-\frac{1}{2}} = x_i^n - \frac{\Delta t}{2} v_i^{n-\frac{1}{2}} \tag{39}$$

By reorganizing Equation (37), the previous position can be given as follows:

$$x_i^n = x_i^{n+1} - \Delta t\, v_i^{n+\frac{1}{2}} \tag{40}$$

Replacing Equation (40) in Equation (39):

$$x_i^{n-\frac{1}{2}} = \left(x_i^{n+1} - \Delta t\, v_i^{n+\frac{1}{2}}\right) - \frac{\Delta t}{2} v_i^{n-\frac{1}{2}} \tag{41}$$

Finally, replacing Equation (36) in Equation (41), results:

$$x_i^{n-\frac{1}{2}} = x_i^{n+1} - \frac{3}{2}\Delta t\, v_i^{n+\frac{1}{2}} + \frac{1}{2}\cdot\frac{F_i^{unb}}{m_i}\cdot\Delta t^2 \tag{42}$$

When the analysis is restarted, the velocities must be computed at the middle point of the previous interval. Recalling that the velocity at time t is given by Equation (43), Equation (44) is obtained.

$$v_i^n = \frac{1}{2}\left(v_i^{n-\frac{1}{2}} + v_i^{n+\frac{1}{2}} \right) = 0 \tag{43}$$

$$v_i^{n-\frac{1}{2}} = -v_i^{n+\frac{1}{2}} \tag{44}$$

By exploiting Equation (44) and Equation (36), the velocity becomes:

$$v_i^{n+\frac{1}{2}} = \frac{1}{2} \cdot \frac{F_i^{unb}}{m_i} \cdot \Delta t \tag{45}$$

where all unbalanced forces, F_i^{unb}, must be evaluated at the $x_i^{n-\frac{1}{2}}$ position using Equation (42).

2.3 Numerical implementation of the PSA3D physics engine

This subchapter gives an overview of the numerical implementation of the PSA3D physics engine. It can be summarized in the Numerical method and the Numerical process.

2.3.1 Numerical method

The Numerical method is the implementation of the Particle System approach (PS), which consists of solving Newton's second law for a set of particles by numerical integration. The first step is to set the geometry by defining the list of particles and the list of rods. Then, the equivalent mass for each rod, m_α, is computed and allocated to each particle in accordance with equations (10) and (11), respectively. Then, the initial conditions and the stopping criterion are set. Finally, the Numerical process (Annex B.6.1) can occur until the stopping criterion is met, as summarized in Figure 2.9.

The Numerical process involves the list of particles and the list of rods. It can be summarized in two fundamental parts, the numerical integration of the equation of motion and the calculation of axial forces in each rod. The numerical integration of the equation of motion consists of transforming the unbalanced forces acting on a particle into acceleration, and then, into motion of the particle. As will be explained later, this process starts by calculating the unbalanced forces for a set of particles, followed by the accelerations. Then, the new positions and velocities are calculated. Finally, the axial forces of the rods are calculated.

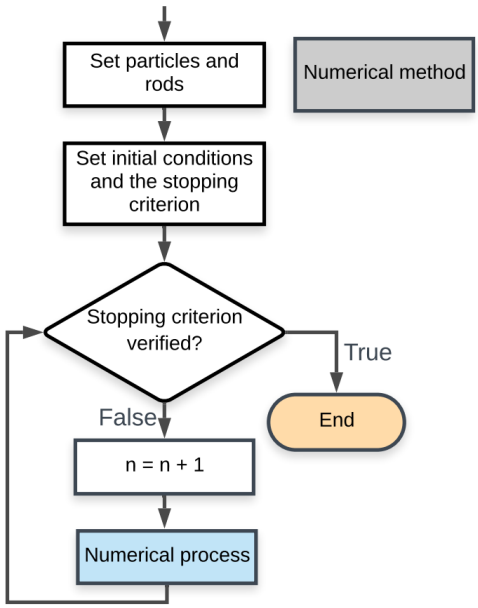

Figure 2.9 – Numerical method flow chart.

As follows, two approaches are presented for the implementation of the Numerical process. Approach 1 considers the small displacements formulation and a damping force approach; Approach 2 considers the large displacements formulation and a kinetic energy damping approach. The following sections will be considered: Numerical process for Approach 1 and Numerical process for Approach 2.

2.3.2 Numerical process – Approach 1

The Numerical process for Approach 1 consists of looping both the list of particles and the list of rods (Annex B.6.1). First, the numerical integration is implemented for each particle by applying the trapezoidal rule. Then, the axial force is calculated for each rod, considering the hypothesis of small displacements. The figure below shows the Numerical process for Approach 1.

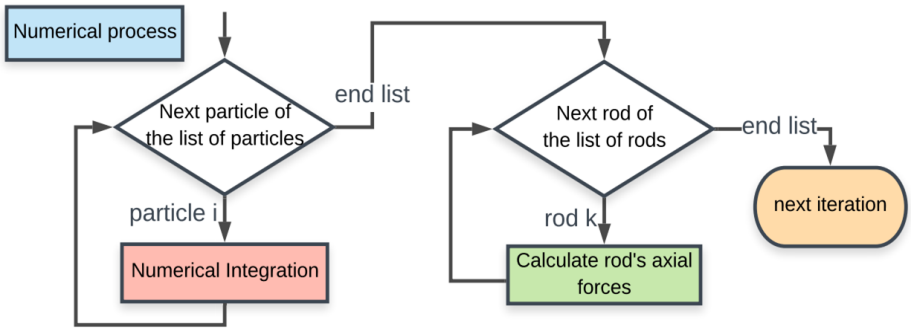

Figure 2.10 – Numerical process – Approach 1 flow chart.

2.3.2.1 Numerical integration of the equation of motion

Several numerical integration techniques may be used for solving the equation of motion [59]. The most common are the Euler's Method, the Verlet Method, and the Runge-Kutta Method [60]. Sometimes it is convenient to reformulate the second-order differential equation as a system of two coupled first-order differential equations [61]. So, by introducing the auxiliary function $\mathrm{v(t)}$ into the system and considering (for the sake of simplicity) the motion of a particle in one dimension, it is now possible to rewrite them in explicit form as follows:

$$\begin{cases} \dfrac{dv}{dt} = a(t), \\ \dfrac{dx}{dt} = v(t) \end{cases} \tag{46}$$

where $x(t)$ is the displacement, $v(t)$ is the velocity and $a(t)$ is the acceleration at time t. The differential equations are to be solved with the initial conditions:

$$x(t_0) = x_0\,;\; v(t_0) = v_0$$

Considering the Taylor series expansions for velocity, $v_{n+1} = v(t + \Delta t)$ and displacement, $x_{n+1} = x(t + \Delta t)$, it follows:

$$v_{n+1} = v_n + a_n \Delta t + O((\Delta t)^2) \tag{47}$$

$$x_{n+1} = x_n + v_n \Delta t + \frac{1}{2} a_n (\Delta t)^2 + O((\Delta t)^3) \tag{48}$$

The Euler algorithm is obtained from the above series by truncating the O(Δt) terms (see [61]), resulting in equations (49) and (50).

$$v_{n+1} = v_n + a_n \Delta t \tag{49}$$

$$x_{n+1} = x_n + v_n \Delta t \tag{50}$$

The trapezoidal rule is a refinement of Euler's method; it consists of using the mean velocity during the interval to obtain a new position [60], and its application can be summarized as:

$$v_{n+1} = v_n + \; a_n \Delta t \tag{51}$$

$$x_{n+1} = x_n + \frac{1}{2}(v_n + v_{n+1}) \Delta t \tag{52}$$

All the steps must be repeated for the other directions.

The numerical integration of the equation of motion algorithm in Approach 1 consists of applying the trapezoidal rule. In this way, the unbalanced forces at the particle are transformed into motion, as shown in Figure 2.11 and Annex B.6.2.1. In the first step, the unbalanced forces (F_i^{unb}) are calculated, Equation (53), and then the acceleration (a_i^n), Equation (54). Later, velocities (v_i^{n+1}) and positions (x_i^{n+1}) are calculated using equations (55) and (56), respectively.

$$F_i^{unb} = \begin{bmatrix} F_{i,x}^{unb} \\ F_{i,y}^{unb} \\ F_{i,z}^{unb]} \end{bmatrix} = \begin{bmatrix} F_{i,x}^{ext} \\ F_{i,y}^{ext} \\ F_{i,z}^{ext} \end{bmatrix} + \sum_{k=1}^{n} \left(\begin{bmatrix} F_{k,x}^{int} \\ F_{k,y}^{int} \\ F_{k,z}^{int} \end{bmatrix} \right) + \begin{bmatrix} F_{i,x}^{reaction} \\ F_{i,y}^{reaction} \\ F_{i,z}^{reaction} \end{bmatrix} \tag{53}$$

$$a_i^n = \begin{bmatrix} \ddot{x}_{x,i}^n \\ \ddot{x}_{y,i}^n \\ \ddot{x}_{z,i}^n \end{bmatrix} = \begin{bmatrix} F_{i,x}^{unb} \\ F_{i,y}^{unb} \\ F_{i,z}^{unb} \end{bmatrix} \Big/ m_j \tag{54}$$

$$v_i^{n+1} = \begin{bmatrix} \dot{x}_{x,i}^{n+1} \\ \dot{x}_{y,i}^{n+1} \\ \dot{x}_{z,i}^{n+1} \end{bmatrix} = \begin{bmatrix} \dot{x}_{x,i}^{n} \\ \dot{x}_{y,i}^{n} \\ \dot{x}_{z,i}^{n} \end{bmatrix} + \Delta t \cdot \begin{bmatrix} \ddot{x}_{x,i}^{n} \\ \ddot{x}_{y,i}^{n} \\ \ddot{x}_{z,i}^{n} \end{bmatrix} \tag{55}$$

$$x_i^{n+1} = \begin{bmatrix} x_{x,i}^{n+1} \\ x_{y,i}^{n+1} \\ x_{z,i}^{n+1} \end{bmatrix} = \begin{bmatrix} x_{x,i}^{n} \\ x_{y,i}^{n} \\ x_{z,i}^{n} \end{bmatrix} + \frac{\Delta t}{2} \cdot \left(\begin{bmatrix} \dot{x}_{x,i}^{n} \\ \dot{x}_{y,i}^{n} \\ \dot{x}_{z,i}^{n} \end{bmatrix} + \begin{bmatrix} \dot{x}_{x,i}^{n+1} \\ \dot{x}_{y,i}^{n+1} \\ \dot{x}_{z,i}^{n+1} \end{bmatrix} \right) \tag{56}$$

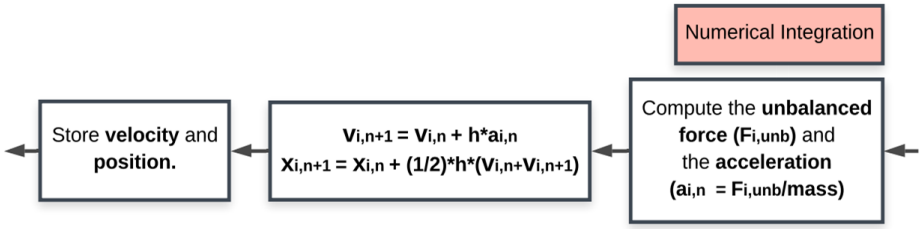

Figure 2.11 – Numerical integration of the equation of motion – Trapezoidal rule flow chart.

2.3.2.2 Rod's axial force

The rod's axial force is the interaction between the particles and is computed by applying Equation (25). Figure 2.12 summarizes the steps for its implementation. Annex B.6.2.2 presents the resulting code. The algorithm starts by calculating the rest length, which only depends on the initial position of the rod. Then, over the iterations, the current length ($L_{k,n+1}$) and strain ($\varepsilon_{k,n+1}$) are computed with equations (24) and (23). Then, the internal force on the local axis ($f^{\text{int}}_{k,\text{local axis}}$) is calculated. The next step consists of getting the velocity from the particles and computing the rod's damping force on the local axis ($f^{\text{dmp}}_{k,\text{local axis}}$) according to Equation (30). The rod's axial force on the axis ($f^{axial}_{k,\text{local axis}}$) results by adding the rod's internal force and rod's damping force, Equation (32). Finally, the axial force in the local axis must be calculated on the global axis and stored as presented in equations (27) and (28). This amount will be latter transmitted to each particle as internal nodal forces and used to calculate the unbalanced forces as summarized in the flow chart of Figure 2.11.

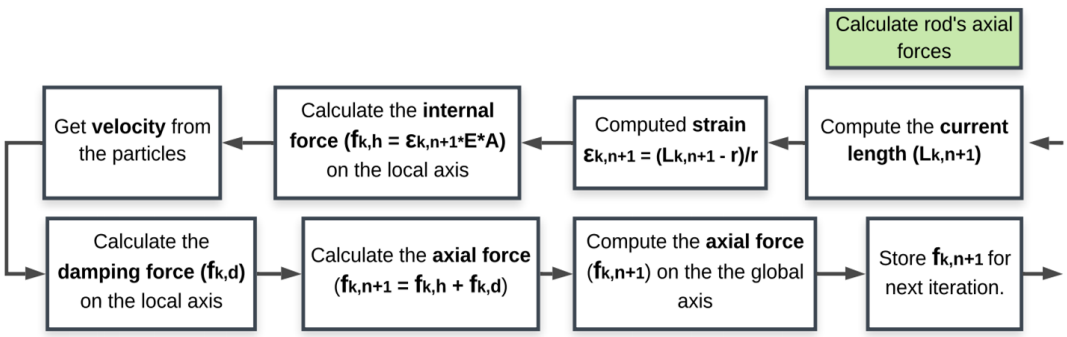

Figure 2.12 – Flow chart for the calculation of rods' axial forces in Approach 1.

2.3.3 Numerical process – Approach 2

Similarly to Approach 1, the Numerical process for Approach 2 consists of looping in sequence the list of particles and the list of rods (Annex B.6.1). First, the numerical integration is carried out for each particle by applying the centered finite difference. Then, the Kinetic Damping step is applied. Finally, the axial force is calculated for each of the rods, considering the formulation for large displacements. The figure below shows the Numerical process for Approach 2.

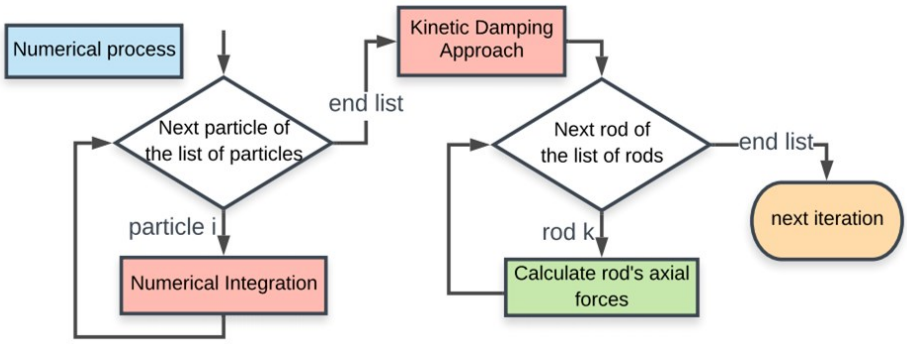

Figure 2.13 – Numerical process – Approach 2.

2.3.3.1 Stage 1 – Numerical integration

As referred before, the relationship between the velocity, the position, and the unbalanced forces can be obtained by performing a double numerical integration of the acceleration. For Approach 2, this step can be performed using the central finite difference form [43].

Figure 2.14 and Annex B.6.3.1 summarize the implementation of the numerical integration in Approach 2. It starts by computing the unbalanced force (F_i^{unb}) and the acceleration ($a_i^t = \frac{F_i^{unb}}{m_i}$). The next step is to check if it is a peak. In case it is a peak, the velocity at the mid-point ($v_i^{n+\frac{1}{2}}$) is calculated with Equation (45). Otherwise, the velocity is calculated with Equation (36). Finally, the position (x_i^{n+1}) is computed with Equation (37). As described in [43], the first iteration may be set as a peak and the velocity can be calculated with Equation (45).

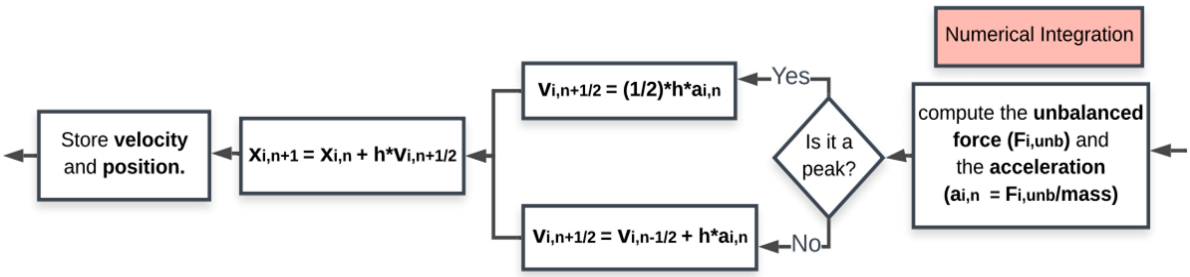

Figure 2.14 – Stage 1 of the Kinetic Damping approach - Numerical integration flow chart.

2.3.3.2 Stage 2 – Kinetic Damping approach

The stage 2 of the Kinetic Damping approach consists of re-initializing the velocities at kinetic energy peaks. The figure below summarizes its implementation, and Annex B.6.3.1 presents the resulting code. The algorithm starts by computing the current kinetic energy (K^{n+1}) according to Equation (38). Then, the current kinetic energy is compared with the previous ones. If condition $K^{n-1} \leq K^n \; and \; K^n \leq K^{n+1}$ is not met, it means that a peak occurs between $\mathrm{t}_1 = t - \Delta t$ and $\mathrm{t}_2 = t$, and the position of each particle must be reevaluated at the position $x_i^{t-\frac{\Delta t}{2}}$, according to Equation (42). Finally, the kinetic energy is reset to zero.

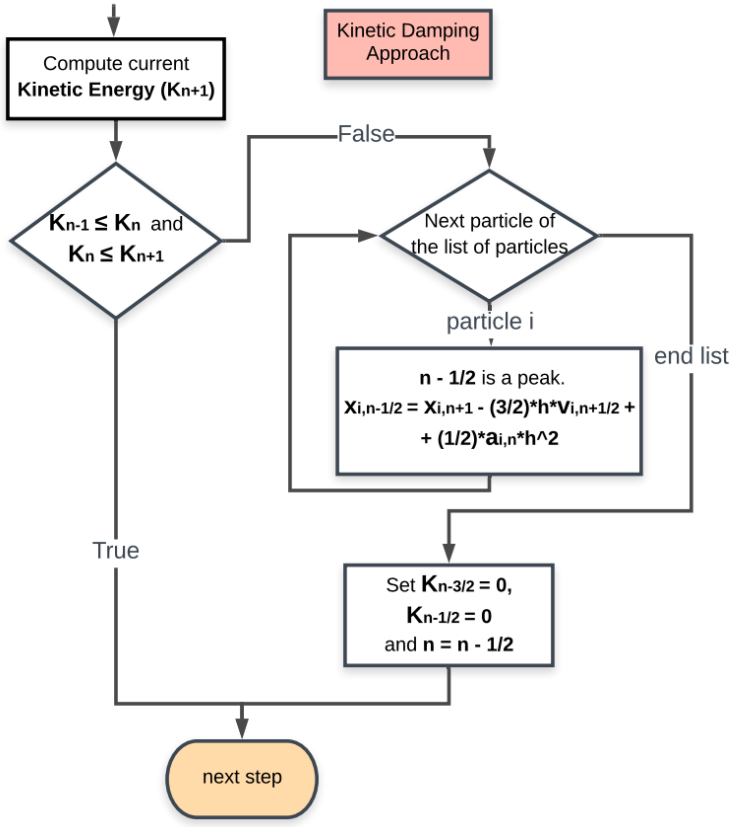

Figure 2.15 – Stage 2 of the Kinetic Damping approach – flow chart.

2.3.3.3 Rod's axial force

Considering the formulation for large displacements, the rod's axial force can be given by Equation (25) and is conveniently recalled here as:

$$f^{\mathrm{int}}_{\mathrm{k,local\ axis}} = \left(\sigma_{\mathrm{k,n}} \mathrm{A_n} + \mathrm{E_n A_n} \varepsilon_{\mathrm{k,n+1}}\right) \mathrm{e}_{1'2'}$$

$$\varepsilon_{\mathrm{k,n+1}} = \frac{\Delta \mathrm{L}}{\mathrm{L_{k,n}}} = \frac{\mathrm{L_{k,n+1}} - \mathrm{L_{k,n}}}{\mathrm{L_{k,n}}}$$

The axial force in each rod can be summarized as presented in Figure 2.16. Annex B.6.3.2 presents the resulting code. The algorithm starts by calculating the current length of the rod k, $L_{k,n+1}$, and the transformation matrix with the approach presented in Equation (22). Then, the strain ($\varepsilon_{k,n+1}$) is computed. Finally, the axial force in the local axis ($f^{int}_{k,local\ axis}$) can be calculated. As presented before, the axial force must be calculated on the global axis and stored as presented in equations (27) and (28). This amount will be latter transmitted to each particle as internal nodal forces and used to calculate the unbalanced forces, as summarized in the flow chart of Figure 2.14. For further iterations, the current stress, $\sigma_{k,n+1} = \frac{f_{k,n+1}}{A_n}$, is calculated and stored along with $L_{k,n+1}$.

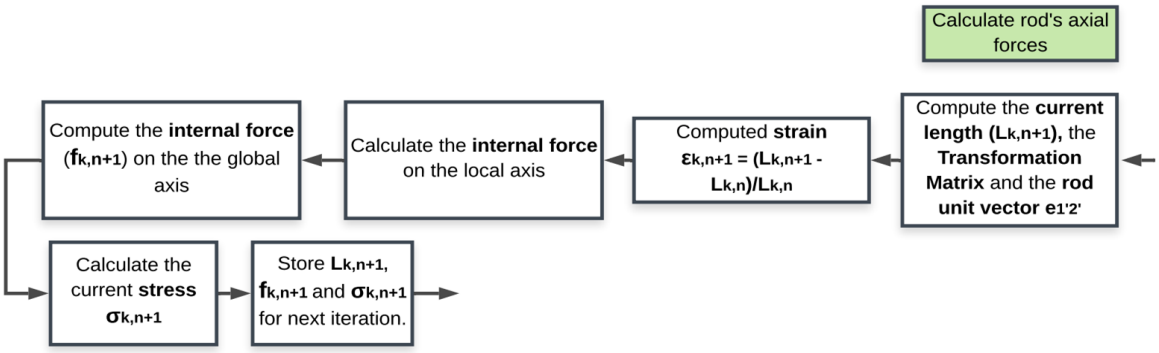

Figure 2.16 – Flow chart for the calculation of rods' axial forces in Approach 2.

2.4 Stopping criterion

An iterative numerical method is used to solve Newton's second law. Thus, this approach calculates successive approximations for the solution of the differential equation (9), which is recalled here for convenience.

$$m_i \begin{bmatrix} \ddot{x}_{i,x} \\ \ddot{x}_{i,y} \\ \ddot{x}_{i,z} \end{bmatrix} = \begin{bmatrix} F^{ext}_{i,x} \\ F^{ext}_{i,y} \\ F^{ext}_{i,z} \end{bmatrix} + \begin{bmatrix} F^{int}_{i,x} \\ F^{int}_{i,y} \\ F^{int}_{i,z} \end{bmatrix} + \begin{bmatrix} F^{reaction}_{i,x} \\ F^{reaction}_{i,y} \\ F^{reaction}_{i,z} \end{bmatrix} = \begin{bmatrix} F^{unb}_{i,x} \\ F^{unb}_{i,y} \\ F^{unb}_{i,z} \end{bmatrix}$$

Such a method involves a sequence of generated steps, an error tolerance, and at each step, an amount that may be related to the simulation error is estimated. Therefore, numerical methods for ordinary differential equations have a stopping criterion that can be simply described as in Equation (57) [75].

$$|\varepsilon - \varepsilon_n| < Tolerance \qquad (57)$$

In the case of the 3D force system, the cartesian approach first requires the definition of the x, y, and z directions. Then, the equations of motion for each direction must be verified. Thus, the presented stopping criterion uses the unbalanced force of each particle, F_{unb}, as a numerical method convergence indicator. This amount corresponds to the unbalanced forces at each particle that generates the nodal acceleration, which keeps the numerical method working. However, it is a difficult task to choose a single meaningful error tolerance, since it mainly depends on the geometry of the structural systems – besides, the combination of different load scenarios may lead to very different results.

The stopping criterion proposed here is:

$$\left|F_i^{unb}\right| \leq Tolerance \tag{58}$$

$$F_i^{unb} = F_i^{ext} + F_i^{int} + F_i^{reaction} \tag{59}$$

where F_i^{unb} is the unbalanced force in axis i, F_i^{ext} is the applied external force, F_i^{int} is the internal nodal force and $F_i^{reaction}$ is the contribution of the support reaction. The formulation of these quantities was expressed before in this chapter.

3 The 3DParticleSystem Software

Many commercial and didactic software allow static structural analysis through the direct stiffness method or finite element analysis (FEA); notable examples are FTOOL [46], ADINA [47], and SAP 2000 [48]. On the other hand, it is not so common to find structural analysis software implemented with numerical approaches usually found in computer games. The herein developed software, called 3DParticleSystem, adds some diversity to the didactic software commonly used in civil engineering courses. It is noteworthy that the developed software allows physically nonlinear analysis by considering nonlinear material models such as the elastic-perfectly plastic model and the bilinear hardening model. In this chapter, the structure of the developed software and some of its features will be presented.

The PSA3D physics engine (PE) (see Chapter 2) is combined with a graphics rendering middleware – our own graphics rendering engine, which uses the Panda3D rendering capabilities [44], and is responsible for rendering the structural engineering phenomena, such as deformation, stress-strain curves, and even collapse. The result of this combination is the 3DParticleSystem software developed in this work. This software gives to the user a unique game-like interaction where structural models respond to input in real-time.

3.1 The 3DParticleSystem GUI

The 3DParticleSystem graphical user interface (GUI) contains some features that are essential for executing the numerical approach presented in Chapter 2. This section summarizes some important features needed to use the developed software correctly. The first set of features is related to physical units. Then the camera control is presented, followed by a general presentation of the 3DParticleSystem GUI. Finally, some features of the 3DParticleSystem Canvas are presented.

3.1.1 Units

Typically, the software that handles physical phenomena requires the use of length, force, mass, and time. Therefore, for the 3DParticleSystem software, the units of the physical quantities must be imported and are exported as follows in Table *3.1*.

Table 3.1 – The units needed for the 3DParticleSystem software input.

Units	
Length	meter (m)
Forces	kilonewton (kN)
time	second (s)
Mass	kilogram (kg)
Area	m^2
Mass per unit volume	kg/m^3
Young's modulus	GPa
Pressure, stress, etc.	MPa

3.1.2 Camera control

The 3DParticleSystem software's mouse control is like the standard Panda3D's camera control system. Table *3.2* shows some keys to handling the navigation in the developed software.

Table 3.2 – Default Panda3D's camera control system.

Key	Action	Alternative (Windows 10)
Left Button	Pan left and right.	-
Right Button	Move forward and backward.	Control+Left Button
Middle Button	Rotate around the origin of the application.	Shift+Left Button
Right and Middle Buttons	Roll the point of view around the view axis.	Control+Shift+Left Button

3.1.3 The 3DParticleSystem GUI overview

The 3DParticleSystem software has two main windows, the menu window, and the canvas window. The first deals with the menu commands, allowing the user to access the different options of software and setting the different system variables. The latter deals with the graphical rendering of the structural system.

3.1.3.1 The 3DParticleSystem menu

Figure 3.1 presents the main menu of the 3DParticleSystem. The menu is divided into several boxes, namely, the simulation menu, the change structure menu, the choose particle menu, the stopping criteria menu, the rendering menu, the output menu, and the physical parameters menu. The file option shows some basic features for handling the input file, such as creating a new model, open file, save file, save as, export, exit, open from CSV, import from DXF. The features on the left side allow the user to reset and update the structural system. It also allows the user to remove rods and change support constraints. On the right side, the user has several features to deal with the parameters of the physics engine and with the parameters of the graphical rendering engine. The right-side features are combined as:

a) Stopping criterion, which allows setting the stopping criterion.
b) Rendering, which allows setting some auxiliary parameters, such as the axial diagram scale, the deformed shape scale, the rendering frequency, and the text scale size.
c) Output, which allows the user to show/hide the original geometry of the structure. It also offers an option to show the stress-strain curve of any rod.
d) Physical Parameter, which allows setting the damping coefficient and the time-step.

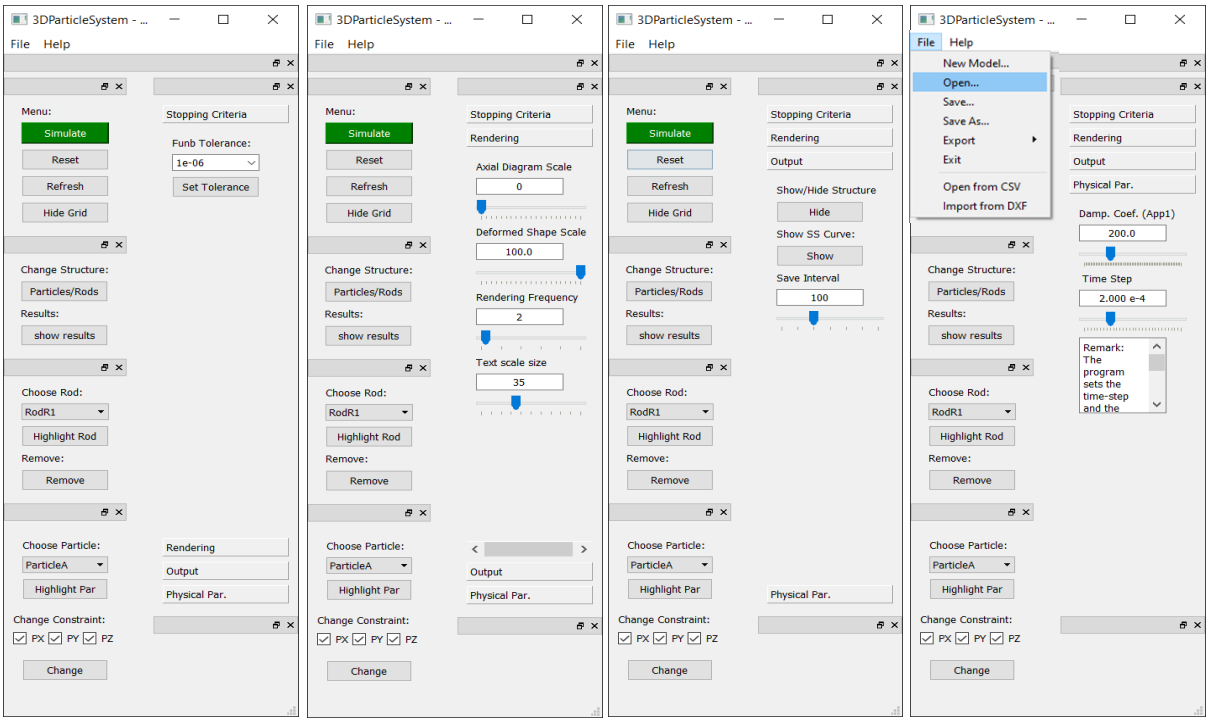

Figure 3.1 – The 3DParticleSystem software menu.

3.1.3.2 The 3DParticleSystem Canvas

The 3DParticleSystem Canvas consists of a window with the Grid button and the Simulation button, in which the structural system is rendered along with its output results. The Grid button allows the user to show/hide the grid and the axes, being useful for designing the structures and analyzing the output results. Each axis is represented with a different color; the red, green, and blue lines correspond to the axes x, y, and z, respectively. The Simulation button controls the state of the simulation. When this button is clicked, the simulation occurs until a given stopping criterion is met or the state of the simulation is changed to pause. Figure 3.2 shows a space tower with a square base, and a horizontal load applied to the top. The following figures sequence graphically shows the evolution of the space truss system while using the 3DParticleSystem software. These figures show the support reactions as green arrows and the loading force as a blue arrow. The red bars are subject to tensile stresses, and the blue bars are subject to compressive stresses.

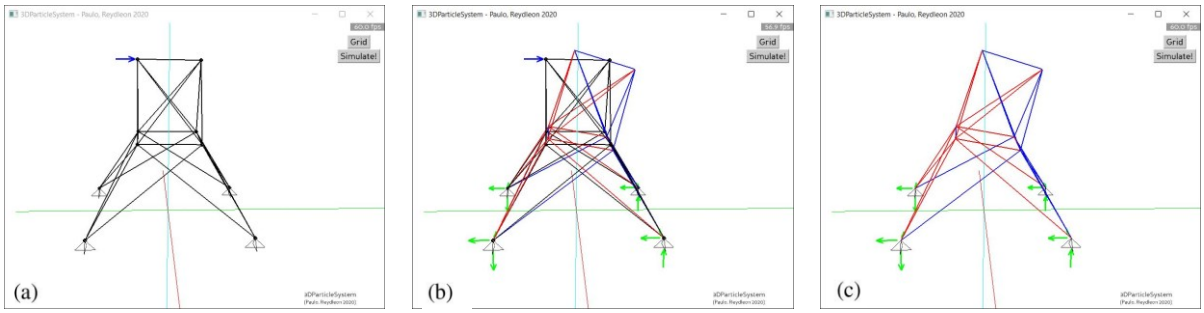

Figure 3.2 – (a) space tower with a square base. (b) deformed shape with the original structure in the back. (c) deformed shape.

3.1.3.3 Setting the 3DParticleSystem Software

The 3DParticleSystem's GUI aims to avoid the feeling of learning software from scratch by creating a software-inspired GUI commonly used by civil engineering students. Thus, some software such as FTOOL [46], ADINA [47], SAP2000 [48], and AutoCAD [62] played a key role in this creative process.

Before launching the 3DParticleSystem, the user must edit the main input file for the input parameters. It consists of setting some essential parameters, as presented in Annex A.2. The user must then write an input file that contains the desired geometry, Annex A.2 (this can be either TXT or CSV). During the simulation, the user can edit the structure geometry, forces, and constraints using the GUI, and proceed with the simulation, considering those changes.

When using structural analysis software, the first step is to define the geometry of the structure to be analyzed. In the developed, it can also be done by editing tables in which points and lines are specified. As with ADINA (Automatic Dynamic Incremental Nonlinear Analysis [63]), the definition of points and lines in the 3DParticleSystem software is first given by defining the points and then the lines. Thus, for each line, the user must choose the corresponding edges from the points already defined.

Figure 3.3 shows the plane truss structure that will be analyzed by the 3DParticleSystem software. All rod elements are considered to have the same cross-sectional area of $20\ \mathrm{cm}^2$, elastic modulus $E = 200\ GPa$ and mass per unit volume $\rho = 7900\ kg/m^3$. Then, the mass per unit length of the rod element is $\lambda = \rho A = 15.8\ kg/m$. The system is loaded with an applied force of $100\ \mathrm{kN}$ along the z-axis at nodes B, C, E, F and G.

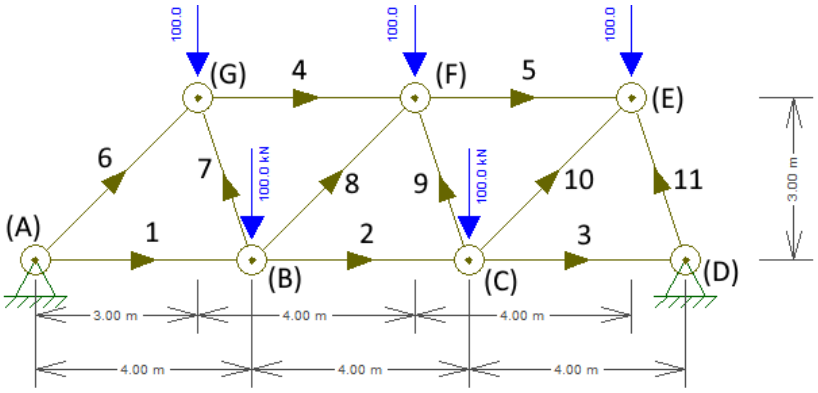

Figure 3.3 – Plane truss. Adapted from FTOOL.

Figure 3.4 and Annex A.2 show the definition of the geometry of the plane truss structure by editing two tables, one for particles and one for rods. Figure 3.4 in the left shows the particles named from A to G, along with its coordinate. Figure 3.4 in the right shows the rod named from 1 to 11. Each rod is composed by two particles, for exemple, rod10 results from the connection of ParticleC and ParticleE.

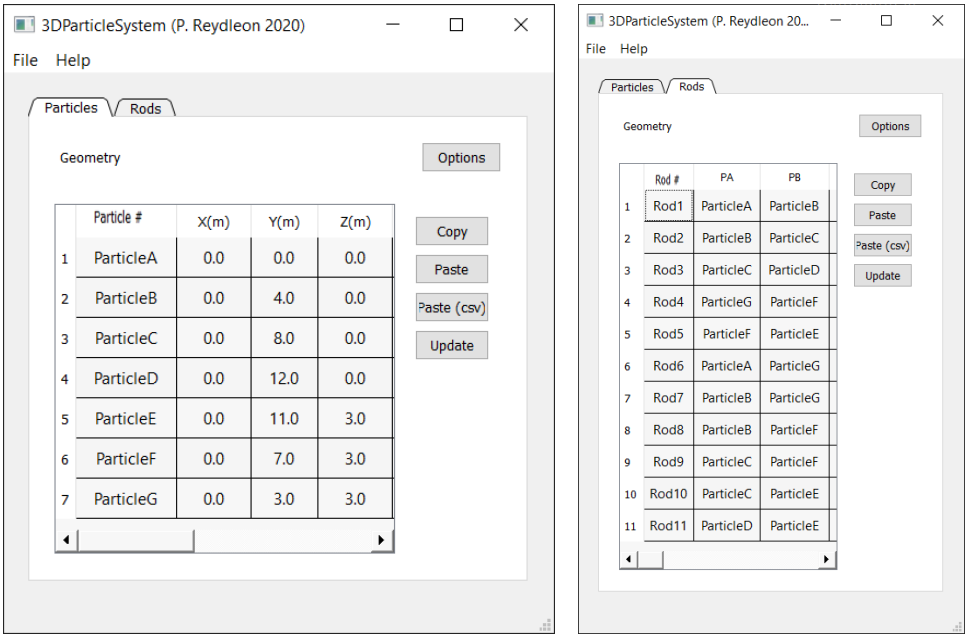

Figure 3.4 – Definition of particles and rods in the 3DParticleSystem software.

Then, it is just a matter of editing the input tables to define support constraints and external forces, as shown in Figure 3.5. This step can be made at any time during the simulation.

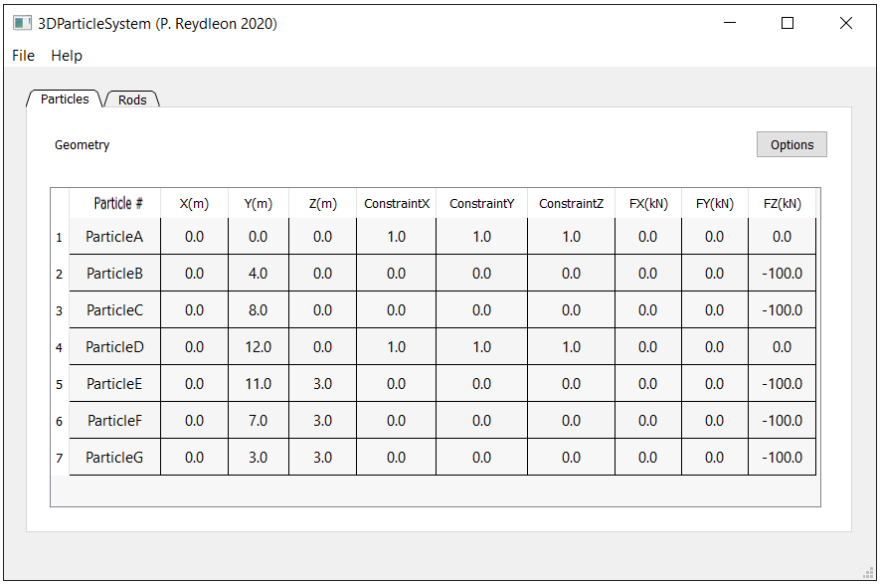

Figure 3.5 – An example of defining support constraints and external forces in the 3DParticleSystem software.

The next step is to define the cross-sectional area, mass per unit volume, and the modulus of elasticity or the stress-strain curve, Figure 3.6.

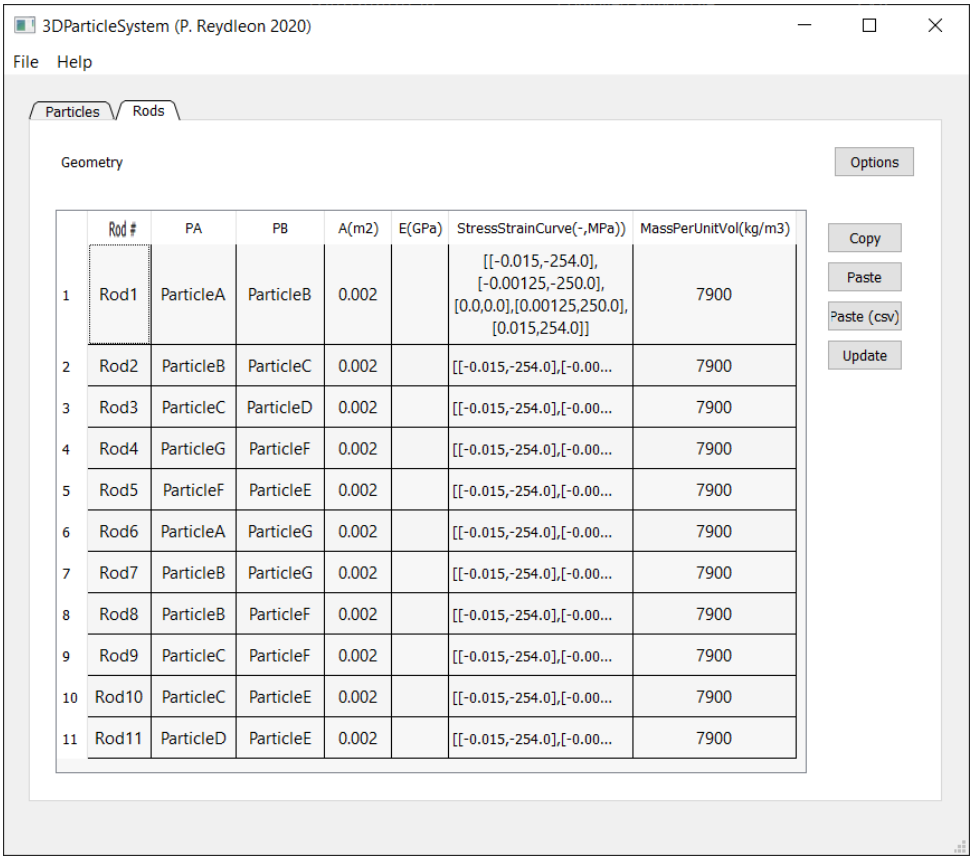

	Rod #	PA	PB	A(m2)	E(GPa)	StressStrainCurve(-,MPa))	MassPerUnitVol(kg/m3)
1	Rod1	ParticleA	ParticleB	0.002		[[-0.015,-254.0], [-0.00125,-250.0], [0.0,0.0],[0.00125,250.0], [0.015,254.0]]	7900
2	Rod2	ParticleB	ParticleC	0.002		[[-0.015,-254.0],[-0.00...	7900
3	Rod3	ParticleC	ParticleD	0.002		[[-0.015,-254.0],[-0.00...	7900
4	Rod4	ParticleG	ParticleF	0.002		[[-0.015,-254.0],[-0.00...	7900
5	Rod5	ParticleF	ParticleE	0.002		[[-0.015,-254.0],[-0.00...	7900
6	Rod6	ParticleA	ParticleG	0.002		[[-0.015,-254.0],[-0.00...	7900
7	Rod7	ParticleB	ParticleG	0.002		[[-0.015,-254.0],[-0.00...	7900
8	Rod8	ParticleB	ParticleF	0.002		[[-0.015,-254.0],[-0.00...	7900
9	Rod9	ParticleC	ParticleF	0.002		[[-0.015,-254.0],[-0.00...	7900
10	Rod10	ParticleC	ParticleE	0.002		[[-0.015,-254.0],[-0.00...	7900
11	Rod11	ParticleD	ParticleE	0.002		[[-0.015,-254.0],[-0.00...	7900

Figure 3.6 – An example of defining the cross-sectional area and the material's mechanical properties in the 3DParticleSystem software.

After the simulation, the numerical results can be displayed as output tables and graphs, as shown below. Figure 3.7 shows the computed results for a set of particles. Figure 3.8 and Figure 3.9 show the stress-strain curve for some bars (rod6 and rod10) with their results (axial force, strain, and stress).

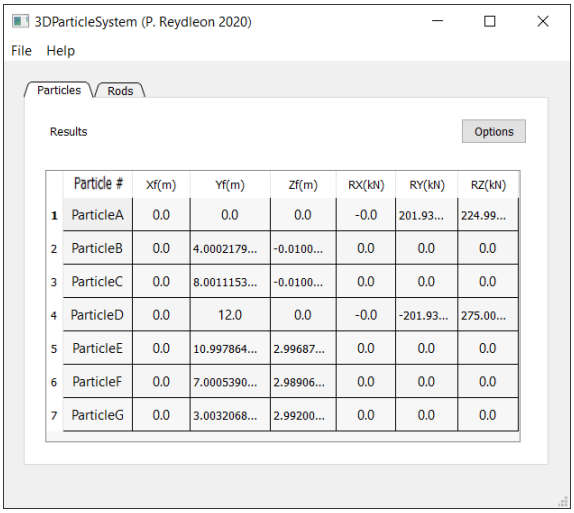

	Particle #	Xf(m)	Yf(m)	Zf(m)	RX(kN)	RY(kN)	RZ(kN)
1	ParticleA	0.0	0.0	0.0	-0.0	201.93...	224.99...
2	ParticleB	0.0	4.0002179...	-0.0100...	0.0	0.0	0.0
3	ParticleC	0.0	8.0011153...	-0.0100...	0.0	0.0	0.0
4	ParticleD	0.0	12.0	0.0	-0.0	-201.93...	275.00...
5	ParticleE	0.0	10.997864...	2.99687...	0.0	0.0	0.0
6	ParticleF	0.0	7.0005390...	2.98906...	0.0	0.0	0.0
7	ParticleG	0.0	3.0032068...	2.99200...	0.0	0.0	0.0

Figure 3.7 – The results of the particles in the 3DParticleSystem software.

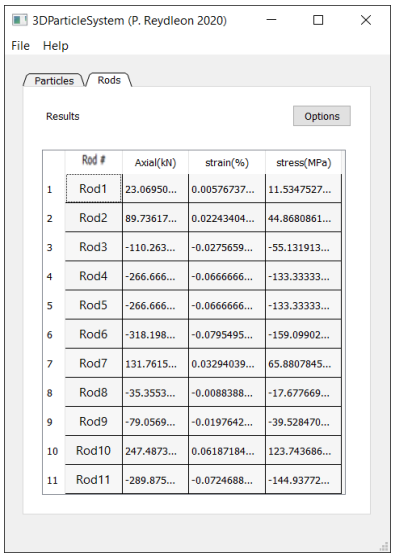

	Rod #	Axial(kN)	strain(%)	stress(MPa)
1	Rod1	23.06950...	0.00576737...	11.5347527...
2	Rod2	89.73617...	0.02243404...	44.8680861...
3	Rod3	-110.263...	-0.0275659...	-55.131913...
4	Rod4	-266.666...	-0.0666666...	-133.33333...
5	Rod5	-266.666...	-0.0666666...	-133.33333...
6	Rod6	-318.198...	-0.0795495...	-159.09902...
7	Rod7	131.7615...	0.03294039...	65.8807845...
8	Rod8	-35.3553...	-0.0088388...	-17.677669...
9	Rod9	-79.0569...	-0.0197642...	-39.528470...
10	Rod10	247.4873...	0.06187184...	123.743686...
11	Rod11	-289.875...	-0.0724688...	-144.93772...

Figure 3.8 – The results of the rods in the 3DParticleSystem software.

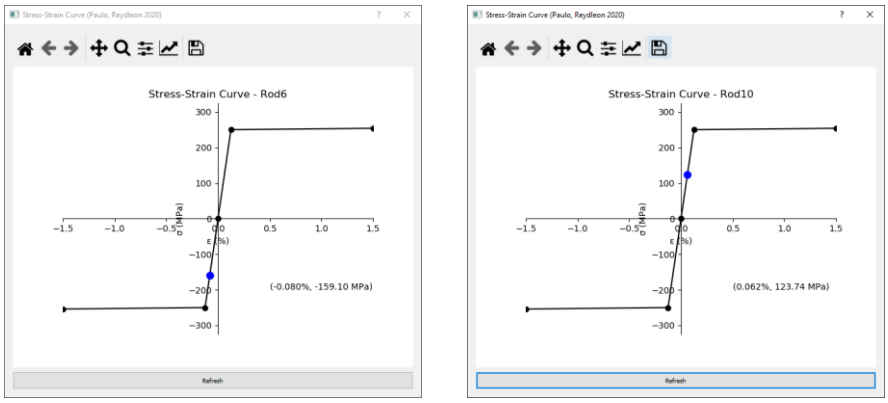

Figure 3.9 – The results of stress and strain in the 3DParticleSystem software.

The 3DParticleSystem software has some computer-aided design (CAD) capabilities. Still, it may be more advantageous to use an advanced CAD/drafting software such as AutoCAD to design the structure geometry. In this way, the resulting files in the DXF format (AutoCAD 2018 Drawing Exchange Format) can be imported from AutoCAD applications to the 3DParticleSystem software, as shown in Figure 3.10.

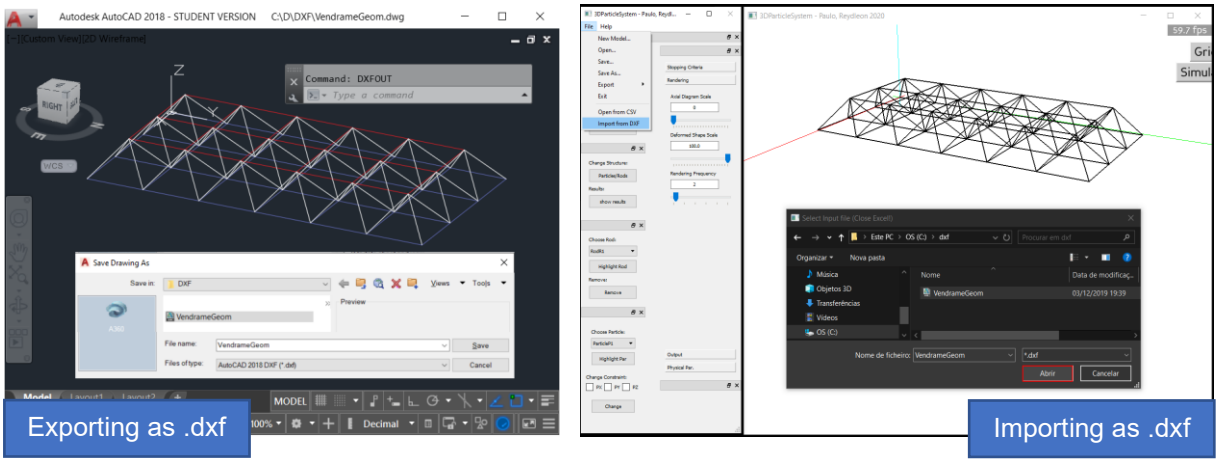

Figure 3.10 – Importing from AutoCAD 2018 to the 3DParticleSystem software.

3.2 Software structure

This subsection explains some topics related to the structure of the developed software. This subsection starts by presenting the tools chosen for this task, Python and Anaconda. Then, the structure of the 3DParticleSystem is presented. Finally, some aspects related to the implementation of the physics engine are presented.

3.2.1 Python and Anaconda

Python is often the first programming language engineering science students are exposed to. In addition, it is one of the fastest-growing platforms for machine learning. This versatility is one of the advantages of this programming language. Besides, Python has excellent online learning resources and is becoming an increasingly popular programming language in many areas due to its large standard library, expressive syntax, and focus on code readability [13]. Python is a high-level, interpreted, cross--platform, and dynamically typed programming language that supports different programming paradigms, such as the functional paradigm and the object-oriented paradigm.

Despite all the advantages above described, a user with poor programming skills may have some difficulties installing packages and programming libraries; these tasks can be daunting and even slow the learning progress. However, these difficulties can be easily overcome by using the Spyder IDE and Anaconda [64] or other similar environments. Anaconda is a highly recommended alternative to the Python distribution for scientific computing, ideal for a novice user who does not know which packages will be needed.

3.2.2 The 3DParticleSystem structure

The 3DParticleSystem software is entirely written in Python and allows the user to draw structures, analyze them, and then export the results. The CAD software has been successfully created from scratch. Thus, the developed software is organized into two distinct modules: one implementing the GUI and the other implementing for the PSA3D physics engine, described in Chapter 2. The 3DParticleSystem GUI was created using two frameworks: PyQt framework and Panda3D game engine. The first is responsible for managing the main features available to the user, such as buttons and menus. The latter is responsible for handling the graphics rendering engine, rendering the geometry of the structure, and presenting numerical results.

The 3DParticleSystem software starts with a simple main file, which is a Python Main function and is presented in Annex B.1. This main method calls the Qt application and the 3DParticleSystem Graphical User Interface (GUI) (class The3DParticleSystemGUI), Annex B.2. The 3DParticleSystem GUI launches the 3DParticleSystem main menu, presented in Figure 3.1 (The3DPsDialog class, Annex B.3), starting the event-loop [65] until the PyQt Application is closed. Then, the 3DParticleSystem Graphical User Interface instantiates the game engine (class GameEngine3DParticleSystem). The game engine uses its Elements‘ instance (PSA3DElements) to read the structural system file with the structural geometry

and saves its content as a list of elements (particles and rods), Annex B.4.1. After reading the input file, the class Element (PSA3DElements) calls the private method named initStructureSystem (Annex B.5.1), which loops through the list of elements (particles and rods), and, for each element, two objects are created, one that handles physical properties (Annex B.6.2 and B.6.3) and the other graphical properties (Annex B.7.3 and B.7.4). After the graphical part element is created, it is also added to the canvas (Annex B.5.2 and B.5.3).

Normally, the game engine has its own event-loop. The game loop of Panda3D is based on the concept of tasks [66]. The tasks are like threads and state the game mode on each loop, for example, either the game is running or not. Thus, the developed software uses a task to control whether the PSA3D physics engine (PE) is running or not, and also to stop the numerical method once the stopping criterion is met (Annex B.4.2 and B.6.1).

The 3DParticleSystem software interacts with the user from a simple window developed with the Qt framework, namely, the 3DParticleSystem GUI main menu (Annex B.2). Then, by controlling the Qt, the user has control of the game engine (Annex B.4), which handles the PSA3D PE (Annex B.6) and the GRE (Annex B.7). Thus, the user can change the state of the simulation at any time, as well as using all the features available in the developed software. Figure 3.11 summarizes the overall responsibilities of each module. Besides, it presents the communication between the different modules.

The double arrow represents that the user can interact with the 3DParticleSystem GUI (Annex B.2). and with the 3DParticleSystem GE (Annex B.4), throughout the canvas. Besides, it allows the user to control features from the canvas, such as the deformed structural scale, axial diagram scale, grid, and camera. Moreover, the PSA3D PE (Annex B.6) gets the properties from the elements and runs the numerical simulation. Then, over the simulations, it updates the numerical data of each element. On the other hand, the GRE handles all the logic behind rendering the space trusses in the canvas.

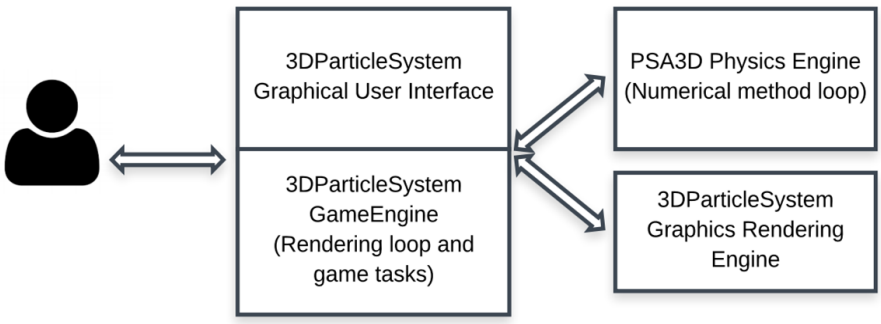

Figure 3.11 – Communication among the user and different modules (GUI, GE, PE, and GRE).

3.2.3 Physics engine programming challenges

During the development of the PSA3D physics engine, there were some programming challenges, two of which stand out: computational performance and maintaining a friendlier programming framework. In this way, auxiliary functions have been written in Python to do basic algebraic operations, corresponding to a thin layer between algebraic operations and Python NumPy [67], allowing for algebraic operations such as sum, addition, and product of vectors and matrices. Among these functions, two stand out, *Matrix Operations* and *Transformation Functions*.

Matrix Operations are a set of auxiliary functions that aim to create and manipulate Python arrays *(Annex B.8.1)*. These functions allow the PSA3D physics engine to perform matrix operations such as sum, addition, and product. *Transform Functions* are a set of auxiliary functions that allow the PSA3D physical engine to handle transformation matrices, allowing operations such as the calculation of unit vectors, cross products, and transformation matrices (Annex B.8.2).

3.3 Qt framework and PyQt

The 3DParticleSystem GUI goal is to give the best usability in the fewest clicks possible. It also seeks to reduce the learning curve of the developed software. Thus, the developed software uses the PyQt framework for this purpose. Qt is a cross-platform framework to develop GUI in C++ that was produced by the Norwegian company Trolltech and, since 2008, is owned by Nokia. The latest version of Qt is 5.12 LTS, released December 6, 2018, and supported for three years [68]. PyQt brings together the cross-platform language Python and the Qt C++ cross-platform application framework [45].

Qt is based on a well-known Signal & Slot paradigm [69]. In this, the buttons have a callback that corresponds to the function of the button. The simplest example is the "Exit" button, which calls the exit method and allows the user to exit the program. Therefore, this paradigm links GUI features such as buttons, tabs, and combo boxes to its respective callback. Thus, Python’s data structure, such as dictionary and list, are widely used in the developed GUI, making easy some tasks such as the signal and callback task, allowing to connect each widget to its respective callback directly.

3.4 Panda3D

This subchapter gives a brief description of Panda3D, introducing some of its essential features. Besides, it gives an overview of the implementation of the drawing the elements: particles and rods.

3.4.1 Brief Panda3D description and basic features

The engine developed by Disney Interactive to create one of its attractions later became the Panda3D game engine. Before that, some popular commercial games such as Toontown (2003), Pirates of the Caribbean Online (2007), and A Vampyre Story (2008) were developed using this tool [70]. Panda3D is a 3D game engine, a library of subroutines for 3D rendering and game development. It is open-source

and free for any purpose, even commercial [70], allowing the creation of games through programs written in Python or C ++ using Panda3D libraries. Annex A shows how to install Panda3D.

Although Panda3D has many features, the use of this framework in the 3DParticleSystem software is minimal as it is not intended to limit the development of this software to the game engine used in this release. The developed CAD software is based on rendering a set of organized lines, which makes it possible to render arrows, circles, grids, nodes, and bars — then building all the needed modules to represent structures with complex geometries.

One of the most important concepts of the graphics rendering engine is Canvas, shown in Figure 3.12. This can be described as the area or screen in which all UI elements should be contained [71]. Thus, it usually has several methods for drawing lines, boxes, circles, text, and adding images. In Panda3D, ShowBase can be considered a Canvas.

3.4.2 ShowBase class

The *ShowBase* class or *DirectStart ShowBase* is a Panda3D application framework responsible for opening the graphical display window, shown in Figure 3.12. In addition, it is responsible for setting up the 3D scene graph, input devices, and other elements needed to render the scene graph to the window, such as camera, keyboard, and mouse control [72]. Moreover, this class creates buttons, sliders, and text.

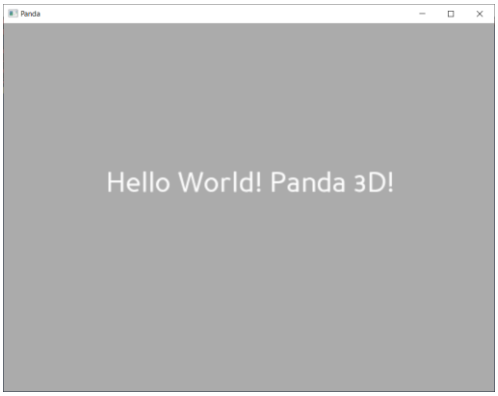

Figure 3.12 – GUI window of Panda3D ShowBase.

3.4.3 LineNodePath class

LineNodePath class is a fundamental class from Panda3D packages, inheriting from the *NodePath* class [73] and allowing the user to render lines by giving as input arguments, thickness, and color (Annex B.7.1). It is then possible to set the starting and ending points for the line by using public methods of *LineNodePath* class. Figure 3.13 shows the inheritance diagram for the *LineNodePath* class.

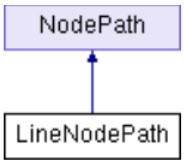

Figure 3.13 – Inheritance diagram for LineNodePath class. Adapted from [88].

It is now possible to extend the *LineNodePath* class to create smarter objects, empowering the developed CAD with functionalities essential to its operation.

3.4.4 ElementaryLine, ElementaryArc and Arrow classes

By arranging lines using pure mathematical logic, it is then possible to render arrows, arcs, circles, triangles, and rectangles. Then, by combining all these simple geometric elements, it is possible to render structural systems with different complexities. Thus, the development of a graphics rendering engine begins by creating the line class, called the *ElementaryLine* class.

3.4.4.1 ElementaryLine class

The *ElementaryLine* class is an extension of the *LineNodePath* class (Annex B.7.1) and receives not only the starting and ending points for the line but also the color and thickness (Annex B.7.2). This extension includes methods that allow changing color and thickness, as well as updating the coordinates, making it easier to render the most crucial element in this graphical interface. Figure 3.14 shows a representation of the lines in a simple Panda3D application and the respective code is presented in Annex B.7.1.

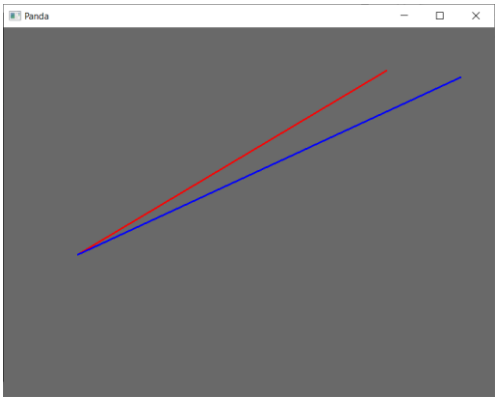

Figure 3.14 – Rendering an ElementaryLine object in a simple Panda3D application.

3.4.4.2 ElementaryArc and Arrow classes

The *ElementaryArc* class is an extension of the *LineNodePath* class and can render arcs and circles by specifying a center and a radius. Moreover, the *Arrow* class is another extension of the *LineNodePath* class and allows the developed CAD to graphically represent arrows by specifying the starting and ending points, color, and thickness. Figure 3.15 shows the representation of lines, arrows, and circles in the 3DParticleSystem software.

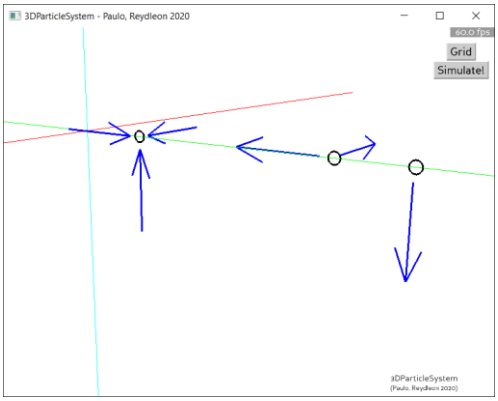

Figure 3.15 – Representation of lines, arrows, and circles in the 3DParticleSystem software.

3.4.5 GameEngine3DParticleSystem class

The *GameEngine3DParticleSystem* class brings together all the elements that make up the graphics rendering engine (Annex B.4). The function of the *GameEngine3DParticleSystem* can be summarized in:

a) Start the DirectStart ShowBase,
b) Start and handle the Graphics Rendering Engine and the screen,
c) Start the grid and define Panda 3D events, such as the escape button, the simulation/stop button, and the grid button,
d) From the resource files, obtain the input parameters, such as the stop/tolerance criteria for the simulation, the Physics Engine parameters and the type of approach, Approach 1 or 2,
e) Start and handle the PSA3D physics engine.

3.5 Elements

The Particle System approach discretizes the space truss structure into simple elements such as particles and rods, as described in Figure 3.16. Thus, for the computational implementation of these elements, the *Elements* class was created (Annex B.5). When particles and rods are created, this class divides each element into its graphical (Annex B.7.3 and B.7.4) and physical parts (Annex B.6.2.2 and B.6.2.1), with the geometry being the linking attribute between these parts.

The first step in rendering a structure is to create particles that define it. Thus, the *Element* class must receive the coordinates of each particle, being the result presented in Figure 3.17, on the left. Then it is possible to create a bar/rod element. Figure 3.17 shows, on the right, the plane truss structure representation in the 3DParticleSystem software.

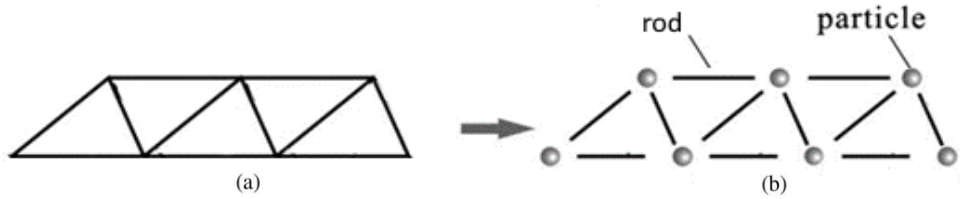

Figure 3.16 – (a) plane truss structure; (b) discretization of the structure in particles and rods.

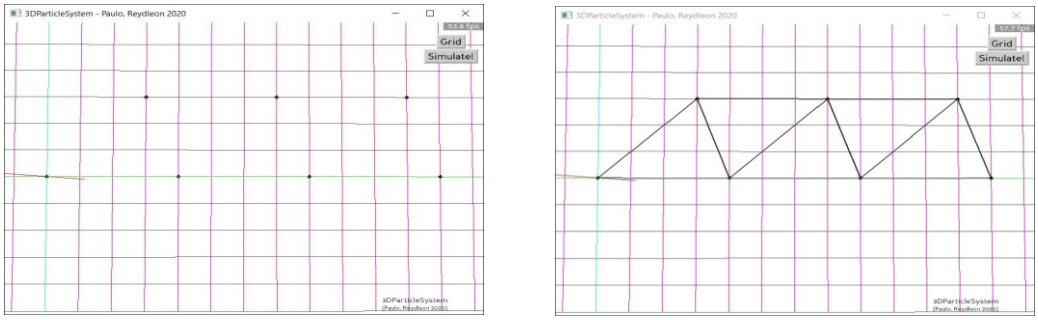

Figure 3.17 – Graphical representation of the particles, on the left, plane truss structure, on the right.

3.5.1 Particles

The particle element carries properties such as coordinates, nodal constraints, and external forces. Then, as a programming approach, each particle is implemented as having physical and graphical components. Regarding the representation of particle elements, it can be a constraint or a loaded node. This is organized into two distinct classes, *NodalConstraint* and *ExternalForce (Annex B.7.3).*

3.5.1.1 NodalConstraints class

Constraints are limits to the motion of particles. The most common 3D nodal constraints are roller constraints, ball-and-socket joints, and ball joints. Therefore, the class that handles the graphical representation of nodal constraints is called Nodal Constraint and imports classes such as LineNodePath, ElementaryArc, and ArrowAlongAxis. Figure 3.18 shows the graphical representation of different types of nodal constraints in the 3DParticleSystem software.

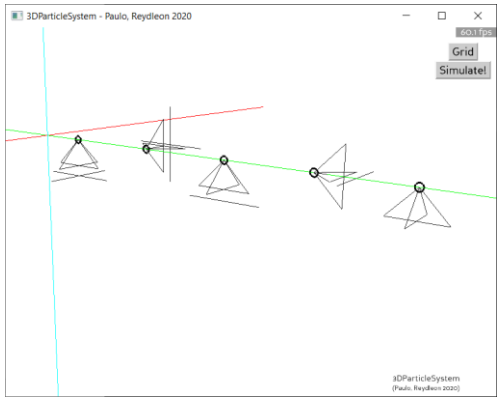

Figure 3.18 – Different types of nodal constraints in the 3DParticleSystem software. From left to right, ball joint in X0Y and Y0Z, roller along y and x, ball-and-socket joint.

3.5.1.2 ExternalForce class

Force is an interaction between bodies and is typically represented by vectors. In addition, vectors are a geometric object that has magnitude, direction, and an application point. The class that handles external forces is called the *ExternalForce* class and imports the *Arrow* class. Figure 3.19 shows on the left the external forces represented by blue arrows; On the right, the supports are also represented and their respective reactions, by green arrows.

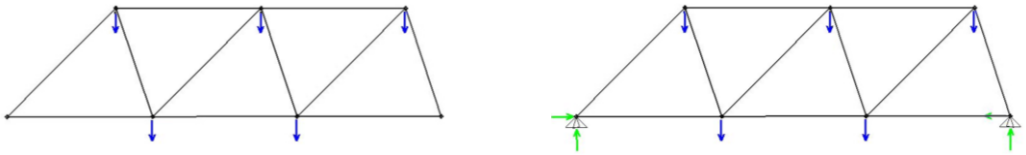

Figure 3.19 – Representation of external forces (left). Representation of a complete plane truss with reaction support results (right).

3.5.2 Rod

Each rod element can be discretized into two particles that contain all their intrinsic properties, namely, original position, deformed position, nodal constraints, and external forces. These coordinates are then used to calculate the rod's length and the local-to-global transformation matrix. Furthermore, each rod must also receive physical parameters, such as the cross-sectional area, the stress-strain curve, and mass per unit volume. It is then possible to characterize the mass of the rod that will be used to compute the mass of each particle, according to equations (10) and (11).

Rods are organized into three classes, namely, *ElementaryRod, AxialDiagram, and DeformedRod* (Annex B.7.4). Even though having common attributes, they have very distinct meanings.

3.5.2.1 ElementaryRod class

The *ElementaryRod* class extends the *ElementaryLine* class, giving 3DParticleSystem software the ability to render rods. This class takes as its argument two coordinates, along with its rendering properties, color, and thickness. The graphical representation of any rod begins by specifying its original geometry and can be updated at any time using its public methods.

3.5.2.2 DeformedRod class

DeformedRod class allows 3DParticleSystem software to render the deformed shape of any structure. To do this, this class inherits basic rendering properties from *ElementaryLine* and *ElementaryRod*, to control color and scale.

Figure 3.20 shows, on the left, the structure with its deformed shape; on the right, it shows the same structure without the original form. The graphical representation of a deformed rod is usually based on its axial force since the structure system changes color according to the magnitude of this parameter. Besides, the DeformedRod class allows the user to amplify the deformed shape by controlling a single

amplification scale parameter. Then, as a property of the ElementaryRod class, it is possible to hide the original form, which is very useful when graphically analyzing complex structural systems.

Figure 3.20 – The deformed and the original shape of a plane truss structure in the 3DParticleSystem software on the left. The deformed shape without the original shape on the right.

3.5.2.3 AxialDiagram

The next step is to render the axial force diagram. Such a diagram has a standard form of representation, so some algebraic manipulation is required to do it properly. It is also useful to introduce a text along with the diagram, which allows the user to track the values of axial forces throughout the evolution of the system. Thus, the *AxialDiagram* class handles the axial force diagram representation, by importing *DeformedRod* and *RendText* classes, the latter being responsible for rendering text in the canvas. Figure 3.21 shows an example of an axial force diagram in the 3DParticleSystem software.

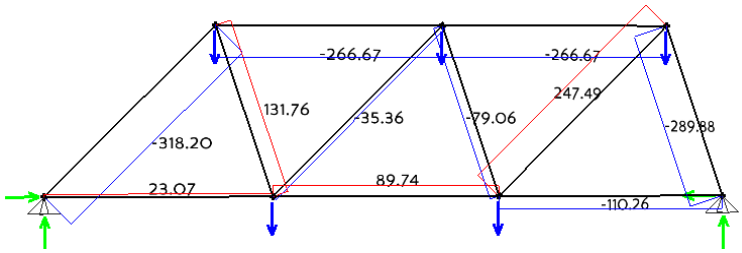

Figure 3.21 – Axial force diagram of a plane truss structure in the 3DParticleSystem.

3.6 Simulation mode

The game loop is the overall flow control for the entire game program, where the game continues performing a series of actions until the user quits [74]. The 3DParticleSystem software game loop consists of the physical engine constantly doing the math according to the loop shown in Figure 2.9, regardless of the graphics rendering engine, until a defined stopping criterion is met. On the other hand, the graphics rendering engine is updated as often as the user deems necessary by controlling the GUI parameter named rendering frequency, which quantifies how often the physics engine updates the graphics rendering engine.

The communication between the physics engine (Annex B.6) and the graphics rendering engine (Annex B.7) plays an essential role in the interactivity of the 3DParticleSystem software throughout the class Elements. The PE refreshes the Elements' GR. Later, the Element class updates the GRE. In this way, the GRE updating is controlled by the physics engine simulation status. This updating is very

straightforward and involves numeric and graphic parts. The communication between these parts has some complexity in the methods that are called. The rendering method starts by accessing the numeric attributes of each element and then updates the graphical environment based on these values (Annex B.5.4). It consists of two main loops, a loop in the rod list and another in the particle list. The first loop consists of updating the axial force of the rods and refreshing the current position of the two particles that make up the rod. The second loop consists of updating new support reaction arrows, according to the support reaction values.

4 Modeling

In this chapter, several case studies are presented and validated. This chapter applies Approach 1 and 2 of the PSA3D physics engine to solve general problems involving trusses with different support and loading conditions and is organized according to the level of complexity of the truss structure systems analyzed with increasing complexity throughout the examples. This chapter is divided into three parts: the first part consists of applying Approach 1 and the small displacements formulation; the second part consists of applying Approach 2 and the large displacements formulation. This chapter concludes by presenting several features of the 3DParticleSystem software, such as simulating structures subjected to changes in support constraints and removing rods during the simulation.

4.1 Relative difference

Let u_i denote the value computed in the 3DParticleSystem and u_{ref} denote the reference solution (which will be the result obtained with ADINA); then the relative difference is defined by:

$$RDif = \frac{|\Delta u|}{|u_{ref}|} = \frac{|u_i - u_{ref}|}{|u_{ref}|} \tag{60}$$

4.2 Numerical simulation – Approach 1

This section applies Approach 1 with the small displacements formulation to simulate a simple 1D problem, a 7-bar plane truss, and a 9-bar space truss. Before starting the analysis, it is required to set the time-step Δt and the damping coefficient c. Moreover, the stopping criterion is set as $|F_i^{unb}| \leq 10^{-6}$ for each axis/direction.

4.2.1 Axial force rod problem

The first example is an one-dimensional axially loaded elastic four meters long rod, as shown in Figure 4.1. The following material properties are considered: modulus of elasticity $E = 200\ GPa$ and mass per unit volume $\rho = 7900\ kg/m^3$. The cross-sectional area is $20\ cm^2$. Then, the mass per unit length of the rod element is $\lambda = \rho A = 15.8\ kg/m$. The bar has a pinned support at one end and has roller support at the other end, where it is loaded with an applied force of $500\ kN$.

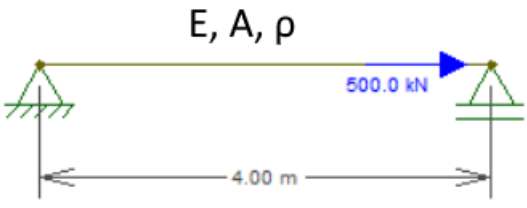

Figure 4.1 – One-dimensional axially loaded rod problem, adapted from FTOOL.

The first step in applying the PS approach is to discretize the system into two (or more) particles and one (or more) rod, as described in Chapter 2. Then, the particle masses should be calculated according to Equation (10). In this case, it can be discretized into two particles and a rod. Some geometrical parameters, such as position and mass, are presented in the tables below.

Table 4.1 – Particles A and B, and their properties.

Particle	x (m)	y (m)	m (kg)
A	0	0	31.60
B	4	0	31.60

Table 4.2 – Rod 1 and its properties.

Rod	PA	PB	L (m)	m (kg)
1	A	B	4	63.20

4.2.1.1 Particle B (roller support)

As expected, Particle B changes its position to solve Newton's equation of motion. As shown in Figure 4.2, the deformed position of the particle changes over iterations until it meets the stopping criterion. Figure 4.2 shows that it takes around 50 iterations to compute a good approximation of the relative displacement, with the relative difference being around 0.05% (4.98 mm).

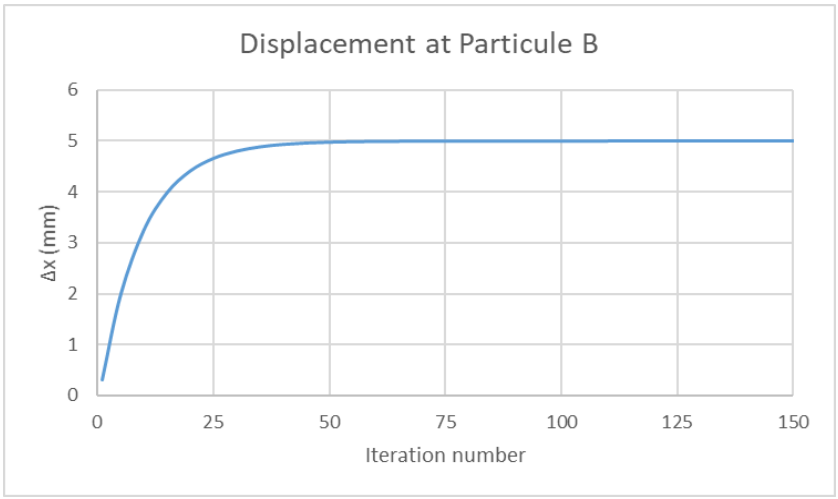

Figure 4.2 – Displacement at Particle B ($\Delta t = 2x10^{-4}$ s and $c = 200$ kN·s/m).

The unbalanced force creates acceleration and velocity in Particle B, which constantly changes its position. Figure 4.3. shows that, at the first iteration, the unbalanced force is the total external force applied. Then, over iterations, this unbalanced force is transformed into the motion of the particle. This motion leads to internal/axial forces that are then placed back at the particle, leading to a new and smaller unbalanced force. After around 25 iterations, the motion is almost null, and the unbalanced force is minimal.

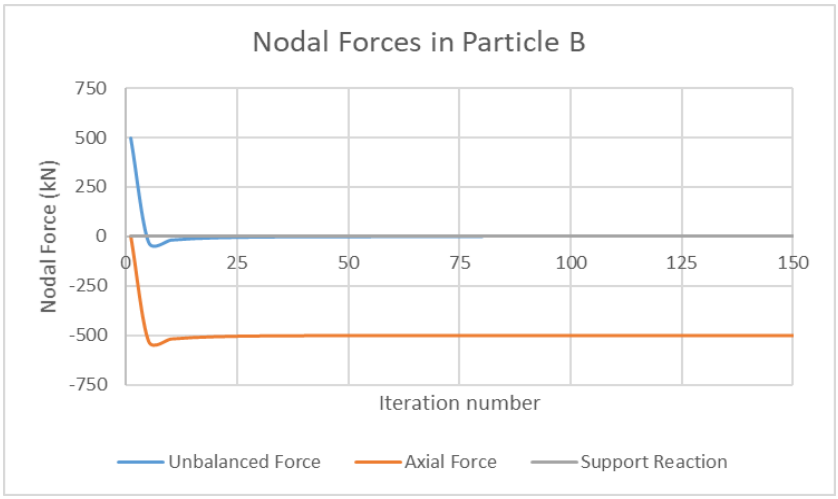

Figure 4.3 – Nodal Forces in Particle B ($\Delta t = 2x10^{-4}$ s and $c = 200$ kN·s/m).

Figure 4.4 shows, on the left, the deformed structure; on the right, the stress-strain curve of Rod 1, with the blue dot being the stress-strain pair after 120 iterations.

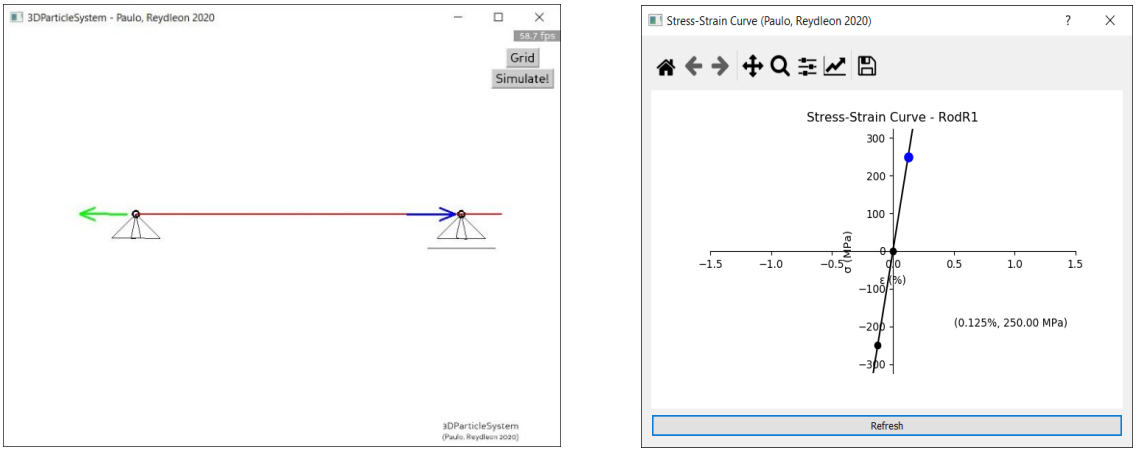

Figure 4.4 – The deformed shape, amplified 100x (left). Stress-strain curve after 120 iterations (right).

4.2.1.2 Particle A (pinned support)

The system has a pinned support at Particle A. Thus, all the axial forces generated by the motion of the Particle B are transmitted to Particle A throughout the rod. As Particle A is constrained, a support reaction arises that balances out the axial force. Figure 4.5 shows two symmetric curves representing, respectively, the axial force and the reaction at the support. After 25 iterations, there is already a good approximation for the support reaction, which is 500 kN.

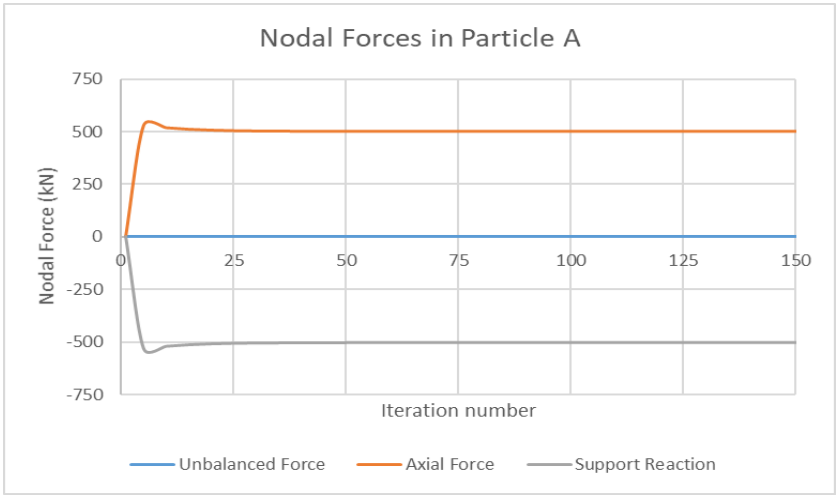

Figure 4.5 – Nodal Forces in Particle A ($\Delta t = 2x10^{-4}$ s and $c = 200$ kN·s/m).

4.2.1.3 Rod 1

Figure 4.6 shows the evolution of the axial force over the iterations. For a bar subjected to traction, the damping force contribution decreases until it reaches zero. On the other hand, the internal force increases until it reaches 500 kN. The axial force is simply the sum between damping and internal forces, as described in Equation (32).

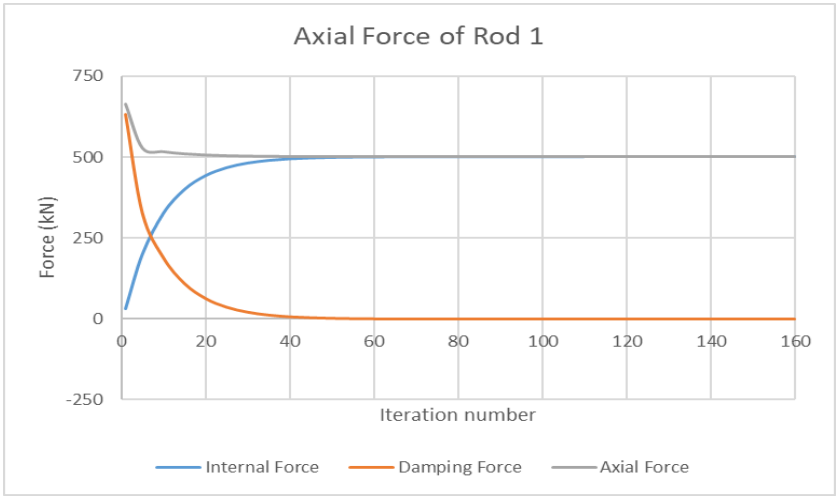

Figure 4.6 – Rod 1. Axial force ($\Delta t = 2x10^{-4}$ s and $c = 200$ kN·s/m).

4.2.1.4 Internal force

The internal force expressed in Equation (23) depends on the stiffness and on the particle displacement, which also depends on the damping coefficient. The figures below show the numerical results while changing the stiffness in three distinct cases, $EA = 4 \times 10^5\ kN$, $EA = 1.2 \times 10^6\ kN$ and $EA = 4 \times 10^6\ kN$ with the same parameters of time-step and damping coefficient. On the left, the figure shows a graph with displacement on Particle B over the iterations; on the right, it shows the internal force in the rod over the iterations.

The figure on the left shows that when $EA = 4 \times 10^6\ kN$, the internal force takes longer to compute a good approximation for the nodal displacement of Particle B. This can be explained once the particle moves slower and takes longer to equilibrate the nodal forces. On the other hand, when $EA = 4 \times 10^5\ kN$, the combination set for the time-step and the damping coefficient, produce faster results. Figure 4.7 shows the relation between the number of iterations and the nodal displacement at Particle B for the three stiffness cases. Figure 4.8 shows the relation between the number of iterations and the internal force of Rod 1 for the three stiffness cases. As expected, the same internal force of 500 kN is reached, but the number of iterations needed increases with increasing stiffness.

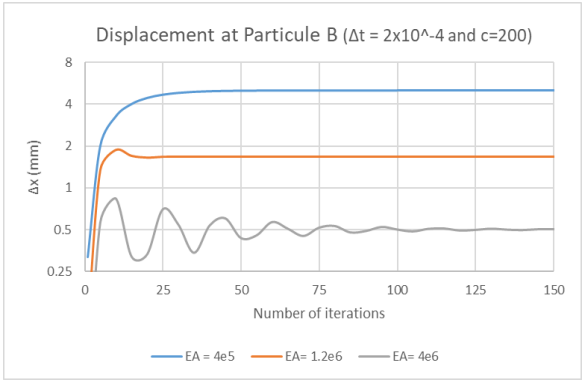

Figure 4.7 – Rod 1. Variation of the displacement with the stiffness.

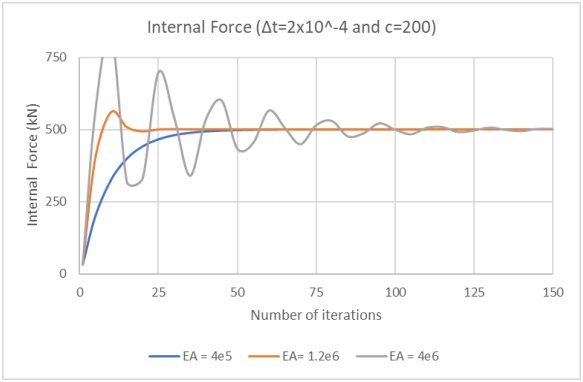

Figure 4.8 – Rod 1. Variation of the internal forces with the stiffness.

4.2.1.5 Damping force

The rod's damping force depends on the damping coefficient and velocities, Equation (29). The damping coefficient only affects how convergence is achieved. However, it should be set to avoid slow convergence due to over or under damping [5].

To study the damping force, two time-steps, $\Delta t = 2 \times 10^{-4}\ s$ and $\Delta t = 2.1 \times 10^{-4}\ s$ were set, and for each time-step, three damping coefficients were considered: $25, 200, \text{and } 300$. The figures below show the response of the rod's damping force over the iterations by setting the time-step and changing the damping coefficient. Both figures show that the curve that yields faster results is the curve that goes to zero without oscillations (blue curve with $c = 200$), corresponding to an overdamped system. On the other hand, after slightly increasing the time-step to $\Delta t = 2.1 \times 10^{-4}\ s$ the gray curve yields the worst results, taking longer to converge to a stable position. It is possible to conclude that the best combination of parameters for analyzing the current structure is $\Delta t = 2 \times 10^{-4}\ s$ and $c = 200\ \text{kNm/s}$, which corresponds to the blue curve combination.

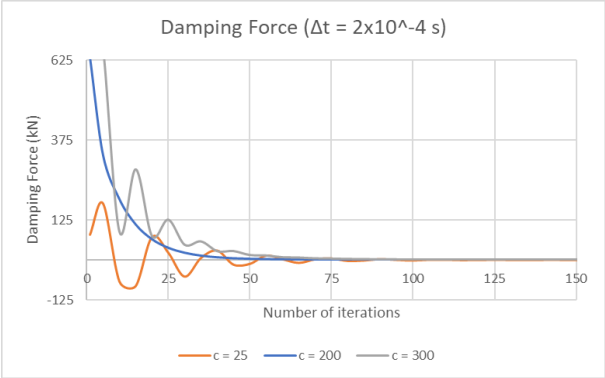

Figure 4.9 – Rod 1. Damping force changing over the damping coefficient. time-step $\Delta t = 2x10^{-4}$ s.

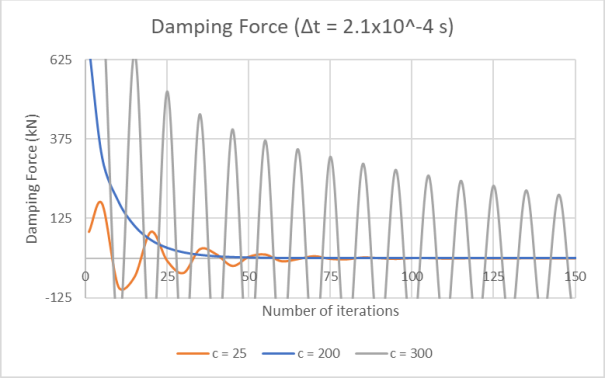

Figure 4.10 – Rod 1. Damping force changing over the damping coefficient. time-step $\Delta t = 2.1x10^{-4}$ s.

4.2.2 7-bar plane truss

To verify the 3DParticleSystem software for two-dimensional problems, a 7-bar plane truss system is analyzed, Figure 4.11. All rod elements are considered to have the same cross-sectional area of $20\ \mathrm{cm}^2$, mass per unit length of $\lambda = \rho A = 15.8\ kg/m$, and elastic modulus $E = 200\ GPa$. The system is loaded with an applied force of $200\ \mathrm{kN}$ along the z-axis at nodes B, D and E. The truss presented is a symmetrical structure with symmetrical loads

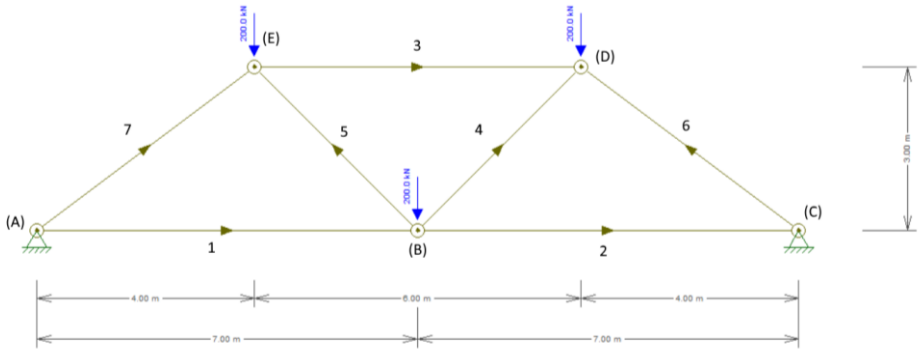

Figure 4.11 – 7-bar plane truss problem (adapted from FTOOL).

For this analysis, the structure is discretized into five particles and seven rods. Furthermore, the rods are oriented as described in Figure 4.11. The following tables present the summary of particle and rod data for the application of the numerical method.

Table 4.3 – Particles A and B, and their properties.

Particle	y (m)	z (m)	m (kg)
A	0	0	94.80
B	7	0	177.63
C	14	0	94.80
D	10	3	120.42
E	4	3	120.42

Table 4.4 – Geometry and properties of the rods.

Rod	PA	PB	L (m)	m (kg)	Angle
1	A	B	7	110.60	0
2	B	C	7	110.60	0
3	E	D	6	94.80	0
4	B	D	4.243	67.03	45º
5	B	E	4.243	67.03	-45º
6	C	D	5	79.00	-36.87º
7	A	E	5	79.00	36.87º

4.2.2.1 Axial forces

The values of the axial forces in each rod are shown in Table 4.5 and in Figure 4.19. In addition, the results of the ADINA analysis (considering small displacements) are presented to validate the reliability and to obtain a quick assessment of the calculated values. The computed results show that it is not fair to consider the hypothesis of small displacements, since the structure cannot support this amount of load, without computing considerable deformations. From the modeling point of view, it would be necessary to increase the stiffness of the structure to obtain smaller displacements, and, consequently, smaller deformations.

The computed results after 822 iterations show that the axial forces in rods 1 and 2 are $F_{axial} = 1.853\ kN$. This value is computed by applying Equation (23) which depends on the displacement of the particles, but also on the stiffness. It is known that the relative displacement of Particle B along the z-direction at the said instant is $\delta_z = 21.318\ mm$. The current length of Rod 1 is around $L = \sqrt{7^2 + (21.318 \times 10^{-3})^2} \approx 7.0000325\ m$, so the rod has lengthened $\Delta L = 3.25 \times 10^{-5}\ m$. Consequently, the internal force is given by $F_{Hooke} = \frac{EA}{L}\Delta L = \frac{200\ Gpa \times 20cm^2 \times 10^2}{7\ m} \times 3.25 \times 10^{-5}\ m \approx 1.85\ kN$. Finally, the axial force corresponds to the sum of the internal force with the damping force. As a simplification, it can be considered that $F_{axial} \approx F_{Hooke}$, even though there is a residual damping force generated by a residual velocity in each particle according to Equation (32).

Table 4.5 – 7-bar plane truss. Axial forces.

Rods	Axial Force (kN)		
	ADINA	3DParticleSystem	RDif (%)
1	0.00	1.85	-
2	0.00	1.85	-
3	-500.00	-500.00	5.17E-08
4	141.42	141.42	2.52E-04
5	141.42	141.42	2.52E-04
6	-500.00	-500.00	1.76E-08
7	-500.00	-500.00	1.76E-08

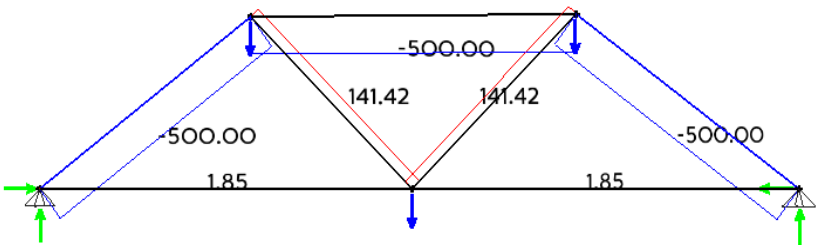

Figure 4.12 – Axial forces in the 7-bar plane truss problem. $EA = 4 \times 10^5\ kN$.

4.2.2.2 Rod's stress and strain and deformed structure

Even though the numerical method returns a good approximation for the axial force at an early stage, it is only valid to compute the stress once the damping force corresponds to a substantial percentage of the rod's axial force (around 10^{-4} %).

Table 4.6 presents the relative displacements in the 7-bar plane truss. The results demonstrate that it takes about 822 iterations to get a good approximation of the displacements. Moreover, it shows that the relative difference of the nodal displacement is about 0.209% when comparing 3DParticleSystem results with ADINA results (small displacements).

Figure 4.13 shows the deformed structure, on the left and stress-strain curve of Rod 3, on the right side. The blue dot on the graph represents the stress-strain pair after 822 iterations.

Table 4.6 – Relative displacements in the 7-bar plane truss.

Particle	ADINA		3DParticleSystem		RDif (%)	
	Δy (mm)	Δz (mm)	Δy (mm)	Δz (mm)	Δy	Δz
B	0.00	-21.29	0.00	-21.32	-	1.31E-01
D	-3.75	-15.42	-3.75	-15.45	1.18E-05	2.09E-01
E	3.75	-15.42	3.75	-15.45	1.18E-05	2.09E-01

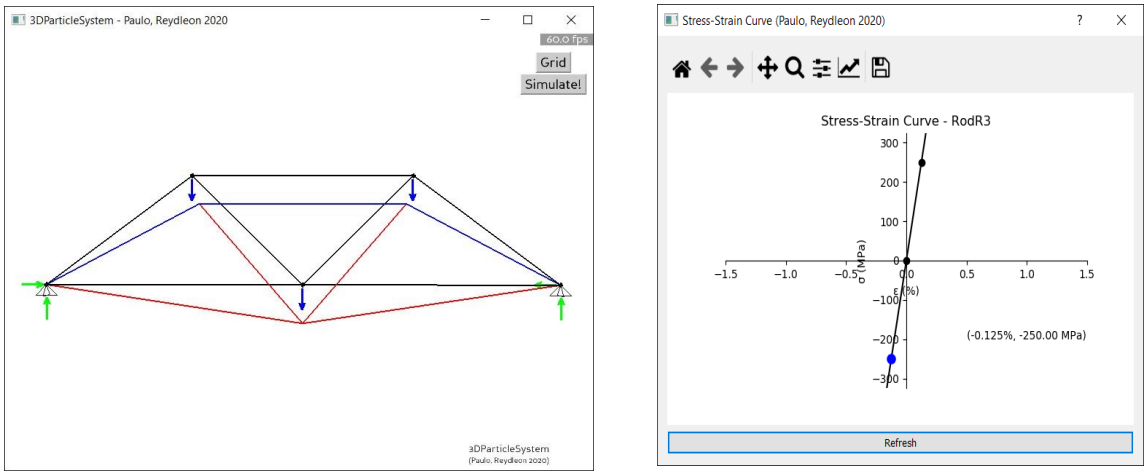

Figure 4.13 – The deformed shape of the 7-bar plane truss, amplified 50x (left). Stress-strain curve after 822 iterations (right).

4.2.2.3 Particle E and Rod 7

The physics engine is constantly correcting each particle velocities and positions throughout the iterations until the unbalanced forces are null everywhere. The internal force in Rod 7 depends on the strain therein. This quantity only corresponds to the relative displacements of Particle E since Particle A has a fixed support, allowing neither motion nor velocity. With similar behavior, the damping force of Rod 7 depends only on the y and z velocity of Particle E. Figure 4.14 shows the axial force in Rod 7 over the iterations, along with the contribution of internal and damping forces on the current structural system.

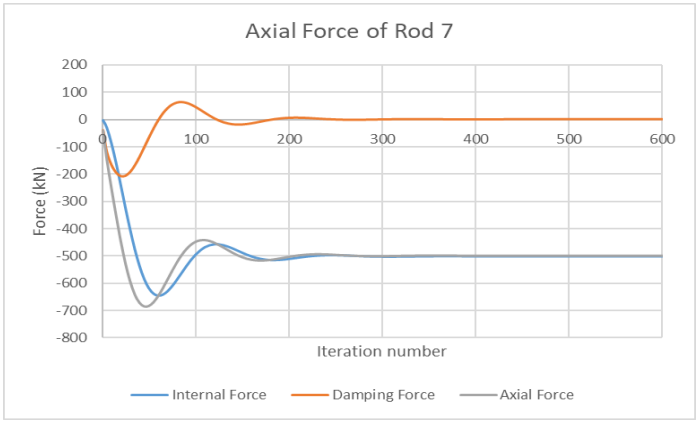

Figure 4.14 – Rod 7. Axial Forces over the iterations.

4.2.2.4 Particle B

The results of the relative vertical displacement of Particle B are stored over the simulation and are shown in Figure 4.15. After 300 iterations, the numerical method already presents a satisfactory result since the relative vertical displacement of Particle B is already around $\delta_z = 21.316\ \mathrm{mm}$.

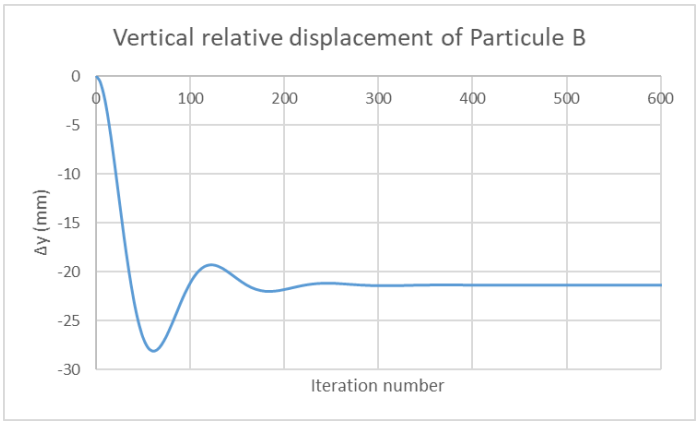

Figure 4.15 – Vertical relative displacement of Particle B over the iterations.

4.2.3 9-bar space truss

In order to verify the 3DParticleSystem software in three dimensions, a space truss system with 9 bars has been analyzed. The truss has a ball-and-socket joint at nodes A, B, C, and D, as shown in Figure 4.16. As with the last validation model, all the rods are composed with the same cross-sectional area with $\mathrm{A} = 20\ \mathrm{cm}^2$; the mass per unit length of the rod element is $\lambda = \rho A = 15.8\ kg/m$ and modulus of elasticity of $\mathrm{E} = 200\ \mathrm{GPa}$. Furthermore, Figure 4.16 also presents the loading case.

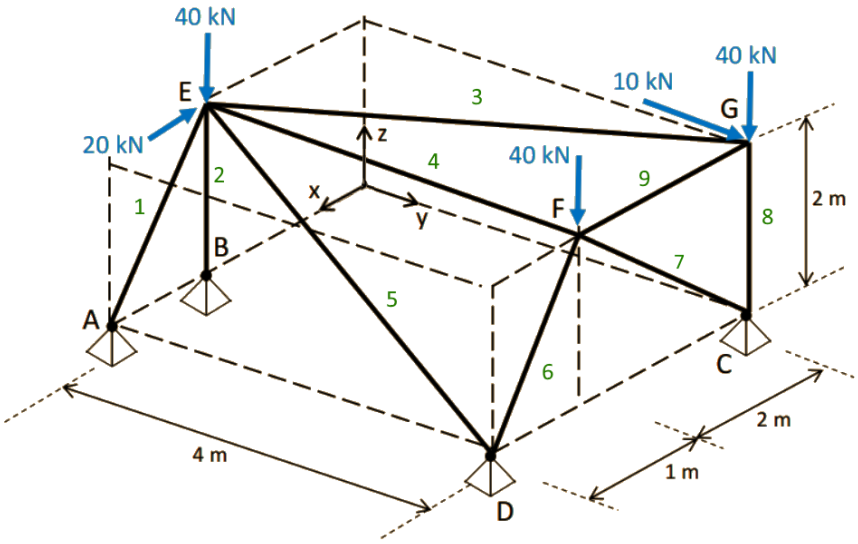

Figure 4.16 – 9-bar space truss. Adapted from [76].

The computed axial forces and relative displacements are summarized in Table 4.7 and Table 4.8, respectively. The 3DParticleSystem takes 1187 iterations to meet the stopping criterion. The maximum relative difference is around 4.86×10^{-3} % when compared with ADINA results (small displacements). This level of accuracy in the application of the 3DParticleSystem to the analysis of 3D trusses is quite good and serves as a validation of the developed code.

Table 4.7 – 9-bar space truss. Axial forces.

Rods	Axial Force (kN)		
	ADINA	3DParticleSystem	RDif (%)
1	61.49	61.49	1.40E-03
2	-90.00	-90.00	5.57E-04
3	11.18	11.18	1.36E-03
4	0.00	0.00	-
5	-11.46	-11.46	4.86E-03
6	-33.54	-33.54	1.75E-04
7	-14.14	-14.14	9.63E-04
8	-40.00	-40.00	6.26E-07
9	-5.00	-5.00	1.92E-03

Table 4.8 – 9-bar space truss. Relative displacements.

Particle	3DParticleSystem results		
	Δy (mm)	Δz (mm)	Δx (mm)
E	-1.67	0.34	-0.45
F	0.05	0.34	-0.19
G	0.07	1.35	-0.20

The figures below show the 3DParticleSystem graphical simulation outcome. Figure 4.17 shows the axial force diagram. Figure 4.18 shows the deformed shape.

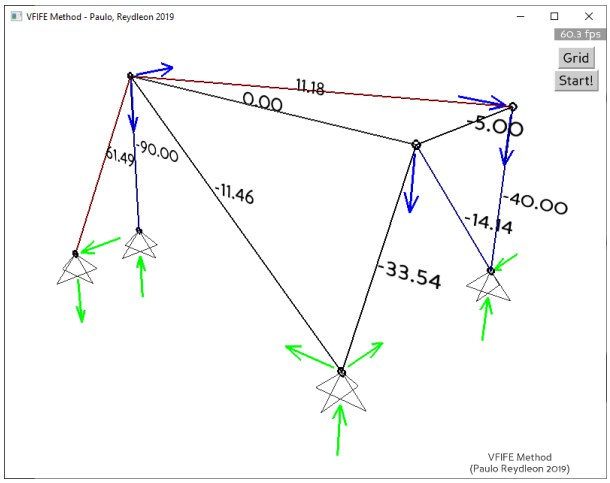

Figure 4.17 – 9-bar space truss. Axial forces.

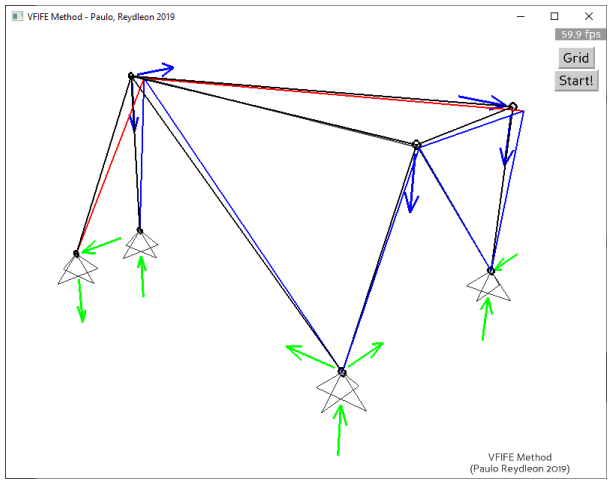

Figure 4.18 – 9-bar space truss. The deformed shape considering a scaling factor of 100.

4.3 Numerical simulation – Approach 2

This section applies Approach 2 with the large displacements formulation to simulate the 7-bar plane truss, a shallow geodesic dome, and a double layer grid. As presented before, Approach 2 applies the kinetic damping to achieve convergence, and the internal forces are calculated using Equation (25). This approach makes the PSA3D physics engine suitable for modeling large displacements, once it follows the movement of the particles.

4.3.1 7-bar plane truss

In this example, the 7-bar plane truss is used to allow for large displacements. The stiffness is decreased ten times. Consequently, the relative displacements increase, and the structure has large displacements.

The values of the axial forces, stresses, and strain on each rod are shown in Table 4.9 and Figure 4.19. The results presented are satisfactory when compared with ADINA results (large displacements mode). Moreover, it shows that the maximum relative difference of the axial forces is about 1.19%, in rods 1 and 2.

Table 4.9 – 7-bar plane truss. Axial forces.

Rods	Axial Force (kN)		
	ADINA	3DParticleSystem	RDif (%)
1	20.48	20.24	1.19
2	20.48	20.24	1.19
3	-522.63	-522.48	0.03
4	138.26	138.28	0.02
5	138.26	138.28	0.02
6	-521.05	-520.91	0.03
7	-521.05	-520.91	0.03

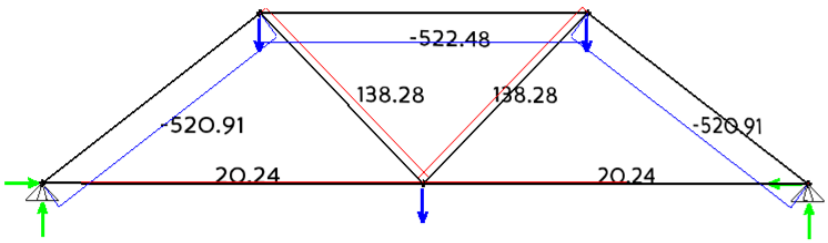

Figure 4.19 – 7-bar plane truss problem. $EA = 4 \times 10^4$ *kN.*

Table 4.11 presents the relative displacements in the 7-bar plane truss. The results show that the maximum relative difference of the nodal displacement is about 0.67%. Moreover, it shows that the relative error in Rod 3 is 1.3062%, which corresponds to compression stress of $2612.41\ MPa$.

Table 4.10 – 24-bar space truss. Stress and strain results.

Rods	ADINA		3DParticleSystem		RDif (%)
	ε (%)	σ (MPa)	ε (%)	σ (MPa)	σ
1	0.0512	102.40	0.0506	101.18	1.19
3	-1.3066	-2613.15	-1.3062	-2612.41	0.03
5	0.3456	691.28	0.3457	691.41	0.02
7	-1.3026	-2605.24	-1.3023	-2604.56	0.03

Table 4.11 – Relative displacements in the 7-bar plane truss.

Particle	ADINA		3DParticleSystem		RDif (%)	
	Δy (mm)	Δz (mm)	Δy (mm)	Δz (mm)	Δy	Δz
B	0	-224.03	0.	-222.71	-	0.59
D	-39.20	-164.90	-38.95	-163.80	0.64	0.67
E	39.20	-164.90	38.95	-163.80	0.64	0.67

4.3.2 24-bar Space Truss (shallow geodesic dome)

A notable example of a Buckminster Fuller's Geodesic Dome is the massive aluminum structure, known as Materials Park, from ASM International in Ohio, USA, Figure 4.20, on the left. Another example of the same architect is the Environment Museum in Montreal, Canada, Figure 4.20, on the right.

Figure 4.20 – ASM International in Ohio, USA, [94] (left). Environment Museum in Montreal, Canada, [95] (right).

This type of structural system is commonly used to perform nonlinear analysis, as in large displacement elastoplastic analysis of space trusses by Freitas et al. [77] and subsequently considering large strains, damage, and plasticity in Driemeier's work [78]. In addition, it is usually analyzed in particle-based methods such as the FPM [6] and the VFIFE method [23]. To demonstrate the versatility of the 3DParticleSystem software, a 24-bar shallow geodesic dome space truss, shown in Figure 4.21, is analyzed.

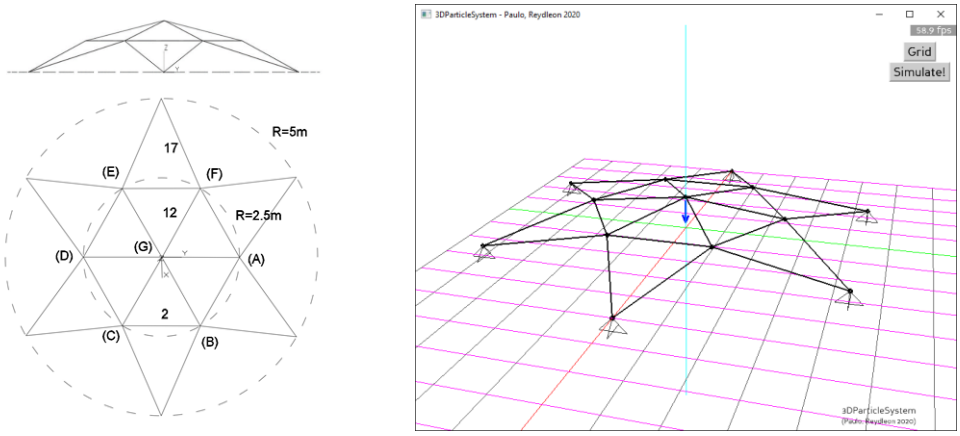

Figure 4.21 – 24-bar space truss (left). Axisymmetric view of the 24-bar space truss in the 3DParticleSystem software (right).

All rod elements are considered to have the same cross-sectional area of $20\ \mathrm{cm}^2$, the mass per unit length of the rod element is $\lambda = \rho A = 15.8\ kg/m$, and elastic modulus of $\mathrm{E} = 200\ \mathrm{GPa}$. The central particle is loaded with an applied force of 500 kN.

The numerical results of the 3DParticleSystem software are presented in the tables below and in Figure 4.22. The following results are validated by comparing them with the ADINA results. Table *4.13* shows that the 3DParticleSystem software returns a very good approximation for the relative displacement of the particles and rods' axial forces. Furthermore, the developed software computes a maximum relative difference in the stress results of only $2.18 \times 10^{-2}\%$.

Table 4.12 – 24-bar space truss. Stress and strain results.

Rods	ADINA		3DParticleSystem		RDif (%)
	ε (%)	σ (MPa)	ε (%)	σ (MPa)	σ
2	0.1387	277.37	0.1386	277.27	3.50E-02
12	-0.2158	-431.66	-0.2158	-431.56	2.18E-02
17	-0.0654	-130.73	-0.0654	-130.72	1.78E-03

Table 4.13 – 24-bar space truss. Displacements results.

Particle	ADINA			3DParticleSystem			RDif (%)		
	Δx (mm)	Δy (mm)	Δz (mm)	Δx (mm)	Δy (mm)	Δz (mm)	Δx (mm)	Δy (mm)	Δz (mm)
A	0.00	3.47	-0.19	0.00	3.47	-0.19	-	0.06	4.30
B	3.00	1.73	-0.19	3.00	1.73	-0.18	0.12	0.24	4.16
C	3.00	-1.73	-0.19	3.00	-1.73	-0.18	0.12	0.24	4.16
D	0.00	-3.47	-0.19	0.00	-3.47	-0.19	-	0.06	4.30
E	-3.00	-1.73	-0.19	-3.00	-1.73	-0.18	0.12	0.24	4.16
F	-3.00	1.73	-0.19	-3.00	1.73	-0.18	0.12	0.24	4.16
G	0.00	0.00	-79.41	0.00	0.00	-79.35	-	-	0.09

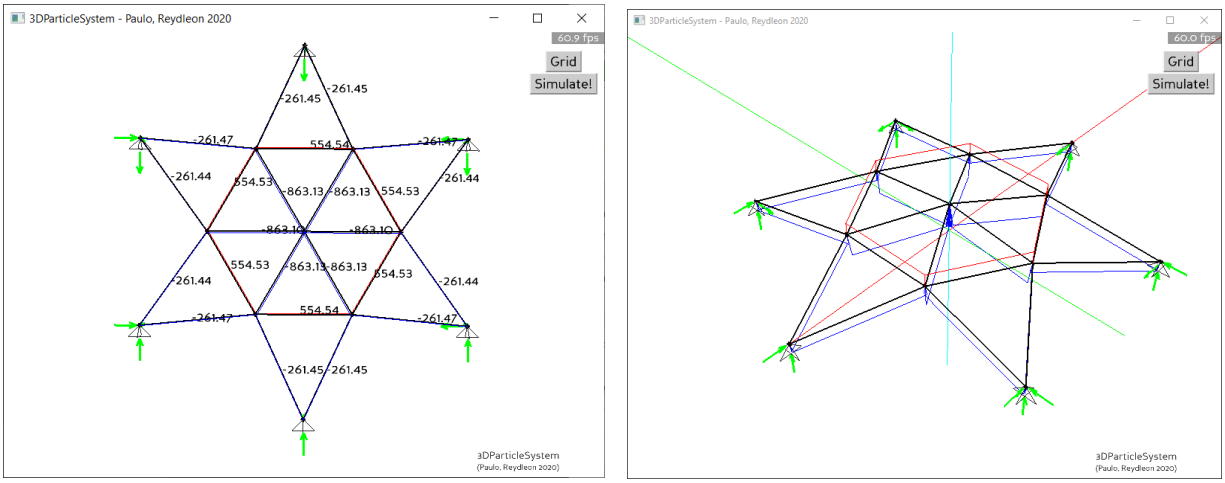

Figure 4.22 – 24-bar space truss. The computed axial forces using the developed software from a top view (left) and axisymmetric view (right).

Finally, Figure 4.23 shows the deformed shape in two different views.

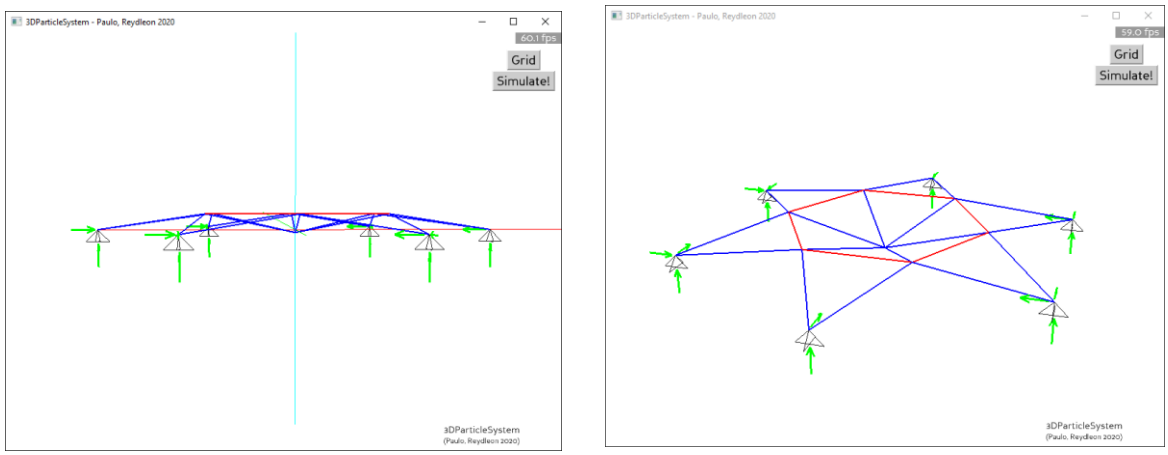

Figure 4.23 – The deformed Shape. Lateral view (left). Axisymmetric view (right)

4.3.3 Double Layer Grid

The Double Layer Grid (DLG), or flat surface space frame, is one of the most common examples of space structures. DLG is a horizontal slab usually composed of interconnected square pyramids and tetrahedral tubular steel struts [79][80].

The DLG used in this case study is based on the experimental model analyzed by Vendrame in [81] and, more recently, by Oliveira [82]. The general scheme of the prototypes tested by Vendrame is shown in Figure 4.24 on the left. This structure is usually denoted as the square-on-square offset space grid system. In this case, it is made up of $2.5m \times 2.5m$ orthogonal square pyramids with a height of $1.5m$. The structures are supported on the four vertices with a span of $7.5m$.

A simplification is here considered as only one of the four supports is a ball and socket support, and all the other three supports are roller supports. As the load case for this analysis, a total of $16000\ kN$ is applied over four nodes highlighted in Figure 4.24 on the left side.

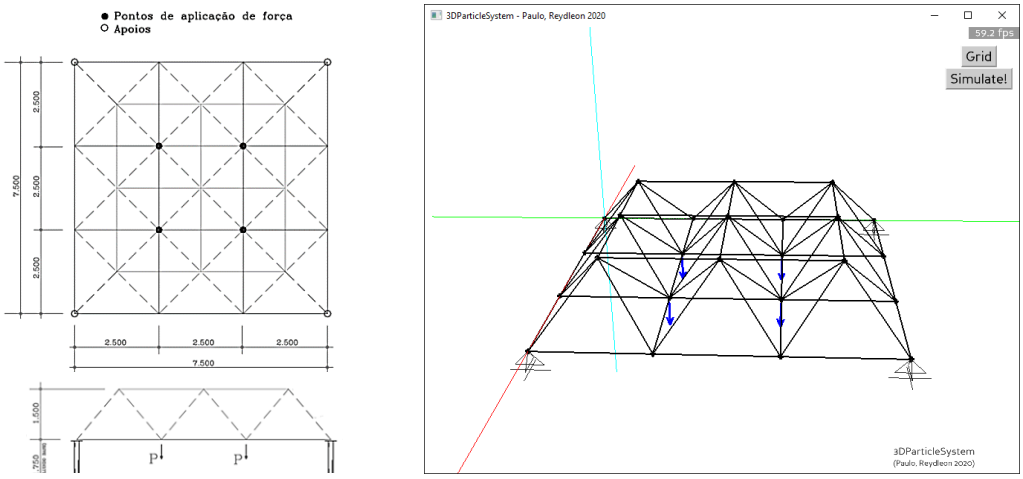

Figure 4.24 – Double Layer Grid (DLG) analyzed by Vendrame. Axisymmetric view of the DLG in the developed software.

As with the last validation model, all rods are composed of the same cross-sectional area with $\mathrm{A} = 20\ \mathrm{cm}^2$ and elastic modulus of $\mathrm{E} = 200\ \mathrm{GPa}$.

4.3.3.1 Stress results

Stress results are summarized and compared with ADINA analysis in the tables below. Thus, the maximum compression stress occurs in the diagonal Rod 72 with approximately $6001.13\ MPa$. The maximum tensile stress occurs in the lower grille flange 2 with approximately $4852.98\ MPa$. Besides, the maximum relative difference is around 0.175% (Rod 27). The figures below show the graphical result of the DLG in different views.

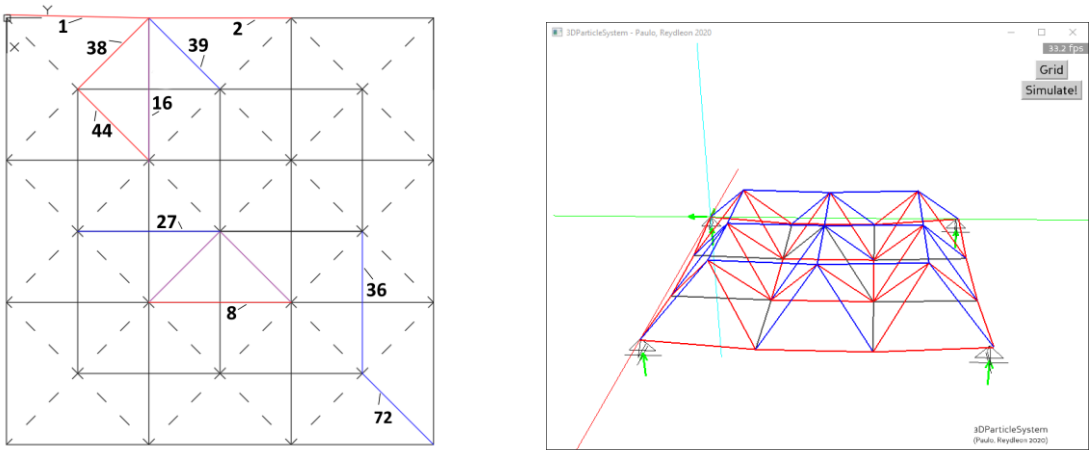

Figure 4.25 – Double Layer Grid (DLG). Top view of the DLG showing the analyzed rods (left). The deformed shape (right).

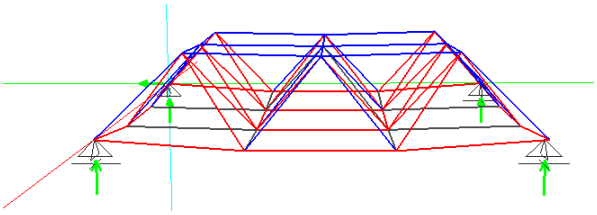

Figure 4.26 – Axisymmetric view of DLG's deformed shape in the 3DParticleSystem software.

Table 4.14 – Double Layer Grid (DLG). Axial forces.

Rods	Axial Force (kN)		
	ADINA	3DParticleSystem	RDif (%)
1	3428.79	3428.50	8.40E-03
2	4852.98	4850.46	5.19E-02
8	2039.07	2041.80	1.34E-01
16	267.60	267.39	8.00E-02
27	-3050.09	-3044.75	1.75E-01
36	-5187.12	-5190.09	5.72E-02
38	1124.88	1123.10	1.58E-01
39	-1557.57	-1554.95	1.68E-01
44	3377.71	3383.13	1.60E-01
72	-6001.13	-6001.69	9.26E-03

Table 4.15 – Double Layer Grid (DLG). Stress and strain results.

Rods	ADINA		3DParticleSystem		RDif (%)
	ε (%)	σ (MPa)	ε (%)	σ (MPa)	σ
1	0.8572	1714.39	0.8571	1714.25	8.11E-03
2	1.2132	2426.49	1.2126	2425.23	5.19E-02
8	0.5098	1019.53	0.5104	1020.90	1.34E-01
16	0.0669	133.80	0.0668	133.69	8.00E-02
27	-0.7625	-1525.05	-0.7612	-1522.38	1.75E-01
36	-1.2968	-2593.56	-1.2975	-2595.04	5.72E-02
38	0.2812	562.44	0.2808	561.55	1.58E-01
39	-0.3894	-778.79	-0.3887	-777.48	1.68E-01
44	0.8444	1688.86	0.8458	1691.56	1.60E-01
72	-1.5003	-3000.56	-1.5004	-3000.84	9.43E-03

4.4 Summary

In this section, a stopping criterion is set as $\left|F_i^{unb}\right| \leq 10^{-6}$ for each axis and all previously analyzed structures are re-analyzed, aiming to compare the various structures and to understand the numerical performance of the 3DParticleSystem software. Table 4.16 summarizes a set of truss structures that analyzes results, along with their geometry characteristics.

The number of iterations corresponds to how often the Numerical process occurs. In other words, a complete iteration corresponds to a cycle in all particles and rods of the analyzed structure, Numerical method, as before summarized in Figure 2.9. The number of iterations depends on the number of particles and rods but also depends on the magnitude of the external force applied. Even though the 9-bar space truss can easily be solved numerically, the shallow geodesic dome turns out to be more complex to solve due to its more demanding geometry.

Table 4.16 – Resume. Geometry and the respective number of iterations required to meet the stopping criterion for several truss structures.

Study Case	Approach	Particles	Rods	Type	Number of iterations
Axial force rod problem	1	2	1	1D	162
7-bar plane truss EA = 4E-5 kN	1	5	7	2D	822
9-bar space truss	1	7	9	3D	1187
Axial force rod problem	2	2	1	1D	39
7-bar plane truss EA = 4E-5 kN	2	5	7	2D	278
7-bar plane truss EA = 4E-6 kN	2	5	7	2D	328
24-bar space truss	2	13	24	3D	507
Double layer grid	2	25	72	3D	729

Table 4.17 summarizes the total times for the simulation of the Double Layer Grid. The analysis was made using a computer with a processor Intel® Core™ i7-8550U CPU @ 1.80GHz 1.99GHz with RAM 16,0 (15,9 usable). Three scenarios are presented: ADINA, the 3DParticleSystem without GUI and the 3DParticleSystem with GUI. ADINA takes around 0.11 seconds to reach a solution (according to its .out file). The 3DParticleSystem without GUI takes between 9 and 15 seconds to meet the stop criterion. In this case, the total time for the simulation depends on the computer processor; after restarting the computer, the 3DParticleSystem was launched using the Anaconda's console, and the total time was just 9 seconds. The 3DParticleSystem with GUI takes at least 17 seconds to meet the stopping criterion. During the simulation, it is possible to check the particle system's evolution and the deformed shape. In this case, the total simulation time depends on the rendering frequency on the canvas. It also depends on how often the results of the mid steps are saved in the output file. This feature is time-consuming, once the positions of the 25 particles must be saved on each iteration, along with the resulting internal forces of the 72 bars. On the other hand, this feature allows the user to easily compute graphs similar to Figure 4.2 and Figure 4.3 presented in section 4.2.1.

Table 4.17 – The total solution time for the simulation of the Double Layer Grid.

	ADINA	**3DParticleSystem (without GUI)**	**3DParticleSystem (with GUI)**
time (s)	~0.11	between 9 and 15	at least 17

4.5 Changing the model during the simulation

The work carried out by Martini with Arcade software [1][21] has proved to be particularly useful in teaching unstable structures and large displacements. In this way, real-time interactive physics software for structural analysis can help students understand some fundamental concepts of structural engineering, such as statically determinate (isostatic,) statically indeterminate, and unstable structures (mechanisms). These topics can be easily understood using two features of the 3DParticleSystem software, namely:

a) Removing rods during the simulation and immediately see the response,

b) Changing the support constraint during the simulation.

4.5.1 Removing rods in a statically indeterminate structure

The 7-bar plane truss, analyzed in chapter 4.2.2, is adopted here to present the feature of removing rods. Since this is a statically indeterminate structure of degree one, one rod may be removed from the structural system without causing it to collapse.

As with Arcade software [21], it is possible to select and remove a rod during a simulation and immediately see the system response to the structure change [83], Figure 4.27. In this example, the rod 1 is removed, which forces the particles to redistribute forces. However, since this structure is one-degree statically indeterminate, the removal of the bar does not cause collapse, as shown in Figure

4.27. Figure 4.28 shows the axial forces after removing Rod 1; in this figure, the color of the members indicates the axial force, with the blue color indicating compression and the red color denoting tension.

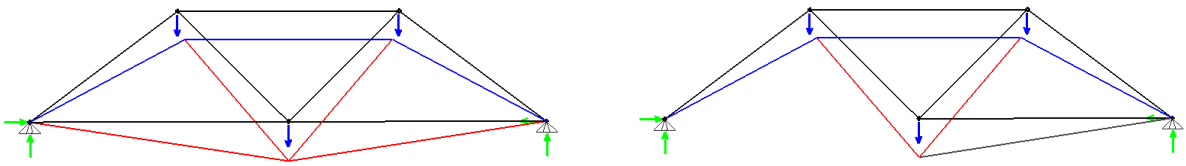

Figure 4.27 – Evolution of the structure system due to the removal of Rod 1.

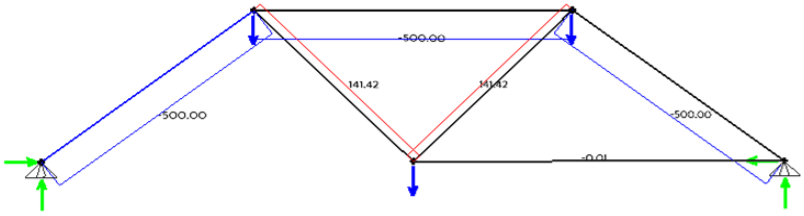

Figure 4.28 – Axial forces for the resulting structure after removing Rod 1.

4.5.2 Changing nodal constraints

Changing the constraint during simulation is another useful feature of the 3DParticleSystem software. In this example, the nodal restriction of Particle C, right-side constraint, is changed; then, this change causes the particles to redistribute the forces aiming to reach the state of equilibrium. Figure 4.29 shows the deformed shape, and Figure 4.30 shows the axial forces.

The figures below show that upon suppressing the horizontal restriction, the system becomes a statically determinate structure. Moreover, Figure 4.30 shows that the horizontal reaction of the suppressed support was 400 kN, which now corresponds to the bar being subjected to traction with equal value.

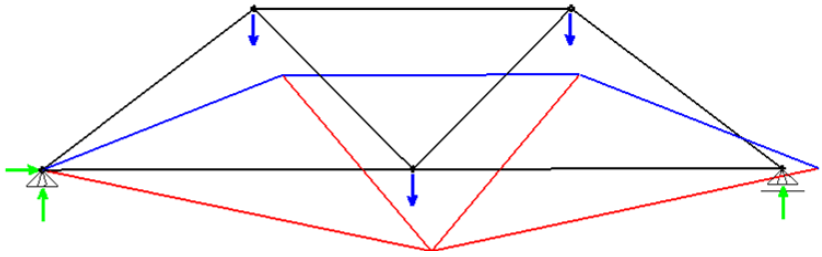

Figure 4.29 – Static equilibrium situation of a 7-bar plane truss system. The deformed shape.

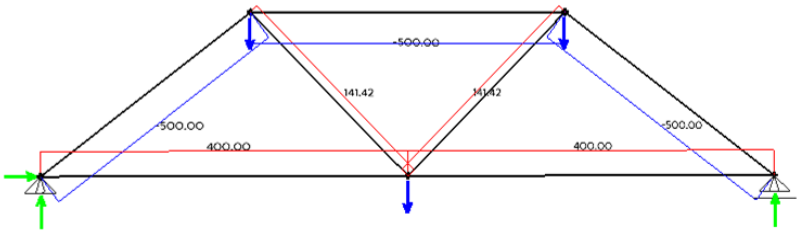

Figure 4.30 – Static equilibrium situation of a 7-bar plane truss system. Axial forces.

Then, Rod 1 is removed. Consequently, the system becomes unstable, as shown in the figure below.

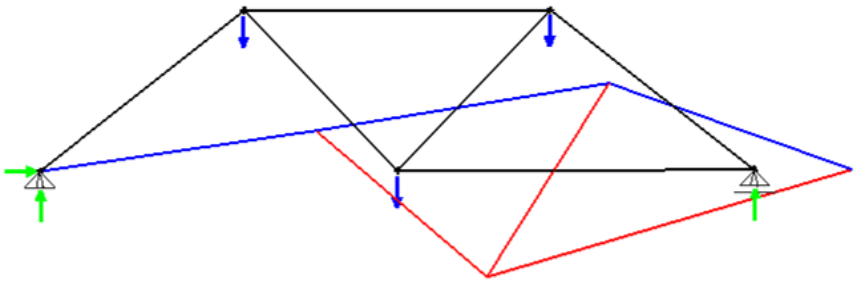

Figure 4.31 – Evolution of the system after changing the nodal constraint and removing a rod.

4.5.3 Removing a rod in the 9-bar Space Truss

An even more interesting feature is to remove rod elements in a three-dimensional structure system. To demonstrate this option, the 9-bar space truss, previously presented in Figure 4.16, was analyzed.

Since the current system is a statically determined structure, the rod removal causes the structure to become a partial mechanism; rods 3 and 8 cannot balance the loads applied to node G; thus, the results are diverging out of any numerical solution, Figure 4.32.

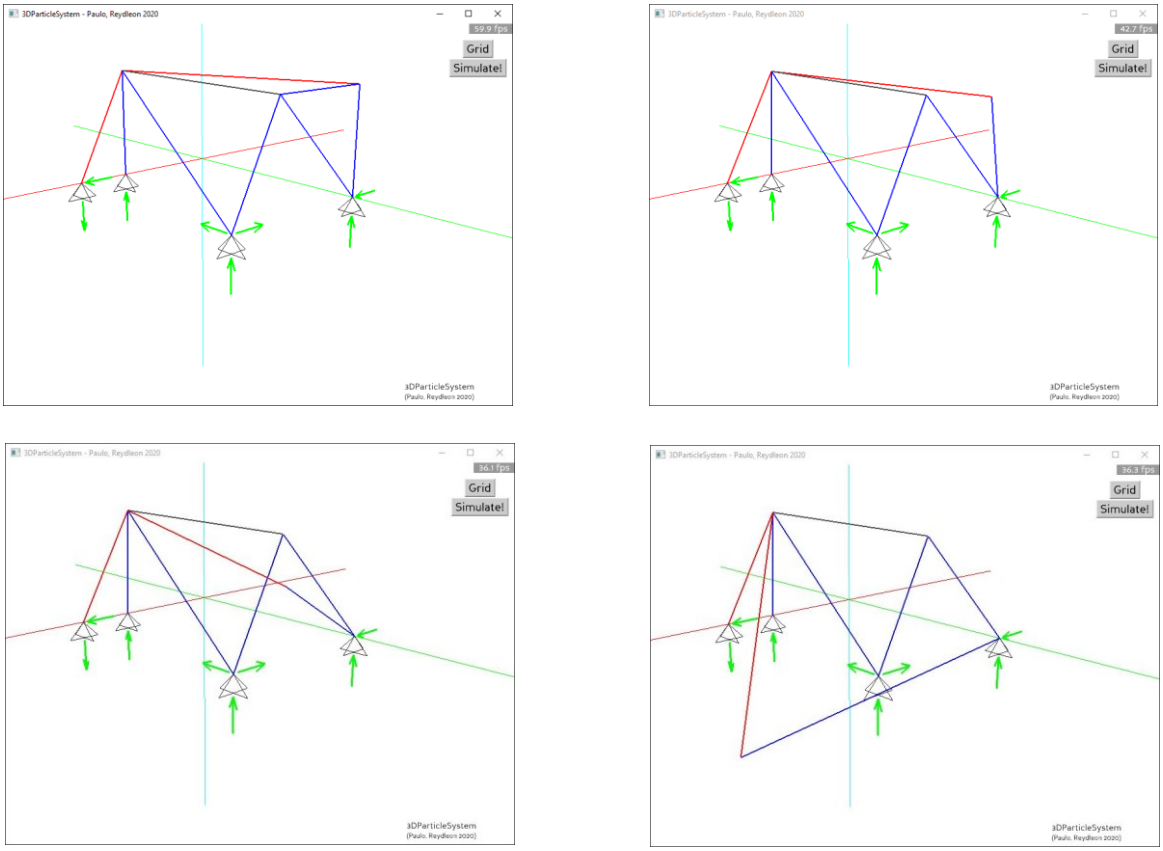

Figure 4.32 – Image sequence showing the collapse of 9-bar space truss when removing Rod 9. The deformed shape scaled 100 times (right).

4.5.4 Analyzing a Double Layer Grid

The complexity of structural analysis increases when analyzing a Double Layer Grid (DLG). Thus, this is commonly the subject of space truss analysis; however, the interpretation of these results may not be trivial due to their spatial geometry. Thus, the user can benefit from the use of 3DParticleSystem software features.

4.5.4.1 Removing rods in a DLG system

The following example shows what happens when several rods are removed in this complex structural system. In this example, first, Rod 16 is removed, followed by rods 57 and 58, all of which are rods with zero axial force, as shown in Figure 4.33. These changes do not cause large motions in the particles, just enough to redirect the unbalanced forces at each node. Thus, the stress and strain results remain unchanged, with equal value to the stage before the changes.

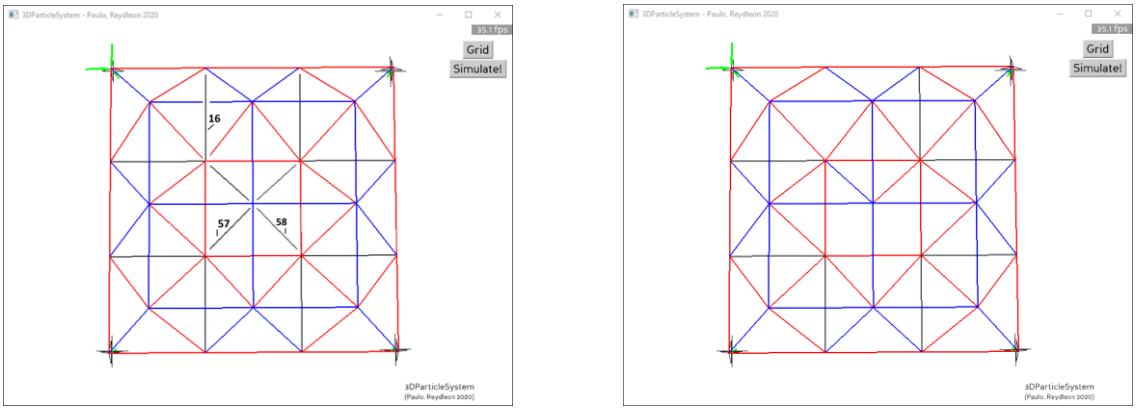

Figure 4.33 – DLG. After removing three zero-force members of the system

Then another nine rods corresponding to zero-force members are also removed, as shown in Figure 4.34. An impressive visual result is that this problem becomes equivalent to a typical form-finding problem. In both cases, the structure system continually tries to find its equilibrium shape/form.

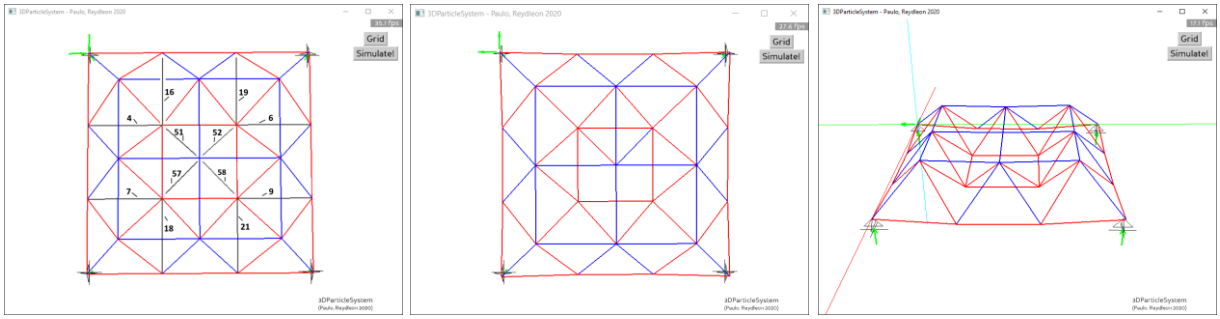

Figure 4.34 – Left to right. The label of the removed rods. DLG results after rods removal, top view, and axisymmetric view.

Later, by removing Rod 72, the collapse is instantaneous. Figure 4.35 shows the resulting computed mechanism.

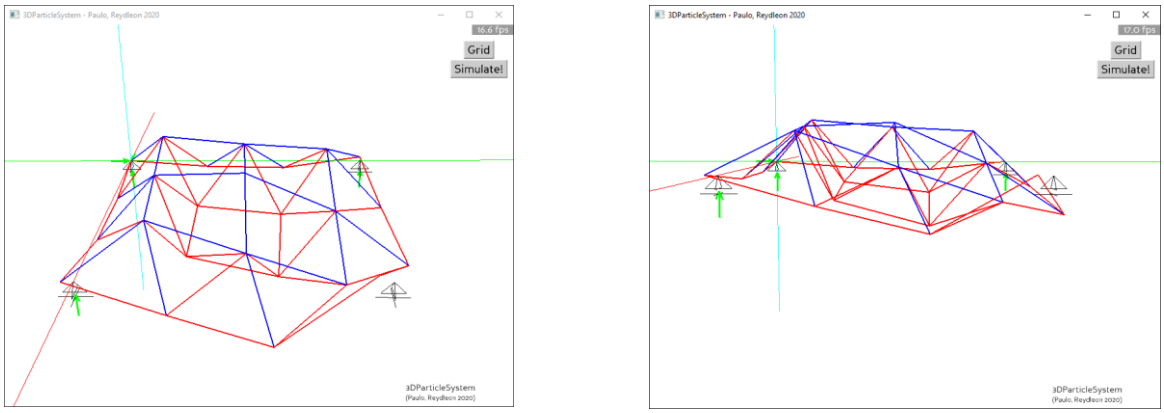

Figure 4.35 – DLG mechanism after removing a fundamental rod.

From the analysis presented above, it is possible to highlight some features of the 3DParticleSystem to follow the failure of structures by removing rods. This is an advantage of particle-based methods since it follows the motion of the particles. The 3DParticleSystem software is proving to be an interesting teaching tool with the potential to analyze various structures.

5 Conclusions

5.1 Main conclusions

The main objective of this thesis was to develop an interactive software that allows solving space trusses. This document explains all the steps for the implementation of a physics engine. It also explains the procedure to create a computer-aided design to render space trusses and their results. This document shows that the approach used in games can be integrated to create an interactive real-time physics software for structural analysis of space trusses and structural design applications. Even though the present approach is limited when compared to the Finite Element Method (FEM), when combined with a graphical rendering engine, it is possible to take advantage of its simplicity. Moreover, this approach enables new types of analyses and modes of interactivity, such as performing linear, nonlinear, and incremental analysis. Finally, it is possible to construct the temporal evolution of a structure where calculations are done in real-time, responding to input from the user. Such advantages are crucial for computer games that model some physical phenomena. The 3DParticleSystem software has great educational potential since the user does not need to have advanced knowledge of structural engineering or even prior knowledge of advanced commercial software to make the most of the developed software.

In this document, the physically-based modeling/particle system dynamics has been revised and implemented with a 3D graphical environment. The 3D graphical environment was developed using cross-platform PyQt and Panda3D frameworks, considering the fundamental principles of the object-oriented programming paradigm. In addition, this environment has some features that allow removing rods and changing the support conditions during the simulation. Besides, a feature that should be highlighted is the ability to display the stress-strain curve along with the simulation, which allows students to learn fundamental concepts of structural analysis.

The analyses presented in this document show good results, especially for the more demanding cases, the Double Layer Grid (DLG), and the shallow geodesic dome analyzes. Moreover, this software contributes to the visual perception of these structures.

5.2 Directions for future work

As future work, some needs may be met, some of which are related to the graphics engine, others related to the physics engine, and the numerical methods used. These needs can be divided into frame analysis, numerical method, nonlinearity, programming improvements, and usability.

5.2.1 Frame analysis

Numerical models like the Particle System approach have been successfully implemented in the analysis of 3D frames. Of these, two stand out. The first is an implementation that combines dynamic relaxation and co-rotational formulation [5] and is the numerical basis of two computer codes,

PushMePullMe [22] and the Catastrophe game [84]. The second corresponds to rotation formulations for dynamic relaxation with application to 3D frame structures with large displacements and rotations [85] presented by J. Li and J. Knippers. Therefore, the physics engine written so far can be upgraded to the analysis of 3D frame structures. However, the graphical rendering engine should be enhanced to handle the spatial frame, as there are some differences in representation, such as shear diagrams, torsional moment diagrams, and bending moment diagrams. Moreover, the established local coordinate system can be used to continue this project as it is designed to implement 3D bending and torsion [42]. In addition, it would be interesting to add beam elements with axial loading and torsion to the model. Further developments should explore the beam-column bending analysis.

5.2.2 Numerical method

In the current version, the 3DParticleSystem software is using the trapezoidal rule to solve the ordinary differential equation of motion. For future work, the implementation of the Runge-Kutta 4 method (RK4) may be considered. To implement this method, a new way of looping should be considered as it requires four structural evaluations per time-step [57]. Finally, it would be interesting to compare the two numerical methods, although the RK4 method is expected to compute better results with fewer iterations [38][60][57].

5.2.3 Nonlinearity

An advantage of the Particle System approach is its application in cases with geometrically nonlinear and physically nonlinear behavior. Regarding the nonlinearity of the material, the 3DParticleSystem software can be further improved by implementing other stress-strain curves, as this is a relatively straightforward task.

5.2.4 Programming improvements

Without changing the physics engine written so far, it is suggested to use parallel computing and use code objects. Code objects are a low-level detail of the CPython implementation [86] and represent a piece of executable code that has not yet been bound to a function. This report also aims to give some clues to change and leverage parallel computing for this type of numerical application [87]. Finally, it would be interesting to rewrite the numerical method in another programming language, such as C ++, aiming for better numerical performance.

5.2.5 Usability

Panda 3D game engine has many functionalities that were not explored in this document. Therefore, it is essential to improve the 3DParticleSystem GUI, as it will give more versatility to the numerical method, as well as allowing a better understanding of the physical phenomena involved in each analysis. Another possible improvement is to connect 3DParticleSystem software with the pymunk physics engine [12]. This combination can add other physical phenomena to the developed software, such as particle collisions, as well as improving numerical efficiency. Finally, the current version works for Desktop only. It would be interesting to have the 3DParticleSystem available as an application for Android and IOS.

References

[1] K. Martini, “Computational Issues in Non-linear Structural Analysis Using a Physics Engine,” in *Proceedings of the ASCE 17th Analysis and Computation Conference*, 2006.

[2] K. Martini, “Nonlinear Dynamics: An Intuitive Digital Representation of Structure,” *J. Educ. Built Environ.*, vol. 8, no. 1, 2013.

[3] A. Kilian and J. Ochsendorf, “Particle-spring systems for structural form finding,” *J. Int. Assoc. Shell Spat. Struct. - IASS*, vol. 46, no. 148, pp. 77–84, 2005.

[4] A. Day, *An Introduction to Dynamic Relaxation*. 1965.

[5] G. Senatore and D. Piker, “Interactive real-time physics: An intuitive approach to form-finding and structural analysis for design and education,” *CAD Comput. Aided Des.*, vol. 61, 2015.

[6] Y. Yu, G. H. Paulino, and Y. Luo, “Finite Particle Method for Progressive Failure Simulation of Truss Structures,” *J. Struct. Eng.*, vol. 137, no. 10, pp. 1168–1181, 2011.

[7] M. K. Yip, E. S. Liu, M. K. Cheung, R. M. Lung, and G. Yu, “Design Decisions in Game Middleware Development : Experiences from Lucid Platform,” 2005.

[8] “Hanov®.” [Online]. Available: http://www.havok.com/. [Accessed: 22-Oct-2019].

[9] PhysX, “No Title.” [Online]. Available: http://www.ageia.com. [Accessed: 22-Oct-2019].

[10] “Open dynamics engine.” [Online]. Available: http://www.ode.org/. [Accessed: 22-Oct-2019].

[11] “Chipmunk.” [Online]. Available: https://chipmunk-physics.net/. [Accessed: 22-Oct-2019].

[12] “Pymunk.” [Online]. Available: http://www.pymunk.org. [Accessed: 22-Oct-2019].

[13] G. van Rossum, “Python,” 2018. [Online]. Available: https://python.org.

[14] “Pygame.” [Online]. Available: https://www.pygame.org. [Accessed: 23-Dec-2019].

[15] A. Bargteil and T. Shinar, *An introduction to physics-based animation*. 2018.

[16] E. Einhorn, T. Langner, R. Stricker, C. Martin, and H. M. Gross, “MIRA - Middleware for robotic applications,” *IEEE Int. Conf. Intell. Robot. Syst.*, pp. 2591–2598, 2012.

[17] E. Todorov, T. Erez, and Y. Tassa, “MuJoCo: A physics engine for model-based control,” *IEEE Int. Conf. Intell. Robot. Syst.*, pp. 5026–5033, 2012.

[18] “Renderware.” [Online]. Available: http://www.renderware.com/. [Accessed: 22-Oct-2019].

[19] “Unity.” [Online]. Available: https://unity.com/. [Accessed: 22-Oct-2019].

[20] “Unreal.” [Online]. Available: http://www.unrealtechnology.com/. [Accessed: 22-Oct-2019].

[21] K. Martini, “Arcade - Interactive Non-linear Structural Analysis and Animation.” [Online]. Available: http://web.arch.virginia.edu/arcade/. [Accessed: 22-Oct-2019].

[22] “PushMePullMe 3D.” [Online]. Available: https://expeditionworkshed.org/workshed/push-me-pull-me-3d/. [Accessed: 22-Oct-2019].

[23] E. C. Ting, C. Shih, and Y. K. Wang, “Fundamentals of a vector form intrinsic finite element: Part I. Basic procedure and a plane frame element,” *J. Mech.*, vol. 20, no. 2, pp. 113–122, 2004.

[24] E. C. Ting, C. Shih, and Y. K. Wang, “Fundamentals of a vector form intrinsic finite element: Part II. Plane Solid Elements,” *J. Mech.*, vol. 20, no. 2, 2004.

[25] C. Shih, Y. K. Wang, and E. C. Ting, “Fundamentals of a vector form intrinsic finite element: Part III. Convected material frame and examples,” *J. Mech.*, vol. 20, no. 2, pp. 133–143, 2004.

[26] C. Y. Wang, C. C. Chuang, R. Z. Wang, and T. Y. Wu, “Nonlinear dynamic analysis of reticulated

space truss structures," *J. Mech.*, vol. 22, no. 3, pp. 199–212, 2006.

[27] X. Lu, X. Lin, and L. Ye, "Simulation of Structural Collapse with Coupled Finite Element-Discrete Element Method," *Comput. Struct. Eng.*, pp. 127–135, 2009.

[28] K. H. Lien, Y. J. Chiou, R. Z. Wang, and P. A. Hsiao, "Vector Form Intrinsic Finite Element analysis of nonlinear behavior of steel structures exposed to fire," *Eng. Struct.*, vol. 32, no. 1, pp. 80–92, 2010.

[29] Y. F. Duan, S. M. Wang, R. Z. Wang, C. Y. Wang, J. Y. Shih, and C. B. Yun, "Vector Form Intrinsic Finite-Element Analysis for Train and Bridge Dynamic Interaction," *J. Bridg. Eng.*, vol. 23, no. 1, p. 04017126, 2017.

[30] Y. Yu and Y. Luo, "Structural collapse analysis based on finite particle method I: Basic approach (in Chinese)," *Jianzhu Jiegou Xuebao/ J. Build. Struct.*, vol. 32, no. 11, pp. 17–2, 2011.

[31] Y. Yu and Y. Luo, "Structural collapse analysis based on finite particle method II: Key problems and numerical examples (in Chinese)," *Jianzhu Jiegou Xuebao/ J. Build. Struct.*, vol. 32, no. 11, pp. 27–35, 2011.

[32] X.-H. Long, R. Yue, Y.-T. Ma, and J. Fan, "Finite Particle Method-Based Collapse Simulation of Space Steel Frame Subjected to Earthquake Excitation," *Shock Vib.*, vol. 2018, pp. 1–19, 2018.

[33] Y. Yu and Y. Luo, "Finite particle method for kinematically indeterminate bar assemblies," *J. Zhejiang Univ. A*, vol. 10, no. 5, pp. 669–676, 2009.

[34] Y. Yu and Y. Z. Luo, "Motion analysis of deployable structures based on the rod hinge element by the finite particle method," *Proc. Inst. Mech. Eng. Part G J. Aerosp. Eng.*, vol. 223, no. 7, pp. 955–964, 2009.

[35] Y. Yu, P. Xia, and C. Yang, "Form finding and collapse analysis of cable nets under dynamic loads based on finite particle method," *C. - Comput. Model. Eng. Sci.*, vol. 117, no. 1, pp. 73–89, 2018.

[36] Y. Yu and X. Zhu, "Nonlinear dynamic collapse analysis of semi-rigid steel frames based on the finite particle method," *Eng. Struct.*, vol. 118, pp. 383–393, 2016.

[37] C. T. Mueller, "Computational Exploration of the Structural Design Space. PhD. thesis MIT," 2014.

[38] K. Martini, "Non-linear Structural Analysis as Real-Time Animation: Borrowing from the Arcade," in *Proceedings of the Computer-Aided Architectural Design Futures 2001 Conference*, 2001, pp. 643–656.

[39] P. M. A. da S. Lopes, "Software development for assistance in the learning of structural analysis," 2015.

[40] J. E. M. de Matos, "Simulação de problemas da mecânica estrutural utilizando 'physics engines' (in Portuguese)," 2017.

[41] A. Witkin, "Physically Based Modeling: Principles and Practice," 1997. [Online]. Available: http://www.cs.cmu.edu/~baraff/sigcourse/. [Accessed: 01-Sep-2019].

[42] D. Baraff, "Rigid Body Dynamics - SIGGRAPH 2001 COURSE NOTES," 2001. [Online]. Available: http://www.cs.cmu.edu/afs/cs/user/baraff/www/sigcourse/. [Accessed: 01-Sep-2019].

[43] M. R. Barnes, "Form Finding and Analysis of Tension Structures by Dynamic Relaxation," *Int. J.*

Sp. Struct., vol. 14, no. 2, pp. 89–104, 1999.

[44] "Panda3D." [Online]. Available: https://www.panda3d.org/.

[45] "Pyqt." [Online]. Available: https://riverbankcomputing.com. [Accessed: 29-Aug-2019].

[46] "Ftool." [Online]. Available: https://www.tecgraf.puc-rio.br/ftool/.

[47] "ADINA." [Online]. Available: http://www.adina.com/. [Accessed: 30-Oct-2019].

[48] "SAP2000 - CSI Portugal." [Online]. Available: https://www.csiportugal.com/software/2/sap2000. [Accessed: 02-Sep-2019].

[49] "ofxMSAPhysics." [Online]. Available: http://www.memo.tv/2009/ofxmsaphysics/. [Accessed: 22-Oct-2019].

[50] "TRAER.PHYSICS 3.0." [Online]. Available: http://murderandcreate.com/physics/. [Accessed: 09-Jan-2020].

[51] F.P. Beer, E. R. Johnston, and J. T. DeWolf, *Mechanics of materials, 5th SI Edition*. .

[52] "ADMET." [Online]. Available: https://www.admet.com/testing-applications/test-types/tension-testing/. [Accessed: 27-Dec-2019].

[53] H. A. Barnes, J. F. Hutton, and K. Walters, *An Introduction to Rheology*, vol. 3. 1989.

[54] University of Strathclyde, "Introduction to PV Design by Analysis." [Online]. Available: http://personal.strath.ac.uk/j.wood/ccopps_dba/notes/dba_intro_content_1.htm. [Accessed: 29-Aug-2019].

[55] MechaniCalc, "Mechanical Properties of Materials." [Online]. Available: https://mechanicalc.com/reference/mechanical-properties-of-materials#stress-strain-approx. [Accessed: 29-Aug-2019].

[56] R. G. Budynas and J. Keith Nisbett, *Shigley's Mechanical Engineering Design*. .

[57] K. Martini, "A Particle-System Approach to Real-Time Non-Linear Analysis," in *Proceedings of the 7th National Conference on Earthquake Engineering*, 2002.

[58] M. Rezaiee-Pajand and H. Rezaee, "Fictitious time step for the kinetic dynamic relaxation method," *Mech. Adv. Mater. Struct.*, vol. 21, no. 8, pp. 631–644, 2014.

[59] H. P. Gavin, "Numerical Integration in Structural Dynamics," *CEE 541. Struct. Dyn.*, 2014.

[60] H. Gould, J. Tobochnik, and W. Christian, *Introduction to Computer Simulation Methods: Applications to Physical Systems third edition*. 2005.

[61] C. Preisinger and M. Heimrath, "Karamba - A toolkit for parametric structural design," *Struct. Eng. Int. J. Int. Assoc. Bridg. Struct. Eng.*, vol. 24, no. 2, pp. 217–221, 2014.

[62] "AutoCad Autodesk." [Online]. Available: https://www.autodesk.com/products/autocad-lt/overview. [Accessed: 30-Oct-2019].

[63] ADINA R & D, "Theory and Modeling Guide," vol. I, no. December, p. 1166, 2012.

[64] "Anaconda." [Online]. Available: https://www.anaconda.com/.

[65] "QEventLoop Class Reference." [Online]. Available: https://doc.qt.io/archives/3.3/qeventloop.html#details.

[66] "The Task Function - Panda3D Manual." [Online]. Available: https://www.panda3d.org/manual/?title=Tasks. [Accessed: 16-Dec-2019].

[67] "NumPy." [Online]. Available: https://numpy.org/. [Accessed: 31-Oct-2019].

[68] Qt, “About Qt.” [Online]. Available: https://wiki.qt.io/About_Qt. [Accessed: 29-Aug-2019].

[69] “Qt Documentation Archives - Signals & Slots.” [Online]. Available: https://doc.qt.io/archives/qt-4.8/signalsandslots.html.

[70] GameDesigning, “In-Depth Panda3D Engine Review.” [Online]. Available: https://www.gamedesigning.org/engines/panda3d/. [Accessed: 29-Aug-2019].

[71] Unity, “Unity User Manual.” [Online]. Available: https://docs.unity3d.com/Manual/UICanvas.html. [Accessed: 29-Aug-2019].

[72] Titangroupco, “Panda3D Manual.” [Online]. Available: http://remote.titangroupco.com:6999/panda3d-manual-python-1.9.2/Main_Page.html. [Accessed: 29-Aug-2019].

[73] Panda3d, “panda3d.core.NodePath.” [Online]. Available: https://docs.panda3d.org/1.10/python/reference/panda3d.core.NodePath. [Accessed: 26-Jul-2020].

[74] S. Madhav, *Game Programming Algorithms and Techniques: A Platform-Agnostic Approach*. 2013.

[75] L. R. Hellevik, “Numerical methods for engineers,” *Math. Comput. Simul.*, vol. 33, no. 3, p. 260, 2003.

[76] Universiti Teknologi Malaysia, “Space Truss - Lecture 8,” *Chapter 6 - Space Trusses*. [Online]. Available: http://engineering.utm.my/civil/chapter-6/. [Accessed: 29-Aug-2019].

[77] J. A. T. de Freitas and A. C. B. S. Ribeiro, “Large displacement elastoplastic analysis of space trusses,” *Comput. Struct.*, vol. 44, no. 5, pp. 1007–1016, 1992.

[78] L. Driemeier, S. P. Baroncini Proença, and M. Alves, “A contribution to the numerical nonlinear analysis of three-dimensional truss systems considering large strains, damage and plasticity,” *Commun. Nonlinear Sci. Numer. Simul.*, vol. 10, no. 5, pp. 515–535, 2005.

[79] T. T. Lan, “Structural Engineering Handbook - Space Frame Structures,” 2005.

[80] M. El-Shami, S. Mahmoud, and M. Elabd, “Effect of floor openings on the capacity of composite space trusses,” *J. King Saud Univ. - Eng. Sci.*, vol. 30, no. 2, pp. 130–140, 2018.

[81] A. M. Vendrame, “Contribution to the study of lattice domes using steel tubular elements (In Portuguese) - MSc Thesis,” *EESC - USP*, p. 139, 1999.

[82] C. M. Oliveira, “Colapso Progressivo de Treliças Espaciais,” 2017.

[83] K. Martini, “Teaching Structural Behavior with a Physics Engine,” in *Proceedings of 2005 Structures Congress*, 2005.

[84] “Catastrophe game.” [Online]. Available: https://expeditionworkshed.org/workshed/catastrophe/. [Accessed: 02-Nov-2019].

[85] J. Li and J. Knippers, “Rotation formulations for dynamic relaxation with application in 3D framed structures with large displacements and rotations,” *Int. Symp. IASS-APCS*, 2012.

[86] “CPython - Python Software Foundation.” [Online]. Available: https://docs.python.org/2/c-api/code.html. [Accessed: 29-Oct-2019].

[87] V. Rek and I. Němec, “Parallel Computing Procedure for Dynamic Relaxation Method on GPU Using NVIDIA’s CUDA,” *Appl. Mech. Mater.*, vol. 821, no. 1, pp. 331–337, 2016.

[88] Panda3d, “Inheritance diagram for LineNodePath.” [Online]. Available: https://docs.panda3d.org/1.10/python/reference/direct.directtools.DirectGeometry. [Accessed: 26-Jul-2020].

[89] “Pymunk and Pygame.” [Online]. Available: http://www.pymunk.org/en/latest/tutorials/SlideAndPinJoint.html. [Accessed: 22-Oct-2019].

[90] D. Yalcin, “Effect of Specimen Geometry on Tensile Testing Results,” 2017. [Online]. Available: https://www.researchgate.net/publication/319773789_How_do_different_specimen_geometries_affect_tensile_test_results. [Accessed: 29-Aug-2019].

[91] S. C. Sharma, “Strength of Materials - Lecture 12.” [Online]. Available: https://nptel.ac.in/courses/112/107/112107146/. [Accessed: 29-Aug-2019].

[92] F. Ziegler, *Mechanics of Solids and Fluids*, vol. 15, no. 2. 1995.

[93] B. Topping and P. Ivanyi, “Computer Aided Design of Cable Membrane Structures,” *Book TMS/FF*. 2007.

[94] archdaily, “ASM International in Ohio, USA.” [Online]. Available: https://www.archdaily.com/212297/asm-international-world-headquarters-renovation-the-chesler-group-and-dimit-architects/asm-international-world-headquarters-materials-park-ohio-architect-john-terrence-kelly-r-buckminster-fuller-6. [Accessed: 29-Aug-2019].

[95] Wikipedia, “Montreal Biosphere.” [Online]. Available: https://upload.wikimedia.org/wikipedia/commons/4/4b/17-08-islcanus-RalfR-DSC_3883.jpg. [Accessed: 29-Aug-2019].

Annex A – Setting the 3DParticleSystem Software

A.1 Some installation notes

The 3DParticleSystem requires PyQt5 and Panda3D modules to be installed for correct operation. Both can be installed via anaconda prompt as an administrator, with the steps below.

```
python -m pip install --upgrade pip
pip install pyqt5
conda install -c kitsune.one panda3d-rp-kitsunetsuki
```

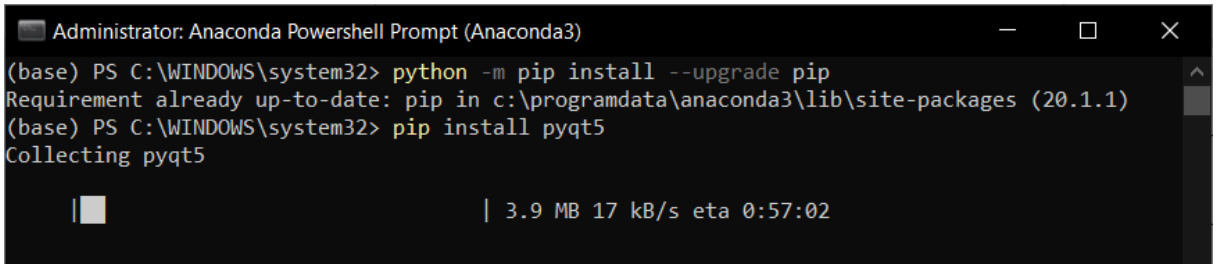

Figure A.1 – Installing Panda3d via Anaconda Prompt, step 1.

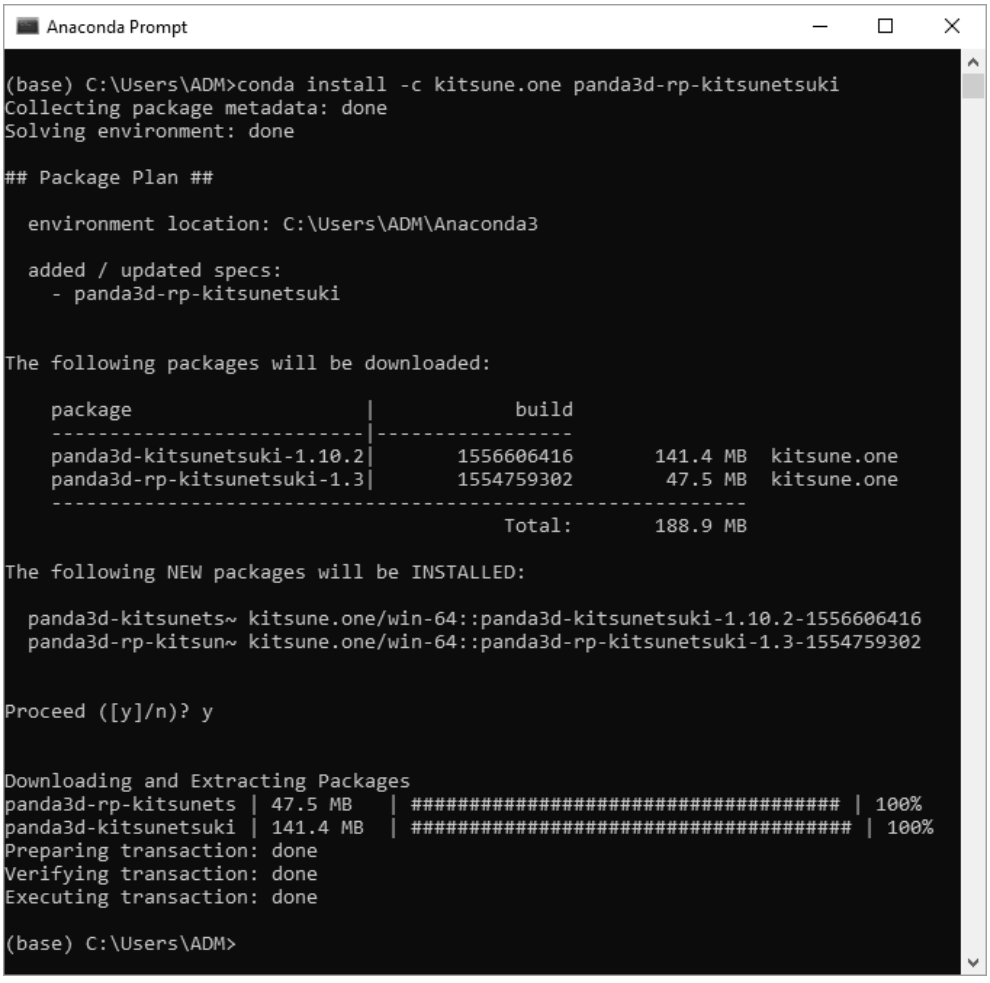

Figure A.2 – Installing Panda3d via Anaconda Prompt, step 2.

A.2 Setting the 3DParticleSystem software

Before launching the 3DParticleSystem software, the user must set two files: the main input file (inputFileOptions.txt) and the structural system file (for example, planeTruss.txt).

A.2.1 Setting the input file

This section shows an example of an input file to set the plane truss shown in Figure 3.3. Here, it is possible to set the directory of the structural system file, the stopping criterion, the parameters of the physics engine (time-step and damping coefficient), and the approach of the desired analysis (either 1 or 2).

```
# -*- coding: utf-8 -*-
"""
Copyright (C) 2020
You should have received a copy of the GNU General Public License
along with this program. If not, see http://www.gnu.org/licenses/.
"""

#Global Var
import os.path
mainDirectory =  os.path.realpath(os.path.dirname(__file__))
FilesInput = 'FilesInput'
filefolder = os.path.join(mainDirectory,FilesInput)

def PSA3DStrucureSystemGeometryAndLoads():

    #--Define the input file directory here--#
    filename = 'planeTruss.txt'
    filenameFull = os.path.join(filefolder,filename)
    return filenameFull

def PSA3DStoppingCriteria():

    #--Set the stopping criterion here--#
    tolerance = 10**-6
    saveInterval = 100
    ContadorLimite = 100000
    return tolerance, saveInterval, ContadorLimite

def PSA3DPhysicsEngineParameters():

    #--Set Physics Engine parameters here--#
    timeStep = 2*10**-4
    dampCoef = 200
    return timeStep, dampCoef

def PSA3DPhysicsAnalysisType():

    #--Set type of analysis here--#
    Approach = 2 #1 or 2

    #--Set if the mid steps axial forces should be printed in console and saved--#
    printSimulationInConsole =  = False

    return Approach
```

A.2.2 Setting the structural system file

The structural system file can be either a CSV or a TXT. This section shows an example of the structural system file to set the plane truss shown of Figure 3.3.

	A	B	C	D	E	F	G	H	I	J
1	Particles	PosX	PosY	PosZ	ConstraintX	ConstraintY	ConstraintZ	ForceX	ForceY	ForceZ
2	A	0	0	0	1	1	1	0	0	0
3	B	0	4	0	0	0	0	0	0	-100
4	C	0	8	0	0	0	0	0	0	-100
5	D	0	12	0	1	1	1	0	0	0
6	E	0	11	3	0	0	0	0	0	-100
7	F	0	7	3	0	0	0	0	0	-100
8	G	0	3	3	0	0	0	0	0	-100
9										
10										
11	Rods	PA	PB	Par1						
12	1	A	B	A:0.002;StressStrainCurve:[[-0.015,-254],[-0.00125,-250],[0,0],[0.00125,250],[0.015,254]						
13	2	B	C	A:0.002;StressStrainCurve:[[-0.015,-254],[-0.00125,-250],[0,0],[0.00125,250],[0.015,254]						
14	3	C	D	A:0.002;StressStrainCurve:[[-0.015,-254],[-0.00125,-250],[0,0],[0.00125,250],[0.015,254]						
15	4	G	F	A:0.002;StressStrainCurve:[[-0.015,-254],[-0.00125,-250],[0,0],[0.00125,250],[0.015,254]						
16	5	F	E	A:0.002;StressStrainCurve:[[-0.015,-254],[-0.00125,-250],[0,0],[0.00125,250],[0.015,254]						
17	6	A	G	A:0.002;StressStrainCurve:[[-0.015,-254],[-0.00125,-250],[0,0],[0.00125,250],[0.015,254]						
18	7	B	G	A:0.002;StressStrainCurve:[[-0.015,-254],[-0.00125,-250],[0,0],[0.00125,250],[0.015,254]						
19	8	B	F	A:0.002;StressStrainCurve:[[-0.015,-254],[-0.00125,-250],[0,0],[0.00125,250],[0.015,254]						
20	9	C	F	A:0.002;StressStrainCurve:[[-0.015,-254],[-0.00125,-250],[0,0],[0.00125,250],[0.015,254]						
21	10	C	E	A:0.002;StressStrainCurve:[[-0.015,-254],[-0.00125,-250],[0,0],[0.00125,250],[0.015,254]						
22	11	D	E	A:0.002;StressStrainCurve:[[-0.015,-254],[-0.00125,-250],[0,0],[0.00125,250],[0.015,254]						

Figure A.3 – An example of a CVS structural system input for the 3DParticleSystem software.

```
type:'Particle';tag:'ParticleA';position:[0 0 0];constraints:[1 1 1];ForceExternal:[0 0 0];appliedAccels:[]
type:'Particle';tag:'ParticleB';position:[0 4 0];constraints:[0 0 0];ForceExternal:[0 0 -100];appliedAccels:[]
type:'Particle';tag:'ParticleC';position:[0 8 0];constraints:[0 0 0];ForceExternal:[0 0 -100];appliedAccels:[]
type:'Particle';tag:'ParticleD';position:[0 12 0];constraints:[1 1 1];ForceExternal:[0 0 0];appliedAccels:[]
type:'Particle';tag:'ParticleE';position:[0 11 3];constraints:[0 0 0];ForceExternal:[0 0 -100];appliedAccels:[]
type:'Particle';tag:'ParticleF';position:[0 7 3];constraints:[0 0 0];ForceExternal:[0 0 -100];appliedAccels:[]
type:'Particle';tag:'ParticleG';position:[0 3 3];constraints:[0 0 0];ForceExternal:[0 0 -100];appliedAccels:[]


type:'Rods';tag:'Rod1';tagPA:'ParticleA';tagPB:'ParticleB';A:0.002;StressStrainCurve:[[-0.015,-254],[-
0.00125,-250],[0,0],[0.00125,250],[0.015,254];
type:'Rods';tag:'Rod2';tagPA:'ParticleB';tagPB:'ParticleC';A:0.002;StressStrainCurve:[[-0.015,-254],[-
0.00125,-250],[0,0],[0.00125,250],[0.015,254];
type:'Rods';tag:'Rod3';tagPA:'ParticleC';tagPB:'ParticleD';A:0.002;StressStrainCurve:[[-0.015,-254],[-
0.00125,-250],[0,0],[0.00125,250],[0.015,254];
type:'Rods';tag:'Rod4';tagPA:'ParticleG';tagPB:'ParticleF';A:0.002;StressStrainCurve:[[-0.015,-254],[-
0.00125,-250],[0,0],[0.00125,250],[0.015,254];
type:'Rods';tag:'Rod5';tagPA:'ParticleF';tagPB:'ParticleE';A:0.002;StressStrainCurve:[[-0.015,-254],[-
0.00125,-250],[0,0],[0.00125,250],[0.015,254];
type:'Rods';tag:'Rod6';tagPA:'ParticleA';tagPB:'ParticleG';A:0.002;StressStrainCurve:[[-0.015,-254],[-
0.00125,-250],[0,0],[0.00125,250],[0.015,254];
type:'Rods';tag:'Rod7';tagPA:'ParticleB';tagPB:'ParticleG';A:0.002;StressStrainCurve:[[-0.015,-254],[-
0.00125,-250],[0,0],[0.00125,250],[0.015,254];
type:'Rods';tag:'Rod8';tagPA:'ParticleB';tagPB:'ParticleF';A:0.002;StressStrainCurve:[[-0.015,-254],[-
0.00125,-250],[0,0],[0.00125,250],[0.015,254];
type:'Rods';tag:'Rod9';tagPA:'ParticleC';tagPB:'ParticleF';A:0.002;StressStrainCurve:[[-0.015,-254],[-
0.00125,-250],[0,0],[0.00125,250],[0.015,254];
type:'Rods';tag:'Rod10';tagPA:'ParticleC';tagPB:'ParticleE';A:0.002;StressStrainCurve:[[-0.015,-254],[-
0.00125,-250],[0,0],[0.00125,250],[0.015,254];
type:'Rods';tag:'Rod11';tagPA:'ParticleD';tagPB:'ParticleE';A:0.002;StressStrainCurve:[[-0.015,-254],[-
0.00125,-250],[0,0],[0.00125,250],[0.015,254];
```

Figure A.4 – An example of a TXT structural system input for the 3DParticleSystem software.

Annex B – Parts of the 3DParticleSystem software code

This section presents parts of the 3DParticleSystem software code, namely: The3DParticleSystem, GameEngine3DParticleSystem, PSA3DElements, PSA3DPhysicsEngine, Graphics Rendering Engine, and Utils functions.

B.1 The3DParticleSystem

The following code corresponds to the initial method that runs the 3DParticleSystem software. It is responsible for calling the The3DParticleSystemGUI, which launches the Graphical User Interface and the canvas.

```
# -*- coding: utf-8 -*-
"""
Copyright (C) 2020
You should have received a copy of the GNU General Public License
along with this program. If not, see http://www.gnu.org/licenses/.
"""


import subprocess
import sys

def installPackage(package):
    subprocess.check_call([sys.executable, "-m", "pip", "install", package])

try:
    import PyQt5
except:
    installPackage('pyqt5')

try:
    import panda3d
except:
    installPackage('panda3d')


from PyQt5.QtWidgets import QApplication
from src.srcThe3DParticleSystemGUI.The3DParticleSystemGUI import The3DParticleSystemGUI

def main():
    app = QApplication(sys.argv)
    The3DParticleSystemGUIRef = The3DParticleSystemGUI() #call Engine

    """
    IMPORTANT:
    called by the The3DParticleSystem.py file

    #Force Panda3D Window ShowBase to Init here (after The3DParticleSystemGUI.show())
    #Merging Qt with Panda
    #from src.GameEngine3DParticleSystem import GameEngine3DParticleSystem #Merging Qt with Panda
    #It must be after PyQt.The3DParticleSystemGUI.show()
    see
https://www.panda3d.org/reference/python/classdirect_1_1showbase_1_1ShowBase_1_1ShowBase.html
    """
    The3DParticleSystemGUIRef.showGE()

    sys.exit(app.exec_())

if __name__ == "__main__":
    main()
```

B.2 The3DParticleSystemGUI

This section shows constructor of the class The3DParticleSystemGUI.

```
class The3DParticleSystemGUI():

    def __init__(self , parent = None):

        #Call the The3DPsDialog and keep its reference
        self.__PyQtReferente = The3DPsDialog()

        #Merging Qt with Panda
        self.GERef = GameEngine3DParticleSystem(self)

        self.The3DPsNodesDialogRef = The3DPsNodesDialog(The3DParticleSystemGUIRef=self)
        self.PSA3DResultsRef = The3DPsResultsDialog(The3DParticleSystemGUIRef=self)
        #
        self.__btnStyle()

        #Setting connections between the UI and the respective actions
        self.__initReferences()
        self.__IteratingOverComboboxDictionary()
        self.__initConnections() #set table and connections
        self.__initConnections2()

        #Calls the sample case structure from the resource file
        self.GERef.sampleCaseStructureFromInputFile()

        #Setting some labels of the interface
        self.__PyQtReferente.slider1_axial.setValue(0)
        self.__PyQtReferente.slider2_deformed.setValue(2*100)
        self.__PyQtReferente.slider2_renderingFrequency.setValue(2)
        self.__PyQtReferente.slider2_textScale.setValue(35)
        self.__PyQtReferente.l_textScale.setText(str(35))

self.__PyQtReferente.slider2_SaveInterval.setValue(self.__PyQtReferente.slider2_SaveInterval.value
())

        #
        self.__PyQtReferente.show() #PyQt.The3DParticleSystemGUIRef.show()
```

B.3 The3DPsDialog

This section shows constructor of the class The3DPsDialog.

```
FORM_CLASS,TYPE_CLASS= get_ui_class('The3DPsGUI.ui')

class The3DPsDialog(TYPE_CLASS, FORM_CLASS):
    """Load "Plugin Interface" from file "*.ui".

    :param TYPE_CLASS: ??.
    :type TYPE_CLASS: ??
    """
    closingPlugin = pyqtSignal()

    def __init__(self, parent=None,titulo=''):
        """Constructor."""
        super(The3DPsDialog, self).__init__(parent)
```

B.4 GameEngine3DParticleSystem

This section shows some relevant methods of the class GameEngine3DParticleSystem: the class constructor and the simulate method.

B.4.1 GameEngine3DParticleSystem.__init__ (Class constructor)

```
class GameEngine3DParticleSystem(DirectObject):

    def __init__(self, PSA3DGUIEngine = None):
        (…)
        #Save reference of PyQt Menu/ Interface
        self.__PSA3DGUIEngine = PSA3DGUIEngine
        self.__PyQtReferente = self.__PSA3DGUIEngine.getPyQtReference()

        #(1) ----Graphics Rendering Engine------#
        #Set base
        self.__base = base #Instance from Panda3d Showbase; responsible for camera, rendering,...
        self.__base.setBackgroundColor(212, 212, 212) #Set background color to white
        self.__base.setFrameRateMeter(True)

        #Graphics Rendering Engine
        #Set Grid
        self.__grid__ = Grid()
        self.__grid__.setStatus(5)
        self.callBackGrid()
        #Set Panda events. Create the escape event
        self.accept('escape', exit)
        #Set Canvas buttons
        self.__setCanvasFeatures__()
        #Global GameEngine vars
        self.__mouseRunStatus = 'isRunning'
        self.__mouseHideShowStatus = 'isNotHidden'

        #(2) ----Input parameters from resource file------#
        self.__setStoppingCriteriaGUI__() #Setting Global Input values for the stopping criterion
        self.__setPhysicsEngineInputParameters__() #Calling Physics Engine parameters and keeping
its reference
        self.__setPhysicsEngineAnalysisTypeGUI__() #Setting Physics Engine Analysis Type

        #(3) ----Physics Engine------#
        #Auxiliary vars
        self.__lastHighlightRod = None
        self.__lastHighlightParticle = None
        #Starts the PSA3D Physics Engine
        self.__PhysicsEngine__()

        #The window starts empty
        self.filenameDirCSV = None
        self.__setStructure__("")

    def __setStructure__(self,filenameDir = None):
        (…)
        self.__PSA3DElementsRef__.loadMode(self.filenameDir)
```

B.4.2 GameEngine3DParticleSystem.__simulate__ (private method)

```
class GameEngine3DParticleSystem(DirectObject):
    (…)
    def __simulate__(self, mode = None):
            (…)
        if self.__mouseRunStatus == 'isPaused': #True:
            self.__mouseRunStatus = 'isRunning'

            if self.__PSA3DPhysicsEngine__.gameTask != "Pause":
                self.__PSA3DPhysicsEngine__.simulate("Pause")
        (…)
        else:
            self.__mouseRunStatus = 'isPaused'
            (…)
            if self.__PSA3DPhysicsEngine__.gameTask != "gameLoop":
                self.__PSA3DPhysicsEngine__.simulate("gameLoop")
```

B.5 PSA3DElements

This section presents the implementation of the PSA3DElements class. After reading the input file, this class calls the private method named *initStructureSystem*. This private method consists of looping into the list of particles and calling the *addParticle* private method. Later, it loops into the list of rods and calls the *addRod* private method. The *PSA3DElements* also contains the method responsive for updating the canvas, named, *updateStructureSystem*, which is explained in section 3.6.

B.5.1 PSA3DElements.__initStructureSystem__ (private method)

```
class PSA3DElements():
    (…)
    def __initStructureSystem__(self):

        #
        for t, vP in self.__ParticleGeometryListInString_.items():
            #Design the structure and setting its properties
            #Defining Particles
            (…)
            #
            self.__addParticle__(tag = tag, pos = position, constraints = constraints,
ForceExternal = ForceExternal, appliedAccels = appliedAccels)

        for t, vR in self.__RodGeometryListInString.items():

            (…)
            self.__addRod__(tag = tag, PA = PA, PB = PB,
                                       E = E, #= 200 #Gpa #Steel
                                       A = A, #m^2
                                       massPerUnitVolume = massPerUnitVolume, #(kg/m^3)
                                       StressStrainCurve = StressStrainCurve
                                       ) #(kN/(m/s))
```

B.5.2 PSA3DElements.__addParticle__ (private method)

```
class PSA3DElements():
    (…)

    def __addParticle__(self, tag = '', pos = [0,0,0], constraints = [0,0,0], ForceExternal =
[0,0,0], appliedAccels = [0,0,0]):

        self.ParticleGeometryList.update({tag: {'tag' : tag, 'pos': pos,'constraints':
constraints, 'RefGREngine': None, 'RefPSA3DPE': None, 'ForceExternal':
ForceExternal,'appliedAccels': appliedAccels}})

        #Graphical Settings
        ParticleGraphics = GraphicsParticles(pos, constraints, ForceExternal)
        (…)
        #Numerical Equations
        ParticleNumerical = PSA3DParticles(original_pos = pos,
        constraint = constraints,
        FextGlobalAxis = ForceExternal,
        appliedAccels = appliedAccels
        )

        #Save Particle Reference
        self.ParticleGeometryList[tag]['RefGREngine'] = ParticleGraphics
        self.ParticleGeometryList[tag]['RefPSA3DPE'] = ParticleNumerical
```

B.5.3 PSA3DElements.__addRod__ (private method)

```
class PSA3DElements():
    (…)
    def __addRod__(self, tag = None, PA = '', PB = '',
                                        E = '', #= 200 #Gpa #Steel
                                        A = '', #m^2
                                        massPerUnitVolume = '', #(kg/m^3)
                                        StressStrainCurve = ''
                                        ):
        #
        self.RodGeometryList.update({tag:{'tag': tag,'PA': PA,'PB': PB, 'RefGREngine': None,
'RefPSA3DPE': None}})

        p1_original_pos = PA.getOriginalPosition()
        p2_original_pos = PB.getOriginalPosition()

        #Graphical Settings
        RodGraphical = GraphicsRods(p1_original_pos, p2_original_pos)
        (…)
        #Numerical Equations
        RodNumerical = PSA3DRods(PA,PB,
                                 E = E, #= 200 #Gpa #Steel
                                 A = A, #m^2
                                 massPerUnitVolume = massPerUnitVolume, #(kg/m^3)
                                 StressStrainCurve = StressStrainCurve,
                                 dampCoef = self.__dampCoef, #(kN/(m/s))
                                 gui = gui
                                 )

        #Save Rod Reference
        self.RodGeometryList[tag]['RefGREngine'] = RodGraphical
        self.RodGeometryList[tag]['RefPSA3DPE'] = RodNumerical
```

B.5.4 PSA3DElements.updateStructureSystem (public method)

```
class PSA3DElements():
    (…)

    def updateStructureSystem(self):
        """
        #Update Canvas
        """

        #Update Rods position
        for RodName, RodData in self.RodGeometryList.items():
            Rod =  RodData['RefGREngine'] # == self.RodGeometryList[RodName]['RefGREngine']

            #get Axial Diagram
            axialValue = RodData['RefPSA3DPE'].getAxialForce()

            #get new Position Particle A
            PA = RodData['PA']
            p1_pos = PA.getDeformedPosition()

            #get new Position Particle B
            PB = RodData['PB']
            p2_pos = PB.getDeformedPosition()

            #Update Axial Diagram
            Rod.axialDiagram.updateAxialValue(axialValue)

            #Update deformed Position
            Rod.deformed.updatePositionAndAxial(p1_pos,p2_pos,axialValue)

        for ParticleName, ParticleData in self.ParticleGeometryList.items():
            P_numerical = ParticleData['RefPSA3DPE']
            P_graphical =  ParticleData['RefGREngine']

            #Update Reaction
            Reaction = P_numerical.getCurrentSupportReactionForces()
            P_graphical.supportReactions(Reaction)
```

B.6 PSA3DPhysicsEngine

This section presents the classes related to the *PSA3DPhysicsEngine*, namely: *PSA3DPhysicsEngine*, *PSA3DRods*, and *PSA3DParticles*.

B.6.1 PSA3DPhysicsEngine Numerical process

This section shows the implementation of the numerical process, presented in Figure 2.10 and Figure 2.13. Notice that, Approach 2 has one more step, which consists of computing the kinetic energy in each iteration.

```
class PSA3DPhysicsEngine():
    (…)
    def __numericalProcess__(self):

        #Step 1 - Part 1
        for ii, item in self.currentParticleGeometryList.items():
            Pii = item['RefPSA3DPE']
            Pii.numericalIntegration()

        #Step 1 - Part 2 - Computing kinetic energy and execute Kinetic Damping Schema
        if self.__kineticdampingschemeOPT == True:

            #Computing kinetic energy
            Uk_n_plus_1 = 0
            for ii, item in self.currentParticleGeometryList.items():
                Pii = item['RefPSA3DPE']
                Uk_i = Pii.calculateKineticEnergy()
                Uk_n_plus_1 = Uk_n_plus_1 + Uk_i

            #Kinetic Damping Approach

            #get Uk_n_less_1 and Uk_n
            Uk_n_less_1 = self.Uk_n_less_1
            Uk_n = self.Uk_n

            #Check if it is a peak Kinetic Energy
            if (Uk_n_less_1 <= Uk_n_plus_1) and (Uk_n <= Uk_n_plus_1):
                #save Ec
                self.Uk_n_less_1 = self.Uk_n
                self.Uk_n = Uk_n_plus_1
                itsPeak = False
            else:
                #Case - peak Kinetic Energy
                for ii, item in self.currentParticleGeometryList.items():
                    Pii = item['RefPSA3DPE']
                    Pii.kineticDamping()

                #Reset Ec
                self.Uk_n_less_1 = 0
                self.Uk_n = 0
                itsPeak = True

        #Step 2 - Calculate Rod's axial force
        for ii, item in self.currentRodGeometryList.items():
            Rii = item['RefPSA3DPE']
            converge = Rii.calculateRodsAxialForce()

        #Step 3 - check the stopping criterion
        if converge == False: #Step 3b - Auxiliar, break if strain>>1!
            print('\nDivergence results. Lower the value of damping coefficient and time-step!')
            stoppingCriterionStatus = True
            self.contador = 1000000
        else:
            FunbMax = 0
            for ii, item in self.currentParticleGeometryList.items():
                Pii = item['RefPSA3DPE']
                Funb = Pii.checkStoppingCriterionStatus()
                FunbMax = max(FunbMax,Funb)

            if FunbMax <= self.tolerance:
                stoppingCriterionStatus = True
```

```
            else:
                stoppingCriterionStatus = False

            #Step 3a - Is it a peak? Needs one more iteration!
            if self.__kineticdampingschemeOPT == True:
                if itsPeak == True:
                    stoppingCriterionStatus = False

        return stoppingCriterionStatus
```

B.6.2 Approach 1

Approach 1 is implemented with two classes: *PSA3DParticlesTrapezoidalRule* and *PSA3DRodsSmallDisplacements*.

B.6.2.1 PSA3DParticlesTrapezoidalRule

This section shows the implementation of the trapezoidal rule, presented before in Figure 2.11.

```
class PSA3DParticlesTrapezoidalRule(PSA3DParticlesElementary):

    def __init__(self,original_pos = [0,0,0],
            constraint = [0,0,0],
            FextGlobalAxis = [0,0,0],
            appliedAccels = [0,0,0]
            ):

        super(PSA3DParticlesArtificialDampingTrapezoidalRule, self).__init__(original_pos =
original_pos,
            constraint = constraint,
            FextGlobalAxis = FextGlobalAxis,
            appliedAccels = appliedAccels
            )

    def __trapezoidalRuleFunction__(self, xn, vn, an, h):
        #
        vn1 = vn + an*h
        xn1 = xn + (1/2)*h*(vn+vn1) #kN #Returns a row
        return xn1, vn1


    def __NumericalIntegration__(self):

        #-------Numerical Method--------

        #
        xn = self.xn
        vn = self.__vn
        tn = self.tn
        h = self.timeStep

        #Trapezoidal rule
        an = self.__computeAcceleration__( tn )
        [xn1,vn1] = self.__trapezoidalRuleFunction__(xn, vn, an, h)

        #Store results
        self.tn += h #time t(n+1)
        self.__vn = vn1 #Velocity in time t(n+1)
        self.xn = xn1 #Position in time t(n+1)

        return None
```

B.6.2.2 PSA3DRodsSmallDisplacements

This section shows the implementation of the internal force calculation considering small displacements, presented in Figure 2.12.

```
class PSA3DRodsSmallDisplacements(PSA3DRodsElementary):

    def __init__(self, ParticleA = '', ParticleB = '',
            E = None, #GPa #Steel
            A = None, #m**2
            massPerUnitVolume = None, #(kg/m^3)
            StressStrainCurve = None,
            dampCoef = None, #(kN/(m/s))
            gui = False
            ):

        super(PSA3DRodsSmallDisplacements, self).__init__(ParticleA = ParticleA, ParticleB =
ParticleB,
            E = E, #GPa #Steel
            A = A, #m**2
            massPerUnitVolume = massPerUnitVolume, #(kg/m^3)
            StressStrainCurve = StressStrainCurve,
            gui = gui
            )

        self.__dampCoef = dampCoef

    def __axialForce__(self):
        '''
        PSA3D Physics Engine by Paulo, Reydleon 2020 (20190528)

        Calculates axial force
        '''

        #Compute the current length (Lk,n+1)
        currentLength = self.__calculateCurrentLength__()

        #Computed strain εk,n+1 = (Lk,n+1 - r)/r
        strain = self.__calculateStrain__(self.restLength, currentLength)

        #Calculate the internal force (fk,h = εk,n+1*E*A)  on the local axis
        Fint = self.Fint = self.__calculateInternalForce__(strain)

        #Get velocity from the particles
        v1 = self.ParticleA.getCurrentVelocity()
        v2 = self.ParticleB.getCurrentVelocity()

        #Calculate the damping force (fk,d) on the local axis
        Fdmp = self.__calculateDampingForce__(v1,v2)

        #Calculate the axial force (fk,n+1 = fk,h + fk,d)
        Fa = Fint + Fdmp

        #Compute the axial force (fk,n+1) on the global axis #(kN)
        ForceAxialGlobal = LocalAxis2Global(self.T_Global2Local,tuple2NpArray([Fa,0,0]))
        #(1x6 vector)
        axialForceGlobal = set1x6SizeVector(ForceAxialGlobal, -ForceAxialGlobal)

        #Store fk,n+1 for next iteration and save for graphical output
        self.axialForceGlobal = axialForceGlobal

        #Compute current Stress in MPa and save for graphical output
        self.__computeCurrentStressAndAxialForce__(axialForceGlobal = axialForceGlobal,
currentTMatrix = self.T_Global2Local)

        return self.converge
```

B.6.3 Approach 2

Approach 2 is implemented with two classes: *PSA3DParticlesKineticDamping* and *PSA3DRodsLargeDisplacements*.

B.6.3.1 PSA3DParticlesKineticDamping

This section shows the implementation of flow charts presented in Figure 2.14 and Figure 2.15.

```
class PSA3DParticlesKineticDamping(PSA3DParticlesElementary):

    def __init__(self,original_pos = [0,0,0],
            constraint = [0,0,0],
            FextGlobalAxis = [0,0,0],
            appliedAccels = [0,0,0]
            ):

        #NOTE: In the case of the Kinetic Damping the velocities are calculated in the midpoint
time (t = t+(1/2)Δt

        super(PSA3DParticlesKineticDamping, self).__init__(original_pos = original_pos,
            constraint = constraint,
            FextGlobalAxis = FextGlobalAxis,
            appliedAccels = appliedAccels
            )

        #set Auxiliary var
        self.isPeak = True

    def __NumericalIntegration__(self):

        #-------Numerical Method--------

        #
        xn = self.xn
        vn_less_f5 = self.vn_plus_f5
        tn = self.tn
        h = self.timeStep

        #kinetic Damping

        #Calculate acceleration
        self.a_n = a_n = self.__computeAcceleration__(tn)

        #Calculate velocity
        if self.__isPeak == True:
            #next iteration
            vn_plus_f5 = (1/2)*h*a_n

            #set Auxiliary var
            self.__isPeak = False

        else:
            vn_plus_f5 = vn_less_f5 + h*a_n

        #Calculate position
        x_n_plus_1 = xn + h*vn_plus_f5 #m #Returns a row

        #Store results
        self.tn = self.tn + h #time t(n+1)
        self.vn_plus_f5 = vn_plus_f5 #Velocity in time t(n+1)
        self.xn = x_n_plus_1 #Position in time t(n+1)

        return None
```

B.6.3.2 PSA3DRodsLargeDisplacements

This section shows the implementation of the internal force calculation considering large displacements, presented before in Figure 2.16.

```
class PSA3DRodsLargeDisplacements(PSA3DRodsElementary):

    def __init__(self, ParticleA = '', ParticleB = '',
            E = None, #GPa #Steel
            A = None, #m**2
            massPerUnitVolume = None, #(kg/m^3)
            StressStrainCurve = None,
            dampCoef = None, #(kN/(m/s))
            gui = False
            ):

        super(PSA3DRodsLargeDisplacements, self).__init__(ParticleA = ParticleA, ParticleB =
ParticleB,
            E = E, #GPa #Steel
            A = A, #m**2
            massPerUnitVolume = massPerUnitVolume, #(kg/m^3)
            StressStrainCurve = StressStrainCurve,
            gui = gui
            )

    def __axialForce__(self):
        '''
        PSA3D Physics Engine by Paulo, Reydleon 2020 (20190528)

        Calculates axial force
        '''

        #Last iteration
        Ln = self.restLength

        #Compute the current length (Lk,n+1), the Transformation Matrix and the rod unit vector
e1'2'
        #(auxiliary step) get current position
        posA = self.ParticleA.getDeformedPosition()
        posB = self.ParticleB.getDeformedPosition()
        #
        Ln_1 = norm3D(posA,posB)
        RodvectorGlobalUCS = posB - posA #tuple2NpArray
        UnitVector, TMatrix = setTransformationMatrixGlobal2Local(RodvectorGlobalUCS) #Local to
global

        #Computed strain εk,n+1 = (Lk,n+1 - Lk,n)/Lk,n
        strain = self.__calculateStrain__(Ln,Ln_1)

        #Calculate the internal force on the local axis
        Fint = self.Fint = self.__calculateInternalForce__(strain)

        #Compute the internal force (fk,n+1) on the global axis
        #Global Axis #(kN) #Note E is in GPa and A in m**2. For that reason, E*A*10^6 == kN/m
        ForceInternalGlobal = Fint*UnitVector #Global2LocalAxis
        #(1x6 vector)
        axialForceGlobal = set1x6SizeVector(ForceInternalGlobal, -ForceInternalGlobal)

        #Calculate the current stress σk,n+1
        currentStress = self.__computeCurrentStressAndAxialForce__(axialForceGlobal =
axialForceGlobal, currentTMatrix = TMatrix)

        #Store Lk,n+1, fk,n+1 and σk,n+1 for next iteration
        self.restLength = Ln_1
        self.axialForceGlobal = axialForceGlobal
        self.__LastStressMPa = currentStress

        return self.converge
```

B.7 Graphics Rendering Engine

This section presents the classes related to the Graphics Rendering Engine, namely: *LineNodePath*, *ElementaryLine*, *GraphicsParticles,* and *GraphicsRods*.

B.7.1 LineNodePath

LineNodePath [88] is one of the basic drawing classes available in Panda3D. It inherits all the features and properties of the *NodePath* class [73]. Some of the methods of this class are: *drawLines*, *moveTo, drawTo, reset, setColor,* and *create.*

```
class LineNodePath(NodePath):
    (…)
    def __init__(self, parent = None, name = None,
                 thickness = 1.0, colorVec = VBase4(1)):

        # Initialize the superclass
        NodePath.__init__(self)

        # Create a lineSegs object to hold the line
        ls = self.lineSegs = LineSegs()
        (…)
    def drawLines(self, lineList):
        """
        Given a list of lists of points, draw a separate line for each list
        """
        for pointList in lineList:
            self.moveTo(*pointList[0])
            for point in pointList[1:]:
                self.drawTo(*point)
    (…)
    def moveTo(self, *_args):
    (…)
    def drawTo(self, *_args):
    (…)
    def reset(self):
    (…)
    def setColor(self, *_args):
    (…)
    def create(self, frameAccurate = 0):
        self.lineSegs.create(self.lineNode, frameAccurate)
```

The following script is an example of how to draw two lines and the result is shown in Figure 3.14.

```
import direct.directbase.DirectStart
from direct.directtools.DirectGeometry import LineNodePath
from pandac.PandaModules import Point3,Vec4

def drawLine(Name,p1 = (0,0,0),p2 = (0,0,0),Color = Vec4(0,0,0,0)):

    #p1 and p2
    arr_ = (p1[0],p1[1],p1[2]); p1 = Point3(arr_[0],arr_[1],arr_[2])
    arr_ = (p2[0],p2[1],p2[2]); p2 = Point3(arr_[0],arr_[1],arr_[2])

    rod = LineNodePath(render,Name,3,Color)
    rod.moveTo(p1)
    rod.drawTo(p2)
    rod.create()
    return rod

def main():
    #Rod1
    rod1 = drawLine(Name = 'Rod1', p1 = (0,0,0), p2 = (3,3,0), Color = Vec4(1,0,0,1))
    #Rod2
    rod2 = drawLine(Name = 'Rod2', p1 = (0,0,0), p2 = (4,3,0), Color = Vec4(0,0,1,0))

main()
run()
```

B.7.2 ElementaryLine

This section introduces the constructor method of the *ElementaryLine* class. It inherits all the properties and methods of the *LineNodePath* class (Annex B.7.1 and [88]). It receives as input the coordinates p1, p2, the color and thickness.

```
class ElementaryLine(LineNodePath):
    (…)

    def __init__(self,p1,p2,strCOLOR = '',thickness = 3):
    (…)
        #Init
        super().__init__( parent = None, name = '',
                    thickness = 3, colorVec = Vec4(0,0,0,0))
```

B.7.3 GraphicsParticles

The GraphicsParticles class is called whenever a particle is created. As explained in 3.5.1, the particle element carries properties such as coordinates, nodal constraints, and external forces. The following code presents the implementation of the graphical part of each particle.

```
class GraphicsParticles():
    (…)

    def __init__(self,originalPosition, constraints = [0,0,0],externalForce = [0,0,0]):
        (…)
        self.NodalConstraint = NodalConstraint(self.__originalPosition, self.__constraints)
        self.ExternalForce = ExternalForce(self.__originalPosition, self.__externalForce,color =
'ColorBlue')
```

B.7.4 GraphicsRods

The GraphicsRods class is called whenever a rod is created. As explained in 3.5.2, the rod element is organized into three classes, namely, ElementaryRod, AxialDiagram, and DeformedRod. Each rod carries properties such as two particles that contain all their intrinsic properties, namely, original position, deformed position, nodal constraints, and external forces. The following code presents the implementation of the graphical part of each rod.

```
class GraphicsRods(ElementaryRod):
    (…)

    def __init__(self,p1,p2,axialDiagramScale = 0.0, RodDeformedScale = 1.0 , strCOLOR =
'ColorBlack', thickness = 1.5):

        #Converts to type (x,y,z)
        p1 = (p1[0],p1[1],p1[2])
        p2 = (p2[0],p2[1],p2[2])

        #Rod
        super().__init__(p1,p2,strCOLOR,thickness)

        #Deformed Rod
        self.deformed = DeformedRod(p1 = p1,p2 = p2, Scale = RodDeformedScale, strCOLOR =
'ColorBlue')

        #Axial Diagram
        self.axialDiagram = AxialDiagram(p1 = p1,p2 = p2, Scale = axialDiagramScale)
```

B.8 Utils functions

Utils functions are a collection of small Python functions, which makes it easier to handle repetitive tasks. It is divided into Matrix Operations and Transformation Functions.

B.8.1 matrixOperations

Matrix Operations functions are a collection of small Python functions based on the Python NumPy [67]. It makes it easier to handle the algebraic operations such as sum, addition, and product of vectors and arrays. The resulting code can be summarized as: *matrixLine2NPArray, tuple2Vec, getSize, MatrixTranspose, Vecs2Matrix, matrixDot, isEqual, set1x6SizeVector,* and *multiplyAandB.*

```
def __matrixLine2NPArray(vecMatrix):
    """
    receive: tupleVec = matrix([x,y,z])
    returns: array([x,y,z])
    """

def __tuple2Vec(tupleVec):
    """
    receive: tupleVec = [1,2,3]
    returns:
    """

def getSize(vecLine):
    """
    receive:

        a) vecLine = [48,54,60]
        b) vecLine =
             [[48]
              [54]
              [60]]

        c) vecLine = Matrix

    returns:
        [numRows , numCols]

    #see https://www.mathworks.com/help/matlab/ref/size.html
    """

def MatrixTranspose(MatrixM):
    """
    receive:
       MatrixM =
        [[ 4  7 10]
         [ 5  8 11]
         [ 6  9 12]]

    returns:
       MatrixM =
        [[ 4  5 6]
         [ 7  8 9]
         [ 10  11 12]]
    """

def Vecs2Matrix(a1,a2,a3):
    """
    receive:
        a1 = [4,5,6]
        a2 = [7,8,9]
        a3 = [10,11,12]

    returns:
       MatrixM =
        [[ 4  5 6]
         [ 7  8 9]
         [ 10  11 12]]
    """

def matrixDot(MatrixM,vecT):
```

```
    """
    receive:
       MatrixM =
        [[ 4  7 10]
         [ 5  8 11]
         [ 6  9 12]]

        vecT = [1 2 3]
        vector line type Size = 1x3
    returns:
        vecRes = [48,54,60]
 """

def isEqual(v1,v2):
    """
    Parameters: a1 ,a2 : array_like Input arrays.

    returns: varBool: bool
            Returns True if the arrays are equal
    """

def set1x6SizeVector(v1, v2):
    """
    Parameters: v1 ,v2 : array_like
                    Input arrays.

    returns: z3_: array_like
                    Outputs 1x6 array.
    """

def multiplyAandB(A,B):
    """
    Parameters: z3: array_like
                    Outputs 1x6 arrays.

    returns: z3: array_like
                    Outputs 1x3 array.

    #See https://stackoverflow.com/questions/25573298/math-error-when-multiplying-float-by-
integer-in-python
    """
```

B.8.2 TransformationFunctions

This section presents some relevant methods of the *TransformationFunctions* class, such as *setTransformationMatrixGlobal2Local, LocalAxis2Global, Global2LocalAxis, crossProduct,* and *normalize3D.*

```
def setTransformationMatrixGlobal2Local(RodvectorGlobalUCS):
    '''
    input:
        RodvectorGlobalUCS = <e1,||RodvectorGlobalUCS||> = [x,y,z]
        Receives a row 1x3 array

    output:
        principalAxisMatrix 3x3 = [e1,e2,e3]

    example:
        RodvectorGlobalUCS = [x y z] = [0, 0.8, 0.6]

        TGlobal2Local = principalAxisMatrix 3x3 =
            [[0.0 0.8 0.6]
             [1.0 0.0 0.0]
             [  0 +0.6 -0.8]]

        RodvectorGlobalUCS = [x y z] = [0, .5*sqrt(2), .5*sqrt(2)]

        TGlobal2Local = principalAxisMatrix 3x3 =
            [[0.0 .5*sqrt(2) .5*sqrt(2)]
             [1.0 0.0 0.0]
             [  0 +.5*sqrt(2) -.5*sqrt(2)]]
    '''

def LocalAxis2Global(TGlobal2Local, VlocalSectionAxis):
    '''
        Transform local Axis to Global
        Return a column 3x1
    '''

def Global2LocalAxis(TGlobal2Local,vGlobal):
    '''
        Transform Global Axis to local Axis
        Return a column 3x1
    '''

#----------------- AUXILIAR METHODS-----------------
def __crossProduct(c1,c2):
    '''
        see https://www.mathworks.com/help/matlab/ref/cross.html
    '''

def __normalize3D(vec):
    '''
        see https://www.mathworks.com/help/matlab/ref/cross.html
    '''
```